Integration of Cellular and Organismal Stress Responses to Light at Night and Simulated Night Shift Work in the Diurnal Zebra Finch and Nocturnal House Mouse

By

Kevin Pham

A dissertation submitted to the Graduate Faculty of
Auburn University
in partial fulfillment of the
requirements for the Degree of
Doctor of Philosophy

Auburn, Alabama
August 9, 2025

Keywords: Light at night; zebra finch; house mouse, oxidative damage; metabolism; hormone; physiology, circadian rhythms

Approved by
Dr. Haruka Wada, Chair, Associate Professor, Biological Sciences
Dr. Wendy Hood, Professor, Biological Sciences
Dr. Jenny Ouyang, Associate Professor, Integrative Biology
Dr. Chris Newland, Professor, Psychology
Outside reader: Dr. Kelsey McCune, Assistant Research Professor, Wildlife

Abstract

The presence and absence of light is a fundamental environmental signal leveraged across the tree of life to synchronize internal biological processes to external, predictable environmental conditions. With the rise of artificial lighting sources and everchanging modern lifestyles, humans and wildlife have been faced with a new challenge – disruption in the nighttime environment through exposure to artificial lighting sources at various spectra, types, intensities, and patterns.

Throughout my PhD, I aimed to elucidate how birds and mammals respond to perturbations in the nighttime environment through aperiodic and alternating lighting conditions, particularly focusing on the physiological costs associated with unnatural light/dark cycles. Birds and mammals offer interesting insights on the role of circadian rhythm disruption due to 1) differences in their ability to receive and relay light information and 2) distinct physiological differences.

Zebra finches (*Taeniopygia guttata castanotis)* are an opportunistic, diurnal social songbird native to Australia, with well-charactered stress physiology and neurobiology. They are generally insensitive to changes in the photoperiod, meaning that we can disentangle unique physiological responses in response to photoperiod manipulations that mimic human patterns without activating alternate pathways sensitive to photoperiodism associated with life-history transitions. Therefore, zebra finches are the ideal model to evaluate the mechanisms underlying physiological and metabolic effects to altered lighting conditions.

The nocturnal mouse (*Mus musculus)* has been the prime model to examine the theoretical and mechanistic basis of circadian rhythm biology. Indeed, the ability to easily manipulate their genome to ask targeted questions regarding the pathogenesis of diseases related to circadian rhythm disruption, in combination with other important factors such as diet and exercise has proven extremely useful. Yet, artificial selection may have removed vital components involved in mediating their physiological and behavioral response to stressors, particularly by making strains more docile, and more reproductively capable. Consequently, the genotypes of many lab strains are virtually the same, and common lab rodents used in circadian rhythm research are done in some strains unable to produce melatonin, a key hormone related to biological timekeeping. Thus, studies capitalizing on the wild-derived house mouse that retains natural sensitivity to stressors bridges together the strength of genetic heterogeneity and plasticity, with the utility of controlled laboratory environments to further evaluate nighttime light disturbances on physiology will prove useful.

These ecologically relevant models are at the forefront of my dissertation, in which I explored neuroendocrine, metabolic, and morphological effects of light at night across four data chapters. In chapters 2 and 3, I examined the role of stress resilience by exposing zebra finches to high intensity constant light and allowing a recovery period. I collected samples to address transient and persistent changes in hypothalamic-pituitary-adrenal (HPA) axis and glucose regulation, body mass, and the abundance of glucocorticoid receptors (Chapter 2).

To further evaluate physiological costs to constant light, I investigated the capacity to which zebra finches displayed ephemeral or persistent cellular damage by measuring a suite of damage markers related to DNA, lipids, and proteins across the blood, liver, and skeletal muscle (Chapter 3). To identify the mechanism(s) associated with cellular damage outcomes, I leveraged

data collected from Chapter 2 to perform path analysis, synonymous to structural equation modelling (SEM), to reveal how light at night altered the physiological regulatory network after exposure and a recovery period.

In Chapter 4, I investigated the bioenergetic mechanisms related to sex and tissue-specific responses to constant light and darkness in the wild-derived house mouse. While HPA axis function could be a mechanism underlying metabolic or cellular damage outcomes to altered lighting conditions, two alternative mechanisms are declines in mitochondrial respiratory function and resting metabolic rate, both of which, are heavily involved in maintaining metabolic homeostasis and underlie metabolic diseases.

In the last data chapter, to bridge together experimental paradigms and findings from chapters 2-4, I exposed zebra finches to simulated night shift work conditions commonly experienced by human shift workers and experimentally done in rodent models. Here, I extended upon hypothalamic-pituitary-adrenal (HPA) regulation by including negative feedback efficiency, the ability to terminate the adrenocortical response to avoid a long duration of elevated glucocorticoid. Moreover, I evaluated circadian rhythmicity of two key hormones reflective of circadian alignment: corticosterone and melatonin.

In Chapter 2, I found that there were time-dependent effects of constant light on the morphology and physiology of zebra finches in addition to varying degrees of stress resilience. Body mass marginally increased after 3 days of constant light, but after 23 days of exposure to constant light, body mass was significantly higher in treatment birds compared to controls. In contrast, baseline glucose levels decreased over the duration of the experiment, yet these effects were transient, as both body mass and glucose levels rebounded to pretreatment levels after the recovery period, indicating stress resilience. Yet, the glucose stress response was blunted due to

constant light, and remained blunted after the recovery period, indicating a persistent effect and a lack of stress resilience. Interestingly, there were no changes in circulating baseline corticosterone, the reactivity of the HPA axis, or the abundance of glucocorticoid receptors in the liver. These data suggest that there is variation in the capacity for different traits to rebound after recovery from a chronic stressor. Yet, questions remain as to if these trends are the result of prioritization of recovery between different traits or is dependent on the length of the recovery period.

In Chapter 3, there were no transient or persistent effects of constant light on global DNA damage in the red blood cells. Furthermore, constant light at night did not result in persistent oxidative damage in the liver or skeletal muscle, measured through protein carbonyls and 4-hydroxynonaneal. However, by leveraging data from chapter 2, a phenotypic integration approach via path analysis revealed interesting associations between traits and their relationship with damage outcomes that were dependent on treatment groups. In control birds, path analysis revealed that HPA axis function was a condition-dependent trait, such that individuals with greater body mass mounted stronger stress responses. Moreover, birds that mounted stronger HPA axis responses also had stronger downstream glucose responses. However, exposure to constant light uncoupled condition-dependency of the stress phenotype, such that after a recovery period, birds previously exposed to light at night had no relationship between body mass, HPA axis function, and the glucose stress response. These data suggest that prior stress history (*i.e.,* exposure and recovery from light at night) may have persistent effects by modifying physiological network linkage between traits within the physiological regulatory network which may underlie damage outcomes.

In Chapter 4, there was a sex and tissue-specific response relating to constant light, but not constant darkness. Specifically, state 3 maximum mitochondrial respiratory function was higher in the liver of female mice exposed to constant light, compared to controls and females under constant darkness. There was not a similar trend in the mitochondrial respiratory response in the male livers, or the skeletal muscles of either sex. While females had greater mitochondrial respiratory function, they did not suffer from greater lipid peroxidation in the liver, indicating that the common assumption between enhanced oxidative phosphorylation capacity and cellular damage is not supported. There were no significant changes in body mass, fat pads, or the resting metabolic rates of mice under constant light or darkness. These data contrast many studies that investigate the effects of light at night in laboratory rodents, emphasizing the importance of individual variation and plasticity. Furthermore, these data highlight that the bioenergetic underpinning of metabolism could improve upon our understanding of metabolic disease to circadian disruption.

In Chapter 5, I found that 24-h corticosterone profiles were inverted an inversion of corticosterone profiles after 63 days of simulated night shift work. There was a similar trend suggesting inversion of melatonin profiles, however, lack of biological samples and statistical power inhibited my ability to capture this effect. I also found that simulated night shift work suppressed HPA axis reactivity, but not negative feedback efficiency. Moreover, simulated night shift work enhanced fatty acid metabolism, indicated by greater number of circulating β-hydroxybutyrate, yet this did not result in changes to body mass or subcutaneous fat deposits. There were no differences in superoxide dismutase 1 or abundance of 4-hydroxynonaneal adducts in the liver. In contrast, there were lower amounts of relative protein abundance of superoxide dismutase 1 in the brain, but no difference between groups in 4-hydroxynonaneal

damage in the brain. Overall, the data gathered here indicate plasticity in circadian mechanisms in response to alternating patterns of light at night that mimic night shift work in humans. Such plasticity was able to alleviate some of the physiological costs to simulated night shift work, indicating resilience to alternating patterns of light.

Acknowledgements

Entering graduate school during the peak of COVID-19 in 2020 was extremely challenging. Such a new environment, coupled with a lack of experience, and knowledge in research almost caused me to quit. However, I was so fortunate to have Haruka and the graduate students in the Wada lab that made the transition a little less scary. I am eternally grateful to Madeline Lazenby for working alongside such a newbie in research, and for showing me the ropes – from literally labeling a tube to the many sampling days that we worked on together. Tori Coutts, Alex Hoffman, Cara Brittain, and Wonil Choi, thank you for creating the environment I needed during Covid. You all were my role models during the pivotal early years at Auburn.

I thank Wendy Hood for adopting me into her lab, and Geoff Hill for letting me crash the Hood/Hill lab meetings. I thank Emma Rhodes and KayLene Yamada for teaching me fundamental lab skills and collaborating on one of my dissertation chapters to investigate the role of light at night on mitochondrial physiology.

I thank Drs. Bruce Smith, Melody Russell, and Taffye Clayton for providing me the opportunity to continue my education through the G-RISE fellowship that enhanced my PhD training here.

To my friends, thank you for their unyielding support throughout my entire academic journey (and listening to all of my many many many complaints).

I want to dedicate this PhD and dissertation to my family. Coming from a first-generation, low-income, immigrant household came with its own challenges that were only further magnified by being in the field of scientific research. My parents went through many

hardships and sacrificed so much in order provide me and my siblings the opportunities that were unobtainable for them and forged me into the person I am today. Thank you for instilling upon me a strong work ethic, perseverance, and resilience.

Finally, I thank my advisor, Haruka Wada. I know for a fact, that I would not have been able to complete a dissertation in anyone else's lab. You never once created the impression that you didn't want what was best for me. I am so grateful that you allowed me to pursue my research without reservations, judgement, or fear of failing. In fact, you expected failure! Failures are what makes us strive to enhance our work, learn more, and help others prevent them. Thank you for accepting me into your lab and giving me the opportunity to make a small contribution to science.

Table of Contents

List of Tables

List of Main Figures

List of Supplementary Figures

General introduction – Chapter 1

Life on earth has evolved under the reliability of photoperiodic cues to govern perhaps all aspects of their biology. However, exposure to light at unnatural times has become a ubiquitous component of modern society. Ecological landscapes have become increasingly urbanized, increasing the prevalence and magnitude of artificial light at night. Additionally, patterns of light at night and sleep/wake have become unpredictable, with differences in susceptibility and vulnerability among age classes, sex, and occupation. Such disruptions in the nighttime environment are thought to affect circadian rhythmicity of physiological processes and hypothesized to be the driver of disease phenotypes detected in the rodent models of shift work and human epidemiological studies. Therefore, how animals circumvent novel challenges that light at unnatural times imposes on their biological responses will be critical to evaluate, given that circadian rhythmicity is at the crux of an organism's biology.

Neuroendocrine axes are likely the most vulnerable to disruption in the nighttime environment, given that the majority of hormones are under circadian control. Additionally, the neuroendocrine system is heavily involved in orchestrating phenotypic adjustments to various environmental inputs and affect multiple tissues and pathways (hormonal pleiotropy), although large variation exists between individuals and between species in the magnitude of these responses (Cockrem, 2013).

One hallmark of the endocrine system, and the focus of this dissertation is the release of glucocorticoids (GCs) by hypothalamic-pituitary-adrenal (HPA) axis. Glucocorticoids are metabolic steroid hormones and under ultradian and circadian control (Oster et al., 2017). The glucocorticoid hormone cascade is released in response to unpredictable challenges (i.e., a threat

to homeostasis), dubbed stress reactivity (among other names). Stress reactivity, coupled with a negative feedback loop mechanism, allows vertebrates to mount strong stress responses, and then subsequently turn off the hormone cascade once the perceived threat is dealt with (Timmermans et al., 2019).

Given the wide distribution of glucocorticoid receptors (GR) and their ability to activate metabolic and oxidative pathways (Breuner et al., 2003; Sapolsky et al., 2000; Lattin et al., 2012; Timmermans et al., 2019; Præstholm et al., 2021), changes in HPA axis regulation through disruption in the nighttime environment may lead to tissue-specific consequences. However, whether glucocorticoids relate to physiological consequences will depend on the magnitude, duration, and capacity of organisms to repair potential damage.

While short-term elevation of glucocorticoids is often beneficial (Sapolsky et al., 2000), long-lasting elevation can cause damage to the body and malfunction of physiological systems (Sapolsky et al., 2000; Romero et al., 2009; Wada, 2019). Despite our understanding glucocorticoid's biphasic effects, it is difficult to ascertain the transition between acute and chronic stress and the emergence of diseases stemming from continuous activation of the HPA axis. Identifying the biphasic effects of glucocorticoids on physiological traits related to downstream physiological consequences will be imperative to reveal how organisms combat stressors on both short-term and long-term scales. Moreover, identifying whether these changes are transient or persistent will be informative to the role that repair and recovery plays in mitigating physiological costs.

Throughout my dissertation chapters, I used the diurnal zebra finch (*Taeniopygia guttata castanotis*) and wild-derived nocturnal house mouse (*Mus musculus)* as model systems to evaluate how light at unnatural times altered morphology, physiology, and cellular damage

markers that are hypothesized to be sensitive to light at night. The overarching goal of my dissertation is to examine the physiological consequences underlying exposure to unnatural lighting conditions.

Overall, my dissertation addresses the following research questions:

1. **What is the capacity for zebra finches to resist or recover from constant exposure to high intensity light at night?**

a. Are there transient or persistent changes in physiological stress mediators after exposure and recovery from light at night? – Chapter 2

b. Do such changes in physiological mediators result in physiological consequences in cellular damage outcomes? – Chapter 2 and Chapter 3

c. What are the mechanisms underlying cellular damage outcomes after recovery from constant light? – Chapter 3

2. **What is the bioenergetic underpinning of a wild-derived house mouse's response to constant light and darkness?**

a. Are there sex-specific consequences to unnatural nighttime conditions? – Chapter 4

b. If so, is there a trade-off in cellular damage? – Chapter 4

c. Do the morphological and physiological consequences of constant light at night resemble that of common patterns found in the literature regarding lab strains? – Chapter 4

3. **Does a diurnal songbird show similar physiological consequences to simulated night shift work that closely mimic human conditions?**

a. How does circadian rhythmicity of melatonin and corticosterone, two important hormones that reflect circadian alignment, change as a result? – Chapter 5

b. What is the role of the hypothalamic-pituitary-adrenal (HPA) axis in mediating stress responsiveness and termination of the response? – Chapter 5

c.) Are there downstream consequences in energy homeostasis and cellular damage? – Chapter 5

References:

Breuner, C.W., Orchinik, M., Hahn, T.P., Meddle, S.L., Moore, I.T., Owen-Ashley, N.T., Sperry, T.S., Wingfield, J.C., 2003. Differential mechanisms for regulation of the stress response across latitudinal gradients. Am. J. Physiol. - Regul. Integr. Comp. Physiol. 285, 1–3. https://doi.org/10.1152/ajpregu.00748.2002

Cockrem, J.F., 2013. Individual variation in glucocorticoid stress responses in animals. Gen. Comp. Endocrinol. 181, 45–58. https://doi.org/10.1016/j.ygcen.2012.11.025

Lattin, C.R., Waldron-Francis, K., Richardson, J.W., de Bruijn, R., Bauer, C.M., Breuner, C.W., Michael Romero, L., 2012. Pharmacological characterization of intracellular glucocorticoid receptors in nine tissues from house sparrow (Passer domesticus). Gen. Comp. Endocrinol. 179, 214–220. https://doi.org/10.1016/j.ygcen.2012.08.007

Præstholm, S.M., Correia, C.M., Goitea, V.E., Siersbæk, M.S., Jørgensen, M., Havelund, J.F., Pedersen, T., Færgeman, N.J., Grøntved, L., 2021. Impaired glucocorticoid receptor expression in liver disrupts feeding-induced gene expression, glucose uptake, and glycogen storage. Cell Rep. 37, 109938. https://doi.org/10.1016/j.celrep.2021.109938

Oster, H., Challet, E., Ott, V., Arvat, E., de Kloet, E.R., Dijk, D.J., Lightman, S., Vgontzas, A., Van Cauter, E., 2017. The functional and clinical significance of the 24-hour rhythm of circulating glucocorticoids. Endocr. Rev. 38, 3–45. https://doi.org/10.1210/er.2015-1080

Præstholm, S.M., Correia, C.M., Goitea, V.E., Siersbæk, M.S., Jørgensen, M., Havelund, J.F., Pedersen, T., Færgeman, N.J., Grøntved, L., 2021. Impaired glucocorticoid receptor expression in liver disrupts feeding-induced gene expression, glucose uptake, and glycogen storage. Cell Rep. 37, 109938. https://doi.org/10.1016/j.celrep.2021.109938

Sapolsky, R.M., Romero, L.M., Munck, A.U., 2000. How do glucocorticoids influence stress responses? Integrating permissive, suppressive, stimulatory, and preparative actions. Endocr. Rev. 21, 55–89. https://doi.org/10.1210/er.21.1.55

Romero, L.M., Dickens, M.J., Cyr, N.E., 2009. The reactive scope model - A new model integrating homeostasis, allostasis, and stress. Horm. Behav. 55, 375–389. https://doi.org/10.1016/j.yhbeh.2008.12.009

Timmermans, S., Souffriau, J., Libert, C., 2019. A general introduction to glucocorticoid biology. Front. Immunol. 10. https://doi.org/10.3389/fimmu.2019.01545

Wada, H., 2019. Damage-Fitness Model: the missing piece in integrative stress models. Stress 22, 548–562. https://doi.org/10.1080/10253890.2019.1614556

Chapter 2: Zebra finches (*Taeniopygia castanotis)* display varying degrees of stress resilience in response to constant light

Published in the Journal of Comparative and General Endocrinology Volume 361,

2025,114644, ISSN 0016-6480 https://doi.org/10.1016/j.ygcen.2024.114644.

(https://www.sciencedirect.com/science/article/pii/S0016648024002077)

Authors: Kevin Pham*[1], Madeline Lazenby[1], KayLene YH Yamada[1], Christine R. Lattin[2], Haruka Wada[1]

[1]Department of Biological Sciences, Auburn University, Auburn, AL 36849, USA

[2]Department of Biological Sciences, Louisiana State University, Baton Rouge, LA 70803, USA

Key words: Light at night, Light pollution, Metabolism, Glucocorticoids, Circadian disruption, Birds

***Note: Slight grammatical corrections were added that is not reflective of the published manuscript online.**

Abstract

The ability for traits to recover after exposure to stress varies depending on the magnitude, duration, or type of stressor. One such stressor is circadian rhythm disruption stemming from exposure to light at night. Circadian rhythm disruption may lead to long-term physiological consequences; however, the capacity in which individuals recover and display stress resilience is not known. Here, we exposed zebra finches (*Taeniopygia guttata castanotis*) to constant light (24L:0D) or a regular light/dark cycle (14L:10D) for 23 days, followed by a recovery period for 12 days. We measured body mass, corticosterone, and glucose levels at multiple timepoints, and relative protein expression of glucocorticoid receptors at euthanasia. Body mass significantly increased over time in light-exposed birds compared to controls, but a 12-day recovery period reversed this increase. Baseline levels of circulating glucose decreased in light-exposed birds compared to controls, but returned to pretreatment levels after the 12-day recovery period. In contrast, the glucose stress response did not show a similar recovery trend, suggesting longer recovery is needed or that this is a persistent effect in light-exposed birds. Surprisingly, we did not detect any differences in baseline corticosterone or stress reactivity between groups throughout the experiment. Moreover, we did not detect differences between relative protein expression of glucocorticoid receptors or a relationship with stress reactivity. Yet, we found a positive relationship between glucocorticoid receptors and the glucose stress response, but only in the light group. Our results indicate that physiological and morphological traits differ in their ability to recover in response to constant light and warrants further investigation on the mechanisms driving stress resilience under a disrupted circadian rhythm.

1. Introduction

With the advent of artificial lighting sources, the nighttime environment has become permanently altered with nearly 83% of the world's population living under some form of artificial light at night (ALAN) (Falchi et al., 2016). Across vertebrates and invertebrates, ecologically relevant levels of ALAN (<35 lux) has been shown to alter a myriad of physiological and behavioral parameters including hormone levels (Ouyang et al., 2015; Secondi et al., 2021), metabolism (Yadav et al., 2022), immune function (Gastón et al., 2019), body condition (Grunst et al., 2020) and behavioral patterns (Levy et al., 2021; Mardones et al., 2023). These physiological and behavioral alterations are thought to be a result of circadian rhythm disruption. Circadian rhythms are 24-hour internal biological clocks that synchronize biological processes (*e.g.,* hormonal release or behavior) to external light/dark cues, such that the timing of these processes coincides with changes in the environment (Gnocchi and Bruscalupi, 2017). A properly functioning circadian system is fundamental to maintain homeostasis. Thus, it is unsurprising to see that circadian rhythm disruption has such a diverse array of biological effects in both nocturnal and diurnal species (Potter et. al., 2016). Indeed, circadian disruption through perturbed light/dark environments is associated with irregular hormone production, metabolic impairments, fat accumulation, weight gain, and disease (Arble et al., 2010; Bedrosian et al., 2016).

The hypothalamic-pituitary-adrenal (HPA) axis is one neuroendocrine system that is subject to circadian rhythm disruption through altered light/dark environments (*e.g.,* constant light or ALAN) (Ouyang et al., 2018). This is because the HPA axis and circadian system have a bidirectional relationship that orchestrates rhythmic secretion of glucocorticoids and hormone precursors (Rao & Androulakis, 2019). Glucocorticoids are metabolic hormones released by the

HPA axis that prime organism physiology and behavior in anticipation to the switch from inactivity to activity (Spencer et al., 2018; Oster et al., 2017). In birds, the main glucocorticoid is corticosterone (hereby referred to as Cort), which exert its effects by binding to mineralocorticoid (MR) and glucocorticoid receptors (GR) in target tissues throughout the body (Kuo et al., 2018; Lattin et al., 2012). Once bound, these receptors play an important role in activating or suppressing genes associated with metabolic, immune, and oxidative pathways through binding of glucocorticoid response elements (GREs) upstream (Kuo et al., 2018; Bekhbat et al., 2017). Thus, up- and/or downregulation of corticosteroid receptors may be an adaptive response that modulates or optimizes the efficiency of the adrenocortical response and downstream physiology to environmental challenges (Jimeno and Rubalcaba, 2024; Jimeno and Zimmer, 2022; Zimmer et al., 2022). However, whether Cort has stimulatory or suppressive effects depends on the duration, magnitude, and type of stressor (Sapolsky et al., 2000).

During immediate or sudden threats to homeostasis (such as in a predator attack), the adrenal medulla releases catecholamines (epinephrine and norepinephrine), signaling for the breakdown of glycogen stores in the liver and upregulation of lipolysis in adipocytes, increasing circulating glucose levels and providing immediate energy to cells for escape and survival (Romero and Butler, 2007). Once released by the HPA axis and bound to intracellular receptors, glucocorticoids redirect glucose to target tissues, such as the brain, by internalizing glucose transports and inhibiting glucose uptake in other tissue to maximize function (Romero and Butler, 2007; Braun and Sweazea, 2008). Furthermore, glucocorticoids readjust and replenish energy stores through GR-mediated transcription of enzyme genes along the gluconeogenesis pathway (Kuo et al., 2018). In doing so, glucocorticoids maintain sufficient energy levels while reallocating resources towards physiological or behavioral processes necessary to maximize

survival and fitness (Rivers et al., 2012; Wada and Breuner, 2008). However, under prolonged stressors, such as in deteriorating environmental conditions (*e.g.,* stochastic weather events, low food availability, or light at night), continuous activation of the HPA axis can increase basal Cort, blunt the reactivity HPA axis, or reduce the strength of negative feedback; all of which, can have deleterious, pathological effects on the body. HPA axis dysregulation is associated with the manifestation of metabolic syndromes such as insulin resistance, obesity, or diabetes and behavioral deficits such as in mental health disorders (Herman et al., 2016; Vegiopoulos and Herzig, 2007). In fact, 16 weeks of unpredictable stressors (forced restraint/water maze) increased plasma Cort and fasted glucose levels in Swiss albino mice and led to increased glycated hemoglobin levels (Raghav et al., 2019). Although it has long been thought that glucocorticoids facilitate an organism's ability to cope with stressors by initiating gene transcription and maintaining energy homeostasis, how glucocorticoids and downstream effects vary after recovery from chronic stress is not well understood. Thus, several theoretical models have been proposed to answer fundamental questions regarding stress tolerance, robustness, and resilience and understanding how they interact to maintain function (Davis et al., 2021; Romero et al., 2009; Wada, 2019)

Here, stress resilience was defined as the ability to restore physiological, morphological, or behavioral traits back to pretreatment or baseline levels after a temporary decline or change (Wada, 2019; Wada and Coutts, 2021). To test this, one experimental approach is to sample before, during, and after the exposure to a stressor (*i.e.,* introduce a recovery period). If posttreatment levels of a parameter after recovery differ from that of pretreatment, or if there is no response to recovery, we would conclude that there is a persistent effect of the stressor (*i.e.,* failure to recover) resulting in a lack of stress resilience. For example, one study found that

female mice (*Mus musculus)* had higher baseline Cort levels than control mice after 10 days of persistent psychological stress, but a 10-day recovery period reversed this rise in Cort (West et al., 2022). However, voiding frequency, a behavioral phenotype associated with bladder dysfunction, did not return to values comparable to the control group after the stress regime ended, suggesting a persistent effect from the chronic stressor or that more time is needed to recover (West et al., 2022). Although this study implemented a recovery period and mice showed differences in the capacity to recover both physiologically and behaviorally, stress resilience cannot be determined because pretreatment levels of Cort and voiding frequency were not measured and compared to posttreatment levels. In contrast, another study measured pretreatment levels of a behavioral phenotype (climbing behavior) in fruit flies (*Drosophila melanogaster)* before administering a cold stressor to the treatment group. They found that an acute 12-hour exposure to cold stress significantly decreased climbing behavior in both sexes of Drosophila. Although climbing performance improved after 72-hours of recovery, neither sexes returned to pretreatment levels, indicating a persistent effect of the cold stressor on a behavioral phenotype and a lack of stress resilience (Garcia and Teets, 2019). It is possible that climbing behavior may have returned to pretreatment levels if the recovery period was extended; however, determining the length of time necessary to mitigate physiological costs or behavioral deficits associated with stress has not been discussed thoroughly in the literature, and may vary depending on the level of damaged incurred by the stressor and the organism's repair capacity (Wada, 2019).

To better understand the physiological costs of light exposure and how organisms recover from stress, we exposed zebra finches to high intensity constant light as a means to disrupt their circadian rhythm and examined how their physiological phenotype changed during treatment and

after recovery from the stressor. Specifically, we tested whether zebra finches displayed stress resilience by exposing them to constant light for 23 days and allowing a recovery period of 12 days. We hypothesized that chronic high intensity constant light would lead to dysregulation of the HPA axis, downstream physiology, and body condition, but that recovery would be able to reverse these effects. In particular, we predicted that birds exposed to constant light would 1) have higher levels of baseline Cort and an attenuated Cort response to capture and restraint; 2) have higher baseline blood glucose levels and a blunted glucose stress response; and 3) have higher body mass, but would all return to pretreatment levels after recovery. Lastly, we predicted that birds exposed to constant light would have higher protein expression of GR.

2. Materials and Methods

2.1 Animal Husbandry

Adult female zebra finches (N = 32) were obtained from Rockefeller University, NY and housed at the Avian Research Laboratory 2, Auburn University, Auburn, AL, USA under a 14L:10D photoperiod commonly used in zebra finch studies and a standard in our laboratory. We chose to only include female zebra finches in this study because they have been shown to be more sensitive to stressors. All individuals were housed separately in cages (38.10 cm width × 45.72 cm depth × 45.72 cm height) provided with a white tarp as a background and were allowed to acclimatize to their new cage for at least 2 months. Within their respective housing rooms, birds were able to see and hear each other. While acclimatizing, all birds were treated with Nystatin, an anti-fungal treatment, to eliminate potential underlying infections for three weeks and further allowed to repopulate fungal microbiome for the remainder of the acclimation period. All individuals had *ad libitum* access to seed (Kaytee Supreme (Finch), Chilton, WI), water, and

cuttlefish bone throughout the entire duration of this study. All procedures done in this experiment were approved by the Institution of Animal Care and use Committee at Auburn University (IACUC) (protocol #2020-3805).

2.2 Experimental Design

To maximize sample size (N = 32), this experiment was done in two phases with 16 birds in each phase following the same experimental protocol and timeline. In phase one (n = 16), birds were randomly assigned to two light regimes, constant light (24L:0D; n = 8) located in Room A or control light/dark cycle (14L:10D; n = 8) located in Room B (**Figure 1**). Eleven days prior to the start of treatment, blood samples and body mass were collected from all individuals to serve as a Pretreatment collection timepoint. Treatment began on Day 0 in which birds were exposed to constant light (24L:0D) while the control group remained under a 14L:10D light cycle. We collected blood samples and body mass after 3 and 23 days of exposure to the light treatment (D3 and D23, respectively). After 23 days of treatment, a 12-day recovery period began for the constant light group by returning to the original 14L:10D light cycle. We collected blood samples and body mass on Day 35 to serve as a Posttreatment collection timepoint. Birds were humanely euthanized the next day, Day 36, via overdose of isoflurane vapors. Liver, pectoralis muscle, pancreas, brain, ovaries, and spleen were collected, and flash frozen in liquid nitrogen for future analyses, concluding phase one. After the conclusion of phase one, each room was thoroughly inspected, cleaned, and disinfected to ensure standardization between phases. To account for any room effect, light treatment of each room from phase one were switched for phase two (indicated by blue arrows; **Figure 1**). In phase two (n = 16), birds were randomly assigned to a control light/dark cycle (14:10D; n = 8) now in Room A or a constant light

(24L:0D; n = 8) now in Room B. Phase two followed the same experimental timeline as phase one for a total sample size of 16 birds per treatment.

All room lighting was provided by 17-Watt MaxLite® light-emitting diodes (LED) at a color temperature of 5000K (model #L17T8DE450-CG120-277V), as this has been shown to affect glucocorticoid levels when birds are exposed at a low light intensity (Alaasam et al., 2018) as well as from a supplementary lamp at the same color temperature that reflected on the white background for even distribution of light. We measured light intensity (lux) at perch level (middle of the cage) in triplicate at pretreatment, D23, and D35 during both phases of the experiment using a Digi-Sense light meter (±3% of reading). Light measurements for their respective rooms were then averaged. The light level was 172.84 lux (±18.02 SD) in Room A, while it was 165.93 lux (±16.79 SD) in room B throughout the entirety of the experiment. Standard personal and protective equipment (shoe covers, disposable gowns, gloves, and masks) was worn during all sampling procedures. All blood samples were taken via the brachial vein using a 26-gauge needle and a sterile bleeding technique in which the feathers were wiped with 70% ethanol, allowed to air dry for 15 seconds without touching or blowing on the area, and repeated a second time after 15 seconds had passed. We followed this collection method to prevent contaminating blood samples drawn for a bacterial killing assay (Choi et al., in prep). All baseline blood samples were taken within 3 min of entering the room (Romero and Reed, 2005) in heparinized microhematocrit tubes and immediately placed in a 4°C refrigerator. Individuals were then restrained in opaque brown paper bags for 30 minutes as a standardized inducer of the adrenocortical response (Wada et al., 2007). Afterwards, a stress-induced blood sample was taken and placed in a 4°C refrigerator. Blood samples were centrifuged at 14,800 x *g* for 10 minutes within 2 hours of collection. Plasma and red blood cells were separated and collected in

0.5mL Safe-Lock Eppendorf tubes. Red blood cells were immediately flash frozen in liquid nitrogen and plasma was stored at 4°C until all samples had been processed. Following sample processing, plasma and red blood cells were transported to the lab and stored at -80°C. All sampling occurred between 0800-hours and 1000-hours.

2.3 Glucose Point-of-Care (POC) Device Validation

Point-of-Care (POC) devices are a promising alternative for quantifying blood metabolites cheaply and efficiently using a small drop of whole blood (<1.5 µL) (Beattie et al., 2022; Morales et al., 2020). We validated the use of the POC device in our study by comparing the coefficient of determination (R^2) across multiple POC devices (ReliOn™ Prime Glucose Monitoring System, Precision Xtra® Ketone and Glucose Monitoring System, and Contour® Next Blood Glucose Monitoring System) to a lab-based enzyme-linked immunosorbent assay (EIA) Cayman Chemicals Glucose assay kit (Cat #10009582)

Male and female zebra finches (N = 15), which were not part of this study, were randomized into various timepoints between 0-60 minutes post-room disturbance to create a range of glucose values. We collected two blood samples per individual (~140 uL total) via the brachial vein using a 26-guage needle. A drop of blood from both blood samples was used to quantify blood glucose levels in duplicate using all three POC devices for a total of 30 data points. The rest of the blood was spun down, plasma samples were prepped at 1:25 dilution, and glucose levels were quantified using Cayman Chemicals Glucose assay kit (Cat #10009582) following manufacture instructions.

The R^2 values from the linear regression between POC devices and lab-based EIA were 0.48, 0.36, and 0.38, respectively (**Figure S1**). From the regression results, we selected the ReliOn POC device for the actual study.

2.4 Hormone and Metabolite Measures

Plasma Cort levels were measured with Enzo Life Sciences Corticosterone ELISA kits (Cat #ADI-900-097). Baseline (within 3 min of disturbance) and stress-induced (after 30 min in an opaque brown paper bag) plasma samples were prepared at a 1:20 dilution with 2.5% steroid displacement buffer and ran in duplicate (Rubin et al., 2021). All samples across multiple collection timepoints (pretreatment, D23, and posttreatment) for each unique individual were run on the same plate and the positions of samples within the plate were randomized. Due to blood volume limitations, we did not measure Cort on D3 of light exposure. Intraplate and interplate coefficients of variation were 2.4% and 11.56%, respectively. Stress reactivity, or the absolute change in Cort, was calculated by subtracting the stress-induced Cort and baseline level per individual at each collection timepoint.

Before centrifugation, baseline and stress-induced whole blood samples collected from each individual were used to quantify blood glucose levels in duplicate using the ReliOn™ POC glucose monitor (Walmart, AR). If blood glucose levels were deemed "too high" by the POC device, a ceiling value of 600 mg/dL was assigned. Out of all blood glucose readings, only 5 replicates of stress-induced blood samples exceeded the meter's capacity and were replaced with the ceiling value. Specifically, only two individuals had 600 mg/dL assigned as their average stress-induced glucose level throughout the experiment. The glucose stress response, or the

absolute change in glucose, was calculated by subtracting the stress-induced blood glucose and baseline level per individual at each sampling timepoint.

2.5 Western Blot

Western blots were conducted on liver tissue collected at death, 13 days after the last exposure period to constant light. We followed methods described in (Parry et al., 2021) with slight modifications. Briefly, approximately 50-100 mg of raw liver tissue was homogenized in a lysis buffer (5 mM Tris HCL, 5 mM EDTA) with a protease inhibitor cocktail (VWR Cat #97063-970) consisting of AEBSF, aprotinin, E-64, bestatin, and leupeptin. Samples were centrifuged at 1500 x *g* for 10 minutes at 4°C and the homogenate was collected. Total protein concentration of the homogenate was obtained against a linear standard curve via Bradford assay (VWR Cat# 97065-020). Homogenates were standardized for western blotting by adding equal parts sample homogenate with 2x Laemmli buffer and raised to a total volume of 200 uL for a final protein concentration of 1.5 µg/µL across all samples. Proteins were separated by polyacrylamide gel electrophoresis using 4-15% Criterion TGX precast gels for ~1 hour at 200 V (Bio-Rad, Hercules, CA). After gel electrophoresis, proteins were transferred to a polyvinylidene difluoride (PVDF) membrane using the wet sandwich method and ran at 200 mA in cold transfer buffer for 2 hours via Bio-Rad Transfer box (Bio-Rad, Hercules, CA). The membrane's non-specific sites were blocked for 2 hours at room temperature while rocking in 5% nonfat milk containing tris-buffered saline with tween (TSB-T). After 3 washes of TBS-T, the membrane was rocked and incubated in a custom polyclonal anti-glucocorticoid receptor primary antibody (LifeTein, raised in rabbits against a portion of the zebra finch GR: C-KVMDSKELLNPLDQDETRK) prepared at a 1:500 concentration with 5% Bovine Serum

Albumin with tween overnight in a 4°C fridge. Membranes were washed 3 more times with TBS-T then rocked and incubated with an anti-rabbit horseradish peroxidase secondary antibody (Cell Signaling Cat# 7074) at a 1:2000 concentration at room temperature for 1 hour. Protein bands were visualized under UV chemiluminescence using ECL Prime (VWR Cat# 89238-012) and images were captured using ImageQuant LAS 4000. Images were all analyzed using Bio-Rad Image Lab (Bio-Rad, Hercules, CA). Ponceau staining was used as a normalizing and transfer control. Western blot images showed two bands between 70 and 100 kDa, corresponding to the two isoforms of zebra finch GR at ~84 kDa and ~88 kDa. We also ran a protein gel of zebra finch brain lysate, stained it with Coomassie blue, excised a portion of the gel in the region where bands were seen (~70-100 kDa), and sent it to the LSU Health Science Center Proteomics Core Facility for analysis via liquid chromatography mass spectrometry. This gel region contained a protein that corresponded to zebra finch GR.

2.6 Statistical Analysis

All statistical analyses were performed using R (Version 4.3.1 "Beagle Scouts") using packages "lme4", "lmerTest", "emmeans", "car", and "nlme"(Bates et al., 2015; Kuznetsova et al., 2017) All plots were generated using "ggplot2". Statistical significance was determined using an alpha value of ($P \leq 0.05$). To test hypotheses related to the duration and effect of experimental treatment on our response variables (body mass, baseline Cort, absolute change in Cort, baseline glucose, absolute change in glucose), global linear mixed effects models were generated with Treatment (two level factor) and Timepoint (four level factor) as fixed effects, an interaction term of Treatment and Timepoint (Treatment*Timepoint), and body mass as a continuous covariate for Cort and glucose response variables. To account for repeated measures (non-

independence) and the hierarchal nature of the experimental design, we used a random nested structure of Bird.ID/Room/Phase in all global and final models. Non-significant ($P > 0.15$) continuous covariates were removed from all final models. Assumptions of linear models (linearity and homoscedasticity) were tested using histograms and residual plots. Grubb's test was used to identify any significant outliers (± 2 standard deviations from the mean; GraphPad) and were removed from the final analysis. Post-hoc tests followed after finding statistically significant or nearly significant interaction terms ($P \leq 0.15$*)* utilizing the "emmeans" package with Tukey's post-hoc correction method for pairwise comparisons of timepoints within treatment groups to control a type I statistical error. Furthermore, comparisons were made between treatment groups at each separate timepoint using the same statistical package.

For the POC device validation, we ran three separate linear regression models with the glucose values obtained from each of the three POC devices compared to lab-based EIA. The R^2 value obtained from each model was used to determine the correlation between the POC device and lab-based EIA, and the ReliOn POC device was used to determine glucose levels for the actual experiment (supplementary materials).

For relative protein abundance of GR, we log-transformed the raw data in order to meet model assumptions to investigate differences between treatment groups. To investigate whether GR could explain variation in Cort responses, we ran two linear regressions between log transformed absolute change in Cort (stress reactivity) and absolute change in glucose (glucose stress response) as the response variable and relative abundance of GR as a continuous covariate.

2.7 Body Mass

To investigate the effect of constant light on body mass throughout the experiment, we ran a linear mixed effects model (LMM). We then ran a type III ANOVA using the "car" package to determine model significance. Tukey's Post-hoc tests followed using the "emmeans" package to make pairwise comparisons between timepoints within treatment groups and between treatment groups within separate timepoints. The final model included Treatment and Timepoint as fixed effects, an interaction term of Treatment:Timepoint, and a random nested structure of Bird.ID/Room/Phase. No values were excluded from analysis

2.8 Cort

To investigate the effect of constant light on baseline Cort (within 3 min of disturbance) and stress reactivity (stress-induced Cort subtracted from baseline value) throughout the experiment, we ran a LMM. In the global model, we initially included body mass as a fixed covariate, but it was later removed as it was not a significant covariate ($P > 0.15$). We then ran a type III ANOVA to determine model significance. The final model chosen was the simpler model which excluded body mass and included Treatment and Timepoint as fixed effects, an interaction term of Treatment*Timepoint, and random nested structure of Bird.ID/Room/Phase. No values were excluded from analysis.

2.9 Glucose

To investigate the effect of constant light on baseline glucose levels (within 3 min of disturbance) and the glucose stress response (stress-induced glucose level subtracted from baseline value) throughout the experiment, we ran a LMM. We included body mass as a fixed

covariate in the global model, however, was removed from the final model as it was not a significant covariate ($P > 0.15$). We ran a type III ANOVA to determine model significance. Tukey's Post-hoc tests followed using the "emmeans" package to make pairwise comparisons between timepoints within treatment groups and between treatment groups within separate timepoints. Out of all baseline glucose levels, one statistical outlier was excluded from analysis (value of 449 mg/dL), resulting in one glucose stress response measure also excluded from analysis as there was no baseline value to subtract from the stress-induced value. Removal of these values were negligible and did not change the main findings of the manuscript (supplementary materials). The final model chosen was the simpler model which excluded body mass and included Treatment and Timepoint as fixed effects, an interaction term of Treatment*Timepoint, and random nested structure of Bird.ID/Room/Phase.

2.10 Glucocorticoid Receptors (GR) and Relationship with Stress Reactivity and the Glucose Stress Response

To investigate the effect of constant light on the relative protein expression of GR, we ran a LMM with Treatment as a fixed effect and a random intercept of gel ID on log transformed data. To investigate the relationship between GR and stress reactivity, we ran a LMM between log transformed protein expression of GR and the absolute change in Cort with Timepoint as a fixed factor, separated by treatment groups, and a random nested structure of Bird.ID/Room/Phase. Furthermore, we ran this model with the glucose stress response as the response variable. One statistical outlier for GR (4.91 arbitrary units) was removed from the control group via Grubb's test (Graphpad). Removal of this outlier did not affect the main result

(supplementary information). Five samples (three control and two treatment) were excluded from the final analysis due to lack of clear binding.

3. Results

3.1 Body mass

We detected a significant interaction between Treatment and Timepoint on body mass such that the effect of constant light depended on the length of the exposure period ($F_{3,90}$ = 10.05, $P < 0.0001$). Within the light group, post-hoc analysis revealed that while body mass did not change after 3 days of treatment ($P = 0.21$), by the time birds were exposed to constant light for 23 days, body mass was significantly higher compared to pretreatment body mass (β = 1.03; 0.56, 1.5 ± 95% CI; $t = 5.715$; $P < 0.0001$; **Figure 2**). Furthermore, after cessation of the light treatment, we found strong evidence that individuals in the light group decreased body mass, (β = -1.28; -1.8, -0.81 ± 95% CI; $t = -7.095$; $P < 0.0001$; **Figure 2**) when comparing D23 and posttreatment timepoints. In light-exposed birds, there were no differences between pretreatment and posttreatment body mass ($P = 0.51$). We found no statistically significant differences in body mass between both groups at the pretreatment, D3 or D23 timepoints ($P \geq 0.14$); however, there was weak evidence showing that the light group had lower body mass when compared to controls at the posttreatment timepoint (β = -0.74; -1.5, 0.04 ± 95% CI; $t = -1.908$; $P = 0.0632$; **Figure 3**).

3.2 Cort

We did not detect a Treatment ($F_{3,90}$ = 0.0003, $P = 0.99$), Timepoint ($F_{2,58}$ = 0.30, P = 0.74), or Treatment:Timepoint ($F_{2,58}$ = 0.33, $P = 0.72$) effect on baseline Cort during the length

of the experiment (**Figure 3**). Further, we did not detect such effects on the absolute change in Cort (**Figure 4**).

3.3 Glucose

We detected a significant interaction between Treatment and Timepoint ($F_{3,87} = 2.69$; $P < 0.0511$) on baseline blood glucose levels. Within the light group, we found no statistically significant differences in baseline blood glucose levels after 3 or 23 days of exposure when compared to pretreatment levels ($P \geq 0.26$). However, after cessation of the light treatment, there was a statistically significant increase in baseline blood glucose levels when comparing D23 and posttreatment timepoints in the light group (β = 37.11; 6.52, 67.71 ± 95% CI; $t = 3.177$; $P = 0.0109$**; Figure 5**), with no differences between pretreatment and posttreatment baseline glucose levels ($P = 0.5055$). We detected weak evidence of the light group having lower baseline blood glucose levels when compared to controls after 3 days of exposure (β = -24.96; -53.9, 4.02 ± 95% CI; $t = -1.711$; $P = 0.0905$), but this difference was larger and became statistically significant after 23 days of exposure (β = -40.08; -69.1, -11.11 ± 95% CI; $t = -2.748$; $P = 0.0072$; **Figure 5**). We detected a nearly significant Treatment:Timepoint interaction ($F_{3,86} = 2.08$; $P = 0.1091$) on the absolute change in blood glucose levels, thus we continued the analysis. Post-hoc analysis revealed that the light group had no statistically significant differences in absolute change in glucose throughout exposure to constant light ($P \geq 0.0995$). However, there was moderate evidence showing that the light group had a lower absolute change in glucose after 23 days of exposure when compared to controls (β = -64.55; -120.4, -8.69 ± 95% CI; $t = -2.293$; $P = 0.0240$; **Figure 6).** Interestingly, there was no statistically significant increase in absolute change in glucose when comparing D23 and posttreatment timepoint ($P = 0.8586$)

3.4 Glucocorticoid receptors (GR) and relationship with stress reactivity and the glucose stress response

We did not detect a significant main effect of treatment on relative protein expression of GR ($F_{1,22} = 0.14$; $P = 0.72$; **Figure 7**). Additionally, we did not find a significant relationship between GR and stress reactivity separated by treatment groups (Control: $F_{1,10} = 0.04$; $P = 0.91$; Treatment: $F_{1,12} = 0.12$; $P = 0.73$; supplementary materials). Yet, we found a positive relationship between GR and the glucose stress response within the light group ($F_{1,12} = 9.92$; marginal $R^2 = 0.24$; conditional $R^2 = 0.30$; $P = 0.008$**; Figure 8**), but no relationship within controls ($F_{1,11} = 0.78$; $P = 0.40$).

4. Discussion

In this study, we sought to quantify stress resilience in the diurnal zebra finch by exposing them to high intensity constant light and allowing them to recover from this stressor. Contrary to our predictions, we did not detect any changes in baseline Cort or the reactivity of the HPA axis throughout the experiment but found that baseline glucose levels in light-exposed birds were lower than control birds. Furthermore, light-exposed birds had a blunted glucose stress response compared to controls. We found that 23 days of constant light exposure was necessary to increase body mass, while 3 days of exposure was not sufficient. However, a 12-day recovery period ameliorated the effects of constant light on both body mass and baseline glucose levels, indicating stress resilience in those traits, but the glucose stress response remained blunted, indicating a persistent effect. We found no differences between groups in relative protein expression of GR in the liver and there was no relationship between GR and stress reactivity. Yet, we found a significant positive relationship between GR and the glucose stress response, but

only within the treatment group. Our findings indicate that diurnal zebra finches were able to maintain adrenocortical responses under constant light. Furthermore, we show that physiological and morphological traits differed in their ability to recover from chronic stress. However, we were unable to determine whether this stress resilience was driven by a trade-off in recovery between traits. There was a significant positive relationship between GR and the glucose stress response in the light group, suggesting that GRs may be a mechanism critical in maintaining sufficient glucose responses under stress. Future studies should characterize whether individuals incur a trade-off when given the opportunity to recover from stress. Furthermore, exploration on the mechanisms that confer stress resilience should be considered, especially in the face of rapid environmental change.

Our finding on an increase in body mass under constant light is consistent with another study in zebra finches (Malik et al., 2020), in which two weeks or longer to light at night is necessary to induce changes. It is possible that this increase in body mass is due to higher food consumption in response to a constant light environment. However, increased feeding rates in great tit nestlings exposed to ecologically relevant levels of light did not lead to an increase in body mass, suggesting patterns in body mass differs between species, light regimes, and life history (Titulaer et al., 2012; Zuo et al., 2023). Alternatively, the rise in body mass may stem from a shift in the timing of food intake, rather than from increased food consumption (Fonken et al., 2010). Indeed, zebra finches under dim light at night showed no differences in food consumption, however stark differences in their feeding pattern during the inactive phase, resulting in excessive weight gain and lipid accumulation in the liver (Batra et al., 2019). However, we found that the effect of constant light on body mass was ephemeral, as the addition of a 12-day recovery period reversed the rise in body mass and returned finches to pretreatment

levels, indicating stress resilience in the trait. Other studies have reported varying durations of recovery periods to reverse the effects of chronic stress on morphological and physiological traits (Gormally et al., 2019; Beattie et al., 2022). For example, in house sparrows (*Passer domesticus*) subjected to repeated cycles of stressors (cage rolling, cage tapping, etc.), individuals declined in body mass, and did not return to pretreatment levels even 2 weeks after cessation of treatment, indicating a persistent effect of a chronic stressor (Beattie et al., 2022). These studies show that the recovery of some traits may be prioritized over others (*i.e.* trade-offs) or that the length of recovery required to illicit beneficial effects differs across traits. Our results, together with published data, suggests variation in the capacity of morphological or physiological traits in avian species to recover from different types of chronic stress.

To understand how physiological systems respond to and recover from constant light, we measured the adrenocortical response and blood glucose levels. Interestingly, we found no differences in either baseline Cort or the reactivity of the HPA axis between treatment groups at any point during the experiment. This could be due to several reasons. First, it is possible that our light treatment was not strong enough to disrupt the birds' circadian rhythm. This is unlikely however, as the light level in our study was well above 150 lux and Prabhat et al. 2020 showed that constant light at 150 lux can disrupt central clock gene expression (*Bmal1, Per2, reverb β)* in the hypothalamus of zebra finches that were reared under constant light as hatchlings (Prabhat et al., 2020). Although we did not measure Cort or clock gene expression over 24-hours, such data would provide more information on whether circadian rhythmicity was maintained or disrupted in light-exposed birds. Second, it is possible that constant light phase delayed, or phase advanced the circadian peak in Cort in the constant light group; thus, circulating levels of Cort at the time of sampling (0800-hours and 1000-hours) may not have been representative between groups.

However, Jha et al. (2021) found that F1 zebra finches under constant light showed no differences in baseline Cort 2 hours before and after lights were turned on, and 4 hours before and after lights turned off, suggesting that constant light may not affect the peak or nadir of Cort in zebra finches (Jha et al., 2021; but see Mishra et al., 2019). Our birds were measured 1 to 2 hours after the lights had turned on; thus, it is reasonable to assume that circulating levels of baseline Cort were representative between groups at the time of sampling. Alternatively, it is possible that female zebra finches may be more resilient to changes in HPA axis function under stress as sex-specific differences in managing stress responses have been reported in a variety of avian species (Edwards et al., 2013; Khan and Robert, 2013; Ninnes et al., 2010; Tetel et al., 2022). Indeed, Jha et al. (2021) further found that there were no changes in baseline Cort in female adult zebra finches under constant light but found that males tended to have lower levels of baseline Cort (Jha et al., 2021). These data suggest that there may be sex-specific differences in how male and female zebra finches maintain HPA axis function under circadian disruption. In our study of female zebra finches, both acute and chronic exposure (at least 23 days) to constant light did not affect baseline levels of Cort, nor stress reactivity. Based on this finding, female zebra finches were able to maintain neuroendocrine responses to acute challenges (*i.e.,* capture and restraint) under a perturbed light environment.

Circulating glucose levels have been widely used as a physiological indicator of wildlife health as they can signify overall condition, but can vary both seasonally and based on environmental quality (McGraw et al., 2020; Remage-Healey and Romero, 2000; Scanes and Braun, 2013). Furthermore, variation in both the baseline and glucose stress response can reflect differences in how glucose is mobilized in response to acute stressors or changes in the environment (Ryan et al., 2023; Schradin et al., 2015). Contrary to our predictions, we found that

baseline levels of glucose decreased in light-exposed birds compared to control birds over the course of the experiment. A similar finding was found in western mosquitofish (*Gambusia affinis)* in which constant light decreased glucose levels in the brain (Miner et al., 2021). Differences in behavior or activity patterns may explain why glucose levels decreased. Although those traits were not measured in our study, light at night has been shown to induce sleep loss and result in higher activity and foraging in many avian species (Lebbin et al., 2007; Raap et al., 2015). This increased energetic demand may result in higher glucose utilization over time and could explain why we detected low circulating levels of baseline glucose in our light-exposed birds. However, this effect was transient, as once the stressor ended, baseline glucose levels in light-exposed birds increased and returned to pretreatment levels, indicating stress resilience. In contrast, Beattie et al. (2022) found that baseline glucose levels in house sparrows (under a fed state) did not return to pretreatment levels and remained elevated 2 weeks after the stress regime had ended (Beattie et al., 2022). These data indicate species-specific differences in how glucose levels may respond to chronic stress and recovery, but also how various stressor types may elicit different glucose patterns. Long periods of hyperglycemia or hypoglycemia could result in cellular damage through glycated hemoglobin or reductions in cellular function because of the lack of sufficient energy provided to cells; thus, further research is warranted on how glucose homeostasis is affected in response to different stressors, and the potential physiological consequences. We also found that the glucose stress response was suppressed after 23 days of high intensity constant light and remained blunted after 12 days of recovery, indicating a persistent effect. It is possible that our zebra finches had a depletion of energy stores due to altered activity levels stemming from constant light (Zuo et al., 2023) and could not mount a strong glucose response to an acute challenge; however, all birds had access to *ad libitum* food.

Nevertheless, a blunted glucose stress response could have implications on survival as a weak response would indicate a lower ability to mobilize glucose to supply energy in face of immediate threats in the environment (Marik and Bellomo, 2013).

In the liver, GR activate genes associated with gluconeogenic pathways through Cort signaling, resulting in stress-induced hyperglycemia that promotes greater cellular glucose uptake and anti-apoptotic pathways to maximize function and aid in survival during and after environmental challenges (Kuo et al., 2018; Marik and Bellomo, 2013). GR are also responsible for regulating the adrenocortical response, particularly by facilitating negative feedback in the brain to terminate elevated levels of Cort (Sapolsky et al., 1984). Thus, the presence of increased GR can augment the organismal and cellular stress response, but may be tissue specific in their effect (Bekhbat et al., 2017; Jimeno and Zimmer, 2022; Lattin and Romero, 2014). In our study, we did not detect differences between experimental groups in relative protein expression of GR in the liver. It is possible we were unable to capture differences due to the timepoint of collection, as we measured GR 13 days after the stressor had ended. While GR are essential in activating molecular pathways, it is possible that chronic stress leads to glucocorticoid receptor resistance, meaning that intracellular receptors have reduced efficiency in activating or repressing genes associated with multiple cellular pathways (immune or metabolic) in response to hormone signaling across tissue (Cohen et al., 2012; Marques et al., 2009). In this context, higher presence of GR would not augment physiological responses. This could explain why the glucose stress response remained blunted in response to capture and restraint after recovery from constant light. Yet, we found an interesting, positive relationship between GR and the glucose stress response in the constant light group. Even though treatment birds had a blunted glucose stress response, they were able to mount adrenocortical responses comparable to controls. This

suggests that GR in the liver is coupled with Cort signaling, such that downstream responses (*i.e.,* the glucose stress response) remains sufficient under stressors such as constant light. This is likely as liver GR proteins are essential transcription factors that regulate glucose homeostasis (Kuo et al., 2018) . However, we are unable to determine whether GR proteins detected in this study are functional. To our knowledge, this is the first study to measure protein levels of GR in the liver of an avian model under constant light. Future studies should evaluate GR as a mechanism modulating HPA axis and downstream physiology across multiple tissues. Glucocorticoid receptors may augment or suppress cellular and molecular responses to stressors, particularly circadian disruption induced by light at night, to maintain metabolic, immune, and organismal function, and a potential mechanism conferring stress resilience (Jimeno & Rubalcaba, 2024).

5. Conclusions

Here, we show varying degrees of stress resilience under high intensity constant light in the zebra finch depending on the morphological or physiological trait of interest. While some metrics return to pretreatment levels 12 days after cessation of constant light, such as body mass and circulating levels of baseline glucose, the glucose stress response remained blunted after the same period. These results suggest that 1.) traits responded differently when given the opportunity to recover from chronic high intensity light 2.) the effects of chronic stressors can persist after stress exposure ends. We found no differences in baseline Cort, stress reactivity, or GR abundance, indicating that zebra finches can maintain HPA axis function under constant light. We found a positive relationship between liver GR and the glucose stress response in the treatment birds only, indicating that GR is essential is modulating glucose levels under constant

light. Future work should characterize how individuals display stress resilience to various environmental perturbations, including light-induced circadian disruption, particularly by probing various aspects of the HPA axis and downstream physiological, behavioral, and morphological traits.

6. Funding Statement

This study was supported by two National Science Foundation (NSF) (IOS-1553657 and IOS-2015802) grants and an Alabama Agriculture Experiment Station grant awarded to H.W. and a National Institutes of Health (NIH) T-32 Graduate Research Training Initiative for Student Enhancement (G-RISE) (Grant number: 5T32GM141739) Fellowship awarded to K.P.

7. IACUC Statement

All procedures done in this experiment were approved by the Institution of Animal Care and use Committee at Auburn University (IACUC) (protocol #2020-3805).

8. Author Statement

K.P. - Conceptualization, Methodology, Investigation, Validation, Writing- Original draft, Review & Editing, Data Curation, Formal Analysis

M.C. - Conceptualization, Methodology, Investigation, Validation, Review & Editing, Data Curation

K.Y. – Methodology, Review & Editing, Formal Analysis

C.R.L – Methodology, Validation, Review & Editing, Formal Analysis

H.W. - Conceptualization, Methodology, Investigation, Review & Editing, Supervision

9. Acknowledgements

We thank Jodi Dawkins, Maren Augustin, and Chloe Moore for their assistance in animal husbandry. We would also like to thank Alex Hoffman, Cara Brittain, Tori Coutts, Wonil Choi, James Utt, Hannah Butterfield, Sydney Wilcoxson, Santana Rojas, Ayden King, Jack Bazzell, Anna Darke, Catherine Florence, and Olivia Riemer for their assistance in blood collection. We thank Dr. Wendy Hood for their feedback on the western blot analysis. Lastly, we thank the Wada, Hood, and Hill labs as well as Dr's. Bruce Smith and Dr. Melody Russell for their valuable input and feedback on an early draft of the manuscript.

References

Alaasam, V.J., Duncan, R., Casagrande, S., Davies, S., Sidher, A., Seymoure, B., Shen, Y., Zhang, Y., Ouyang, J.Q., 2018. Light at night disrupts nocturnal rest and elevates glucocorticoids at cool color temperatures. J. Exp. Zool. Part A Ecol. Integr. Physiol. 329, 465–472. https://doi.org/10.1002/jez.2168

Arble, D.M., Ramsey, K.M., Bass, J., Turek, F.W., 2010. Circadian disruption and metabolic disease: Findings from animal models. Best Pract. Res. Clin. Endocrinol. Metab. 24, 785–800. https://doi.org/10.1016/j.beem.2010.08.003

Bates, D., Mächler, M., Bolker, B.M., Walker, S.C., 2015. Fitting linear mixed-effects models using lme4. J. Stat. Softw. 67. https://doi.org/10.18637/jss.v067.i01

Batra, T., Malik, I., Kumar, V., 2019. Illuminated night alters behaviour and negatively affects physiology and metabolism in diurnal zebra finches. Environ. Pollut. 254, 112916. https://doi.org/10.1016/j.envpol.2019.07.084

Beattie, U.K., Ysrael, M.C., Lok, S.E., Romero, L.M., 2022. The Effect of a Combined Fast and Chronic Stress on Body Mass, Blood Metabolites, Corticosterone, and Behavior in House Sparrows (Passer domesticus). Yale J. Biol. Med. 95, 19–31.

Bedrosian, T.A., Fonken, L.K., Nelson, R.J., 2016. Endocrine Effects of Circadian Disruption. Annu. Rev. Physiol. 78, 109–131. https://doi.org/10.1146/annurev-physiol-021115-105102

Bekhbat, M., Rowson, S.A., Neigh, G.N., 2017. Checks and balances: The glucocorticoid receptor and NFκB in good times and bad. Front. Neuroendocrinol. 46, 15–31. https://doi.org/10.1016/j.yfrne.2017.05.001

Braun, E.J., Sweazea, K.L., 2008. Glucose regulation in birds. Comp. Biochem. Physiol. - B Biochem. Mol. Biol. 151, 1–9. https://doi.org/10.1016/j.cbpb.2008.05.007

Cohen, S., Janicki-Deverts, D., Doyle, W.J., Miller, G.E., Frank, E., Rabin, B.S., Turner, R.B., 2012. Chronic stress, glucocorticoid receptor resistance, inflammation, and disease risk. Proc. Natl. Acad. Sci. U. S. A. 109, 5995–5999. https://doi.org/10.1073/pnas.1118355109

Davis, J.E., Kolozsvary, M.B., Pajerowska-Mukhtar, K.M., Zhang, B., 2021. Toward a Universal Theoretical Framework to Understand Robustness and Resilience: From Cells to Systems. Front. Ecol. Evol. 8, 1–9. https://doi.org/10.3389/fevo.2020.579098

Edwards, D.B., Chin, E.H., Burness, G., Gilchrist, H.G., Schulte-Hostedde, A.I., 2013. Linking sex differences in corticosterone with individual reproductive behaviour and hatch success in two species of uniparental shorebirds. Comp. Biochem. Physiol. - A Mol. Integr. Physiol. 166, 169–176. https://doi.org/10.1016/j.cbpa.2013.05.024

Falchi, F., Cinzano, P., Duriscoe, D., Kyba, C.C.M., Elvidge, C.D., Baugh, K., Portnov, B.A., Rybnikova, N.A., Furgoni, R., 2016. The new world atlas of artificial night sky brightness. Sci. Adv. 2, 1–26. https://doi.org/10.1126/sciadv.1600377

Faught, E., Vijayan, M.M., 2022. The Mineralocorticoid Receptor Functions as a Key Glucose Regulator in the Skeletal Muscle of Zebrafish. Endocrinol. (United States) 163, 1–14. https://doi.org/10.1210/endocr/bqac149

Fonken, L.K., Workman, J.L., Walton, J.C., Weil, Z.M., Morris, J.S., Haim, A., Nelson, R.J., 2010. Light at night increases body mass by shifting the time of food intake. Proc. Natl. Acad. Sci. U. S. A. 107, 18664–18669. https://doi.org/10.1073/pnas.1008734107

Garcia, M.J., Teets, N.M., 2019. Cold stress results in sustained locomotor and behavioral deficits in Drosophila melanogaster. J. Exp. Zool. Part A Ecol. Integr. Physiol. 331, 192–200. https://doi.org/10.1002/jez.2253

Gastón, M.S., Pereyra, L.C., Vaira, M., 2019. Artificial light at night and captivity induces differential effects on leukocyte profile, body condition, and erythrocyte size of a diurnal toad. J. Exp. Zool. Part A Ecol. Integr. Physiol. 331, 93–102. https://doi.org/10.1002/jez.2240

Gnocchi, D., Bruscalupi, G., 2017. Circadian rhythms and hormonal homeostasis: Pathophysiological implications. Biology (Basel). 6, 1–20. https://doi.org/10.3390/biology6010010

Gormally, B.M.G., Estrada, R., Yin, H., Romero, L.M., 2019. Recovery from repeated stressors: Physiology and behavior are affected on different timescales in house sparrows. Gen. Comp. Endocrinol. 282. https://doi.org/10.1016/j.ygcen.2019.113225

Grunst, M.L., Raap, T., Grunst, A.S., Pinxten, R., Parenteau, C., Angelier, F., Eens, M., 2020. Early-life exposure to artificial light at night elevates physiological stress in free-living songbirds. Environ. Pollut. 259. https://doi.org/10.1016/j.envpol.2019.113895

Herman, J.P., Mcklveen, J.M., Ghosal, S., Kopp, B., Wulsin, A., Makinson, R., Scheimann, J., Myers, B., 2016. Response. Compr. Physiol. 6, 603–621. https://doi.org/10.1002/cphy.c150015.Regulation

Jha, N.A., Taufique, S.K.T., Kumar, V., 2021. Born without night: The consequence of the no-night environment on reproductive performance in diurnal zebra finches. J. Exp. Biol. https://doi.org/10.1242/jeb.242996

Jimeno, B., Rubalcaba, J.G., 2024. Modelling the role of glucocorticoid receptor as mediator of endocrine responses to environmental challenge. Philos. Trans. R. Soc. B Biol. Sci. 379. https://doi.org/10.1098/rstb.2022.0501

Jimeno, B., Zimmer, C., 2022. Glucocorticoid receptor expression as an integrative measure to assess glucocorticoid plasticity and efficiency in evolutionary endocrinology: A perspective. Horm. Behav. 145, 105240. https://doi.org/10.1016/j.yhbeh.2022.105240

Khan, N., Robert, K., 2013. Does sex matter? Differential responses to corticosterone administration in the zebra finch. Zoology 116, 293–299. https://doi.org/10.1016/j.zool.2013.08.001

Kuo, Taiyi; McQueen, Allison; Chen, Tzu-Chieh; Wang, J.-C., 2018. Regulation of Glucose Homeostasis by Glucocorticoids Taiyi 99–126. https://doi.org/10.1007/978-1-4939-2895-8

Kuznetsova, A., Brockhoff, P.B., Christensen, R.H.B., 2017. lmerTest Package: Tests in Linear Mixed Effects Models. J. Stat. Softw. 82, 1–26. https://doi.org/10.18637/JSS.V082.I13

Lattin, C.R., Romero, L.M., 2014. Chronic stress alters concentrations of corticosterone receptors in a tissue-specific manner in wild house sparrows (Passer domesticus). J. Exp. Biol. 217, 2601–2608. https://doi.org/10.1242/jeb.103788

Lattin, C.R., Waldron-Francis, K., Richardson, J.W., de Bruijn, R., Bauer, C.M., Breuner, C.W., Michael Romero, L., 2012. Pharmacological characterization of intracellular glucocorticoid receptors in nine tissues from house sparrow (Passer domesticus). Gen. Comp. Endocrinol. 179, 214–220. https://doi.org/10.1016/j.ygcen.2012.08.007

Lebbin, D.J., Harvey, M.G., Lenz, T.C., Andersen, M.J., Ellis, J.M., 2007. Nocturnal migrants foraging at night by artificial light. Wilson J. Ornithol. 119, 506–508. https://doi.org/10.1676/06-139.1

Levy, K., Wegrzyn, Y., Efronny, R., Barnea, A., Ayali, A., 2021. Lifelong exposure to artificial light at night impacts stridulation and locomotion activity patterns in the cricket Gryllus bimaculatus. Proc. R. Soc. B Biol. Sci. 288. https://doi.org/10.1098/rspb.2021.1626

Malik, I., Batra, T., Das, S., Kumar, V., 2020. Light at night affects gut microbial community and negatively impacts host physiology in diurnal animals: Evidence from captive zebra finches. Microbiol. Res. 241, 126597. https://doi.org/10.1016/j.micres.2020.126597

Mardones, M.L., Lambert, J., Wiedenmann, J., Davies, T.W., Levy, O., D'Angelo, C., 2023. Artificial light at night (ALAN) disrupts behavioural patterns of reef corals. Mar. Pollut. Bull. 194, 115365. https://doi.org/10.1016/j.marpolbul.2023.115365

Marik, P. E., Bellomo, R. 2013. Stress hyperglycemia: an essential survival response. Critical Care 1–7. https://10.1186/cc12514

Marques, A.H., Silverman, M.N., Sternberg, E.M., 2009. Glucocorticoid dysregulations and their clinical correlates: From receptors to therapeutics. Ann. N. Y. Acad. Sci. 1179, 1–18. https://doi.org/10.1111/j.1749-6632.2009.04987.x

Marelli, S.P., Terova, G., Cozzi, M.C., Lasagna, E., Sarti, F.M., Cavalchini, L.G., 2010. Gene expression of hepatic glucocorticoid receptor NR3C1 and correlation with plasmatic corticosterone in Italian chickens. Anim. Biotechnol. 21, 140–148. https://doi.org/10.1080/10495391003608621

McGraw, K.J., Chou, K., Bridge, A., McGraw, H.C., McGraw, P.R., Simpson, R.K., 2020. Body condition and poxvirus infection predict circulating glucose levels in a colorful songbird that inhabits urban and rural environments. J. Exp. Zool. Part A Ecol. Integr. Physiol. 333, 561–568. https://doi.org/10.1002/jez.2391

Miner, K.A., Huertas, M., Aspbury, A.S., Gabor, C.R., 2021. Artificial Light at Night Alters the Physiology and Behavior of Western Mosquitofish (Gambusia affinis). Front. Ecol. Evol. 9, 1–12. https://doi.org/10.3389/fevo.2021.617063

Mishra, I., Knerr, R.M., Stewart, A.A., Payette, W.I., Richter, M.M., Ashley, N.T., 2019. Light at night disrupts diel patterns of cytokine gene expression and endocrine profiles in zebra finch (Taeniopygia guttata). Sci. Rep. 9, 1–12. https://doi.org/10.1038/s41598-019-51791-9

Morales, A., Frei, B., Leung, C., Titman, R., Whelan, S., Benowitz-Fredericks, Z.M., Elliott, K.H., 2020. Point-of-care blood analyzers measure the nutritional state of eighteen free-living bird species. Comp. Biochem. Physiol. -Part A Mol. Integr. Physiol. 240, 110594. https://doi.org/10.1016/j.cbpa.2019.110594

Ninnes, C.E., Waas, J.R., Ling, N., Nakagawa, S., Banks, J.C., Bell, D.G., Bright, A., Carey, P.W., Chandler, J., Hudson, Q.J., Ingram, J.R., Lyall, K., Morgan, D.K.J., Stevens, M.I., Wallace, J., Möstl, E., 2010. Comparing plasma and faecal measures of steroid hormones in Adelie penguins Pygoscelis adeliae. J. Comp. Physiol. B Biochem. Syst. Environ. Physiol. 180, 83–94. https://doi.org/10.1007/s00360-009-0390-0

Oster, H., Challet, E., Ott, V., Arvat, E., de Kloet, E.R., Dijk, D.J., Lightman, S., Vgontzas, A., Van Cauter, E., 2017. The functional and clinical significance of the 24-hour rhythm of circulating glucocorticoids. Endocr. Rev. 38, 3–45. https://doi.org/10.1210/er.2015-1080

Ouyang, J.Q., Davies, S., Dominoni, D., 2018. Hormonally mediated effects of artificial light at night on behavior and fitness: Linking endocrine mechanisms with function. J. Exp. Biol. 221. https://doi.org/10.1242/jeb.156893

Ouyang, J.Q., De Jong, M., Hau, M., Visser, M.E., Van Grunsven, R.H.A., Spoelstra, K., 2015. Stressful colours: Corticosterone concentrations in a free-living songbird vary with the spectral composition of experimental illumination. Biol. Lett. 11. https://doi.org/10.1098/rsbl.2015.0517

Parry, H.A., Randall, R.B., Hyatt, H.W., Hood, W.R., Kavazis, A.N., 2021. Short and long-term effect of reproduction on mitochondrial dynamics and autophagy in rats. Heliyon 7, e08070. https://doi.org/10.1016/j.heliyon.2021.e08070

Potter, G.D.M., Skene, D.J., Arendt, J., Cade, J.E., Grant, P.J., Hardie, L.J., 2016. Circadian rhythm and sleep disruption: Causes, metabolic consequences, and countermeasures. Endocr. Rev. 37, 584–608. https://doi.org/10.1210/er.2016-1083

Prabhat, A., Malik, I., Jha, N.A., Bhardwaj, S.K., Kumar, V., 2020. Developmental effects of constant light on circadian behaviour and gene expressions in zebra finches: Insights into mechanisms of metabolic adaptation to aperiodic environment in diurnal animals. J. Photochem. Photobiol. B Biol. 211, 111995. https://doi.org/10.1016/j.jphotobiol.2020.111995

Raghav, A., Ahmad, J., Naseem, I., 2019. Chronic unpredictable environmental stress impair biochemical and physiological homeostasis: Role in diabetes mellitus. Diabetes Metab. Syndr. Clin. Res. Rev. 13, 1021–1030. https://doi.org/10.1016/j.dsx.2019.01.020

Rao, R., Androulakis, I.P., 2019. The physiological significance of the circadian dynamics of the HPA axis: Interplay between circadian rhythms, allostasis and stress resilience. Horm. Behav. 110, 77–89. https://doi.org/10.1016/j.yhbeh.2019.02.018

Raap, T., Pinxten, R., Eens, M., 2015. Light pollution disrupts sleep in free-living animals. Sci. Rep. 5, 1–8. https://doi.org/10.1038/srep13557

Remage-Healey, L., Romero, L.M., 2000. Daily and Seasonal Variation in Response to Stress in Captive Starlings (Sturnus Vulgaris): Glucose. Gen. Comp. Endocrinol. 119, 60–68. https://doi.org/10.1006/gcen.2000.7492

Rivers, J.W., Liebl, A.L., Owen, J.C., Martin, L.B., Betts, M.G., 2012. Baseline corticosterone is positively related to juvenile survival in a migrant passerine bird. Funct. Ecol. 26, 1127–1134. https://doi.org/10.1111/j.1365-2435.2012.02025.x

Romero, L.M., Dickens, M.J., Cyr, N.E., 2009. The reactive scope model - A new model integrating homeostasis, allostasis, and stress. Horm. Behav. 55, 375–389. https://doi.org/10.1016/j.yhbeh.2008.12.009

Romero, M.L., Butler, L.K., 2007. Endocrinology of Stress. Int. J. Comp. Psychol. 20. https://doi.org/10.46867/ijcp.2007.20.02.15

Romero, L.M., Reed, J.M., 2005. Collecting baseline corticosterone samples in the field: Is under 3 min good enough? Comp. Biochem. Physiol. - A Mol. Integr. Physiol. 140, 73–79. https://doi.org/10.1016/j.cbpb.2004.11.004

Rubin, A.M., Choi, M.P., Hoffman, A.J., Beyl, H.E., Mendonça, M.T., Wada, H., 2021. Periodic Cooling during Incubation Alters the Adrenocortical Response and Posthatch Growth in Zebra Finches. Physiol. Biochem. Zool. 94, 110–123. https://doi.org/10.1086/713023

Ryan, T.A., Taff, C.C., Zimmer, C., Vitousek, M.N., 2023. Cold temperatures induce priming of the glucose stress response in tree swallows. Comp. Biochem. Physiol. -Part A Mol. Integr. Physiol. 280, 111419. https://doi.org/10.1016/j.cbpa.2023.111419

Sapolsky, R.M., Krey, L.C., McEwen, B.S., 1984. Glucocorticoid-sensitive hippocampal neurons are involved in terminating the adrenocortical stress response. Proc. Natl. Acad. Sci. U. S. A. 81, 6174–6177. https://doi.org/10.1073/pnas.81.19.6174

Sapolsky, R.M., Romero, L.M., Munck, A.U., 2000. How do glucocorticoids influence stress responses? Integrating permissive, suppressive, stimulatory, and preparative actions. Endocr. Rev. 21, 55–89. https://doi.org/10.1210/er.21.1.55

Scanes, C.G., Braun, E., 2013. Avian metabolism: Its control and evolution. Front. Biol. (Beijing). 8, 134–159. https://doi.org/10.1007/s11515-012-1206-2

Schradin, C., Pillay, N., Kondratyeva, A., Yuen, C.H., Schoepf, I., Krackow, S., 2015. Basal blood glucose concentration in freeliving striped mice is influenced by food availability, ambient temperature and social tactic. Biol. Lett. 11. https://doi.org/10.1098/rsbl.2015.0208

Secondi, J., Mondy, N., Gippet, J.M.W., Touzot, M., Gardette, V., Guillard, L., Lengagne, T., 2021. Artificial light at night alters activity, body mass, and corticosterone level in a tropical anuran. Behav. Ecol. 32, 932–940. https://doi.org/10.1093/beheco/arab044

Spencer, R.L., Chun, L.E., Hartsock, M.J., Woodruff, E.R., 2018. Glucocorticoid hormones are both a major circadian signal and major stress signal: How this shared signal contributes to a dynamic relationship between the circadian and stress systems. Front. Neuroendocrinol. 49, 52–71. https://doi.org/10.1016/j.yfrne.2017.12.005

Tetel, V., Tonissen, S., Fraley, G.S., 2022. Sex differences in serum glucocorticoid levels and heterophil:lymphocyte ratios in adult pekin ducks (Anas platyrhynchos domesticus). Gen. Comp. Endocrinol. 317, 113975. https://doi.org/10.1016/j.ygcen.2021.113975

Titulaer, M., Spoelstra, K., Lange, C.Y.M.J.G., Visser, M.E., 2012. Activity Patterns during Food Provisioning Are Affected by Artificial Light in Free Living Great Tits (Parus major) 7, 5–8. https://doi.org/10.1371/journal.pone.0037377

Vegiopoulos, A., Herzig, S., 2007. Glucocorticoids, metabolism and metabolic diseases. Mol. Cell. Endocrinol. 275, 43–61. https://doi.org/10.1016/j.mce.2007.05.015

Wada, H., 2019. Damage-Fitness Model: the missing piece in integrative stress models. Stress 22, 548–562. https://doi.org/10.1080/10253890.2019.1614556

Wada, H., Coutts, V., 2021. Detrimental or beneficial? Untangling the literature on developmental stress studies in birds. J. Exp. Biol. 224. https://doi.org/10.1242/jeb.227363

Wada, H., Breuner, C.W., 2008. Transient elevation of corticosterone alters begging behavior and growth of white-crowned sparrow nestlings. J. Exp. Biol. 211, 1696–1703. https://doi.org/10.1242/jeb.009191

Wada, H., Hahn, T.P., Breuner, C.W., 2007. Development of stress reactivity in white-crowned sparrow nestlings: Total corticosterone response increases with age, while free corticosterone response remains low. Gen. Comp. Endocrinol. 150, 405–413. https://doi.org/10.1016/j.ygcen.2006.10.002

West, E.G., McDermott, C., Chess-Williams, R., Sellers, D.J., 2022. Partial recovery of voiding function in female mice following repeated psychological stress exposure. PLoS One 17, 1–14. https://doi.org/10.1371/journal.pone.0266458

Yadav, A., Kumar, R., Tiwari, J., Vaish, V., Malik, S., Rani, S., 2022. Effect of artificial light at night on sleep and metabolism in weaver birds. Environ. Sci. Pollut. Res. 29, 80422–80435. https://doi.org/10.1007/s11356-022-20875-x

Zimmer, C., Woods, H.A., Martin, L.B., 2022. Information theory in vertebrate stress physiology. Trends Endocrinol. Metab. 33, 8–17. https://doi.org/10.1016/j.tem.2021.10.001

Zuo, L., Ahmad, I.M., Liu, Y., Wang, L., Fang, S., Li, D., 2023. Effects of constant light and dark conditions on the locomotor activity, body mass, and body temperature rhythms of Eurasian Tree Sparrows (Passer montanus). Avian Res. 14, 100126. https://doi.org/10.1016/j.avrs.2023.100126

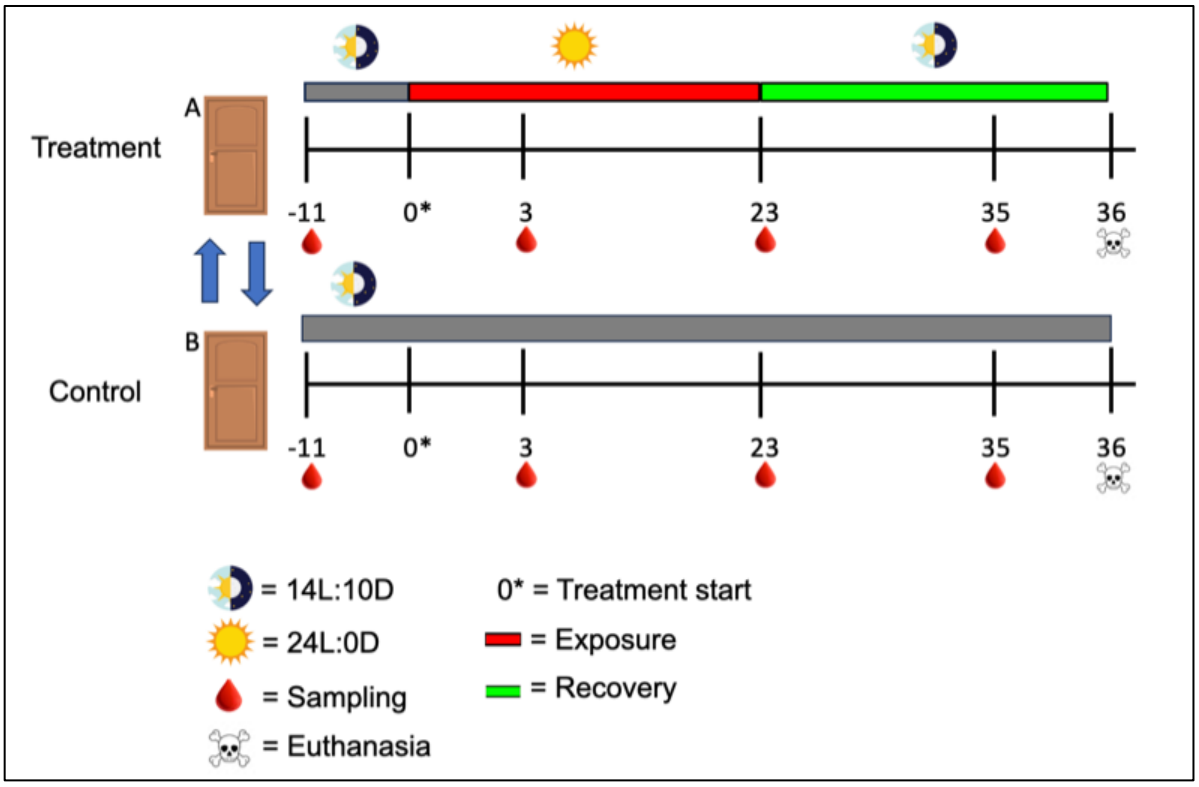

Figure 1: Illustration of the experimental timeline. Both treatment and control individuals were exposed to the same experimental timeline simultaneously. On the figure lines, -11, 3, 23, and 35, correspond to sampling collection timepoints (Pretreatment, D3, D23, and Posttreatment, respectively) with red blood drops indicating blood and body mass data collection. The "0" corresponds to when experimental treatment began when birds were exposed to 24-hours of constant light. Euthanasia is indicated by a skull and crossbones icon. 24L:0D and 14L:10D photoperiods illustrated by a full sun icon and a sun/moon icon, respectively. At the conclusion of phase one, rooms were thoroughly cleaned and inspected in preparation for phase two (where treatment and control rooms were switched as indicated by the blue arrows).

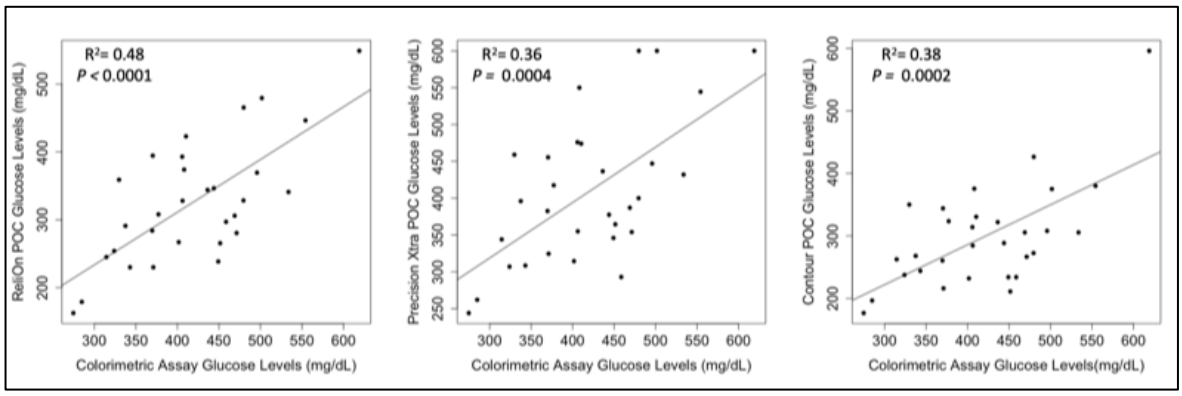

Figure S1. **Linear regression of blood samples used to quantify blood glucose levels vs a lab-based EIA (N = 30).** Colorimetric EIA glucose levels (mg/dL) are indicated on the x-axis, and ReliOn, Precision Xtra, and Contour POC glucose levels (mg/dL) are indicated on the y-axis.

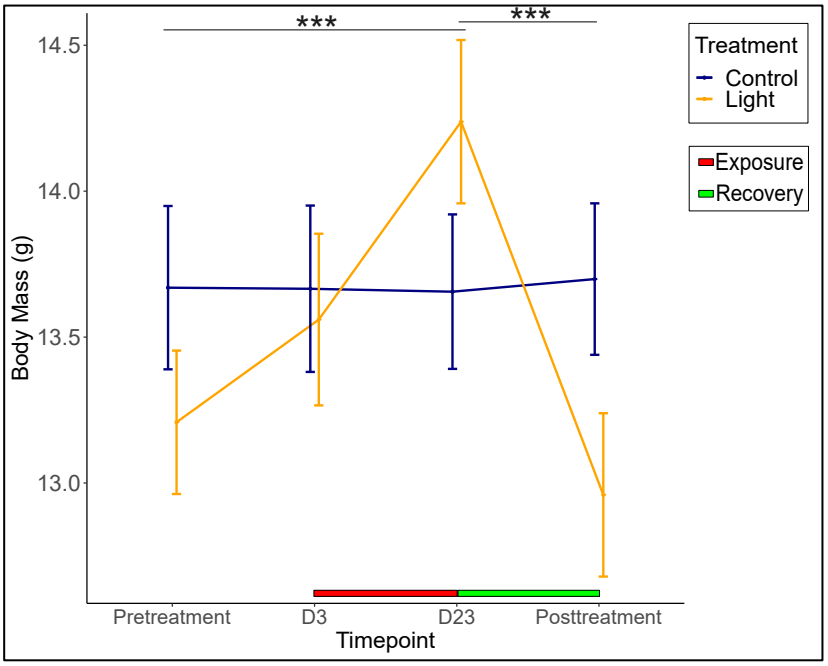

Figure 2. Body mass. Treatment birds (n=16) are indicated by the orange line while control birds (n=16) are indicated by the navy line**.** The solid red bar represents the exposure period of the light treatment (23 days total), while the green bar represents the recovery period (12 days total). Average body mass (g) of both groups is plotted across timepoints using raw data with

error bars indicating ± the standard error of the mean (SEM). Statistical significance within the light group (light-exposed birds) is shown with a solid black line with asterisks denoting associated p values (post hoc analysis*;* *$P \leq 0.05$; ** $P \leq 0.01$, *** $P \leq 0.001$). See supplementary materials for entire statistical output.

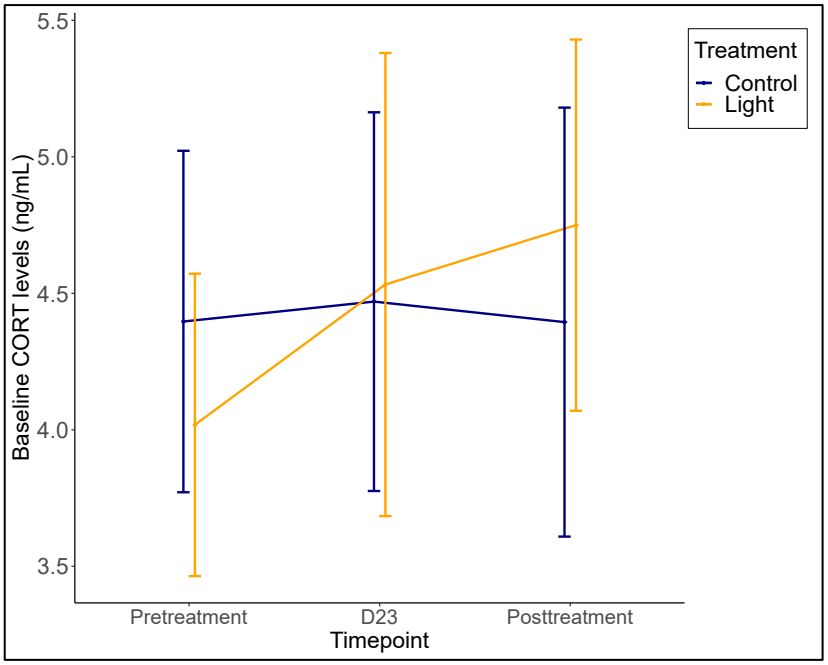

Figure 3. Baseline plasma Cort levels within 3 min of disturbance. Treatment birds (n=16) are indicated by the orange line while control birds (n=16) are indicated by the navy line. Average baseline Cort levels (ng/mL) is plotted across timepoints using raw data (not log transformed) with error bars indicating ± the standard error of the mean (SEM). Due to blood volume limitations, we did not quantify Cort on D3.

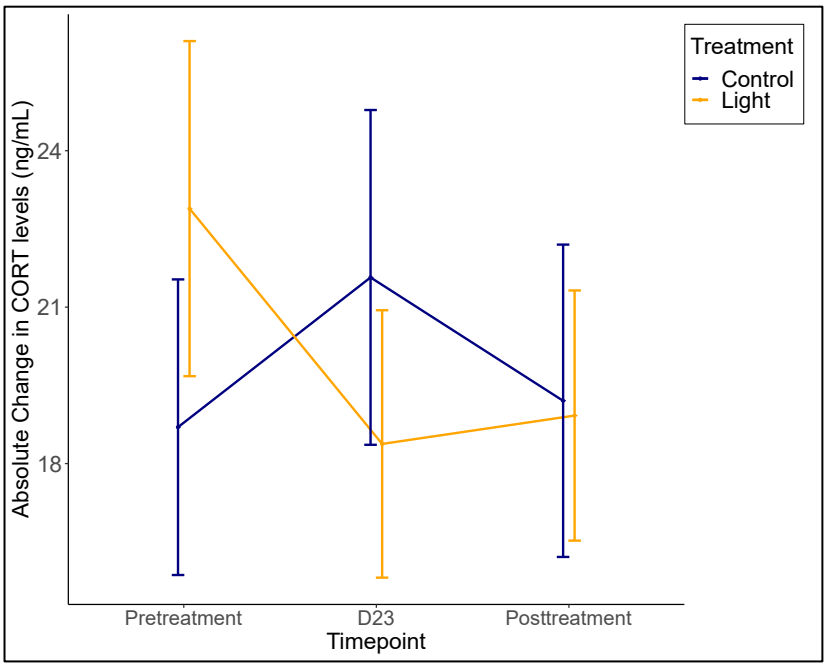

Figure 4. Absolute change in corticosterone (Cort) levels within 30 min of capture and restraint stress. Treatment birds (n=16) are indicated by the orange line while control birds (n=16) are indicated by the navy line. Average absolute change in Cort levels (ng/mL) is plotted across timepoints using raw data (not log transformed) with error bars indicating ± the standard error of the mean (SEM). Due to blood volume limitations, we did not quantify Cort on D3

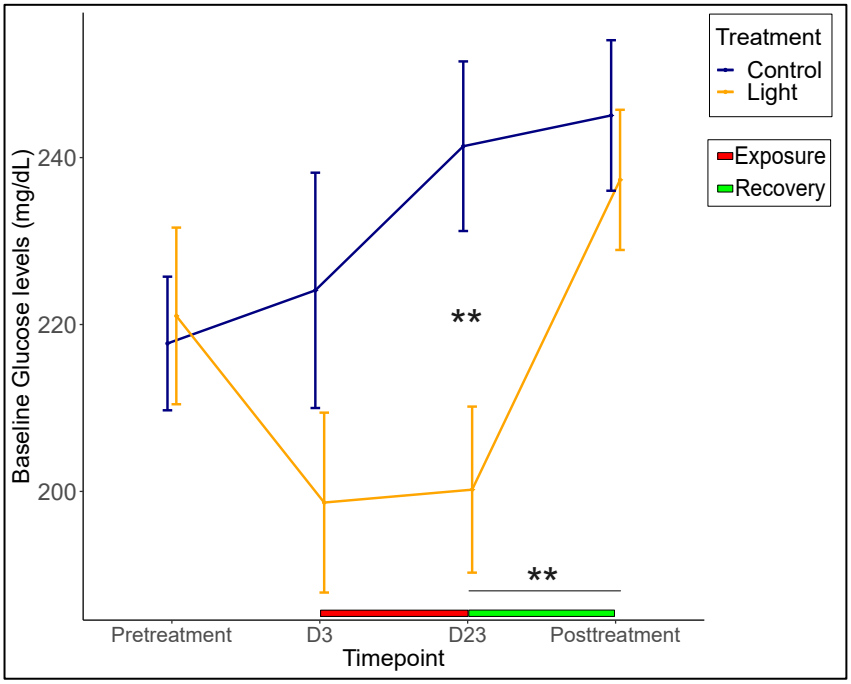

Figure 5. **Baseline glucose level.** Treatment birds (n= 16) are indicated by the orange line while control birds (n=16) are indicated by the navy line. The solid red bar represents the exposure period of the light treatment (23 days total), while the green bar represents the recovery period (12 days total). Average baseline glucose levels of both groups are plotted across timepoints using raw data with error bars indicating ± the standard error of the mean (SEM). Statistical significance within the light group (light-exposed birds) is shown with a solid black line with asterisks denoting associated p values (post hoc analysis; *$P \leq 0.05$; ** $P \leq 0.01$, *** $P \leq 0.001$). Statistical differences between groups at a particular timepoint are shown with just asterisks.

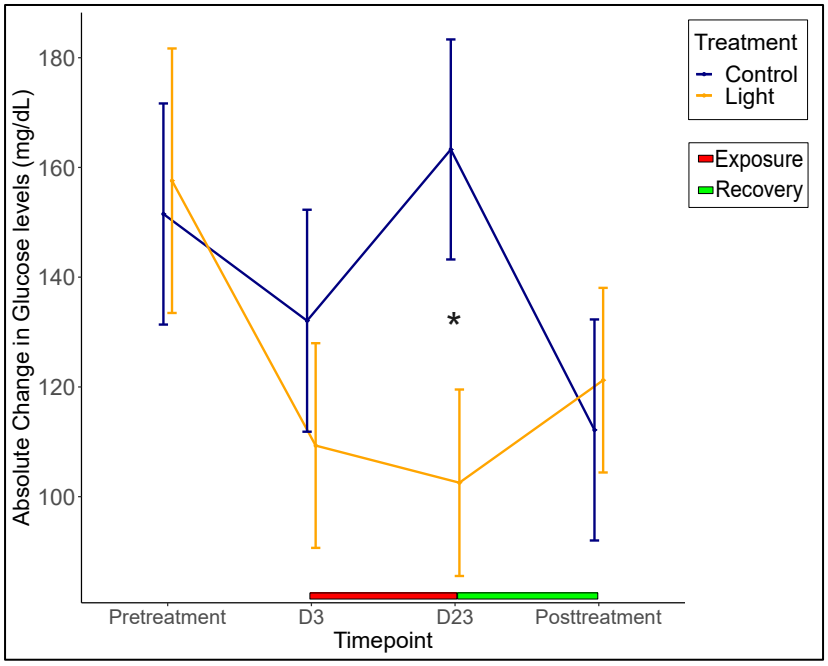

Figure 6. Glucose stress response. Treatment birds (n=16) are indicated by the orange line while control birds (n=16) are indicated by the navy line. The solid red bar represents the exposure period of the light treatment (23 days total), while the green bar represents the recovery period (12 days total). Average absolute change in glucose levels (mg/dL) of both groups is plotted across timepoints using raw data with error bars indicating ± the standard error of the mean (SEM). Statistical significance within the light group (light-exposed birds) is shown with a solid black line with asterisks denoting associated p values (post hoc analysis; *≤ 0.05; **≤ 0.01, ***≤ 0.001). Statistical differences between groups at a particular timepoint are shown with just asterisks.

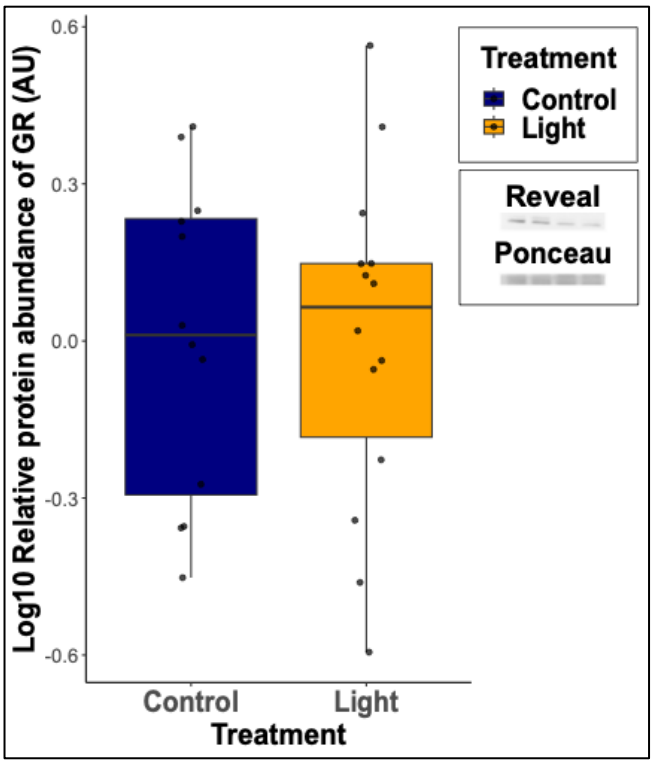

Figure 7. Relative glucocorticoid receptor (GR) protein levels (measured post-euthanasia). Treatment birds (n=14) are indicated by the orange, while control birds (n=12) are indicated by the navy bar. Relative abundance of liver GR (arbitrary units; AU) is plotted between groups using a boxplot with the solid black line indicating the median value on log transformed data. Western blot reveal image is of the raw data (two control samples on the left and two treatment samples on the right). Normalization ponceau stain is also shown.

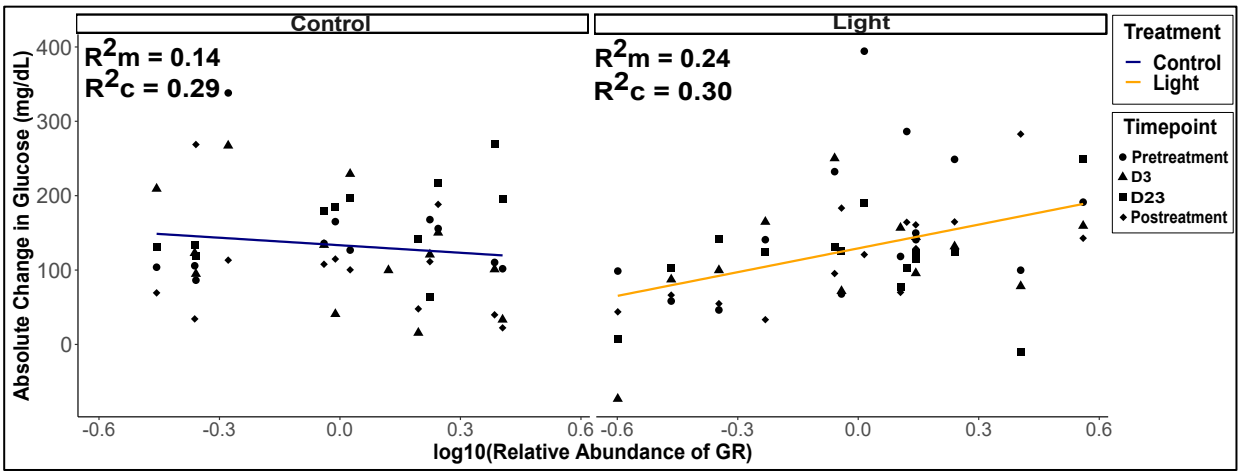

Figure 8. Relationship between GR and the glucose stress response. Absolute change in glucose at each timepoint is represented by circles (posttreatment), triangles (D3), squares (D23) and diamond (posttreatment). Treatment birds (n =14) are indicated by the orange line while control birds are indicated by the navy line (n =12). The marginal and conditional R^2 are listed from two separate linear regression model outputs, one with just Control and one with just Treatment birds. Best fit lines are depicted.

Chapter 3: Physiological responses vary with molecular damage outcomes after recovery from constant light

*Published in the Journal of Integrative and Comparative Biology

https://doi.org/10.1093/icb/icaf075

Authors: Kevin Pham*[1], Madeline Lazenby[1], Natalie R. Gassman[2], Christine R. Lattin[3], Haruka Wada[1]

[1]Department of Biological Sciences, Auburn University, Auburn, AL 36849, USA

[2]Department of Pathology, Heersink School of Medicine, University of Alabama at Birmingham, Birmingham, AL 35294, USA

[3]Department of Biological Sciences, Louisiana State University, Baton Rouge, LA 70803, USA

Key words: Light at night, Path analysis, Phenotypic integration, DNA damage, Oxidative damage

Abstract:

The Damage-Fitness model describes how stress is linked to damage and repair pathways that drive health and fitness outcomes across taxa. However, we lack an understanding of how variation in hypothalamic-pituitary-adrenal (HPA) responses (*i.e.,* endocrine flexibility) affects damage, especially after recovery from stressors. In this study, adult female zebra finches were exposed to a normal photoperiod or constant light for 23 days followed by a recovery period. Using path analysis, we combined a suite of morphological and physiological traits to examine the mechanisms related to cellular damage outcomes. In control individuals, HPA axis reactivity was condition-dependent, such that birds with higher body mass had stronger HPA axis reactivity. HPA axis reactivity was associated with two specific relationships: a strong, positive, relationship with glucose reactivity and a slightly negative relationship with liver 4-hydroxynonaneal that covaried. Interestingly, this condition-dependency disappeared in birds recovering from constant light. While HPA axis reactivity was positively associated with glucose reactivity, this path relationship was not associated with any damage marker. Liver glucocorticoid receptor abundance was negatively associated with liver protein carbonyl damage in control birds, but this relationship was lost in birds recovering from light. These patterns indicate that long-term exposure to a stressor such as constant light can alter biologically linked relationships, even after cessation and recovery from that stressor. Yet, whether rewiring of physiological network connectivity is related to adaptive physiological outcomes, fitness-related traits, or performance remains unclear.

1. Introduction:

The glucocorticoid stress response (*i.e.,* the reactivity of the hypothalamic-pituitary-adrenal (HPA) axis) has been proposed to be critical for vertebrates to cope with and recover from unpredictable challenges (Angelier and Wingfield, 2012; Crino et al., 2024). Glucocorticoids are steroid hormones that regulate a suite of physiological and behavioral processes under basal and stressful conditions through binding of corticosteroid receptors across tissues (Breuner et al., 2003; Lattin et al., 2012; Sapolsky et al., 2000; Timmermans et al., 2019). Under basal conditions, glucocorticoids occupy high affinity mineralocorticoid receptors (MR) in tissues such as the hippocampus and amygdala to regulate neurogenesis, emotion, and spatial memory (De Kloet and Reul, 1987; ter Heegde et al., 2015). Following exposure to a stressor, elevated glucocorticoid levels occupy low-affinity glucocorticoid receptors (GR) throughout the body and bind to glucocorticoid response elements, activating cellular response pathways in a tissue-specific manner to reestablish homeostasis (Kuo et al., 2015; Cohen et al., 2012; Sapolsky et al., 2000).

On one hand, the baseline and magnitude of the glucocorticoid stress response is thought to mediate transitions between key life history events and trade-offs between self-maintenance and reproduction (Angelier et al., 2010; Crespi et al., 2013; Wada, 2008; Wingfield and Kitaysky, 2002), although relationships between glucocorticoids and reproductive investment often vary based on context and species (Bonier et al., 2009). On the other hand, excess glucocorticoid secretion is deleterious and commonly associated with metabolic syndromes, mental health disorders, and age-related diseases (Cohen et al., 2012; Forget et al., 2016). In either case, glucocorticoids may facilitate adaptive or maladaptive responses, as they affect multiple intrinsically linked pathways throughout the physiological regulatory network (Cohen et al.,

2012; Sapolsky et al., 2000; Williams, 2008). These pathways include genomic and non-genomic effects on immunity, oxidative balance, and metabolism across tissues (Cohen et al., 2012; Mir et al., 2021). For instance, GR that bind to positive liver glucocorticoid response elements augment glycolytic processes and free fatty acid and protein catabolism, presumably to replenish energy stores after stressful events (de Guia, 2020; Kuo et al., 2015). Alternatively, GR that bind to negative glucocorticoid response elements in the hypothalamus and pituitary suppress production of neuropeptides and hormone precursors involved in the glucocorticoid hormone cascade, triggering negative feedback to bring glucocorticoid levels back to baseline (Timmermans et al., 2019).

One potential consequence of glucocorticoid secretion is oxidative stress. Oxidative stress is the imbalance between pro-oxidants (e.g., reactive oxygen and nitrogen species) and antioxidants (e.g., superoxide dismutase, glutathione peroxidase, or catalase). If pro-oxidants overwhelm the antioxidant system, oxidative damage can occur to DNA, lipids, and proteins; this damage is implicated in multiple chronic health diseases, in aging, and is a potential driver of ecological trade-offs (Harman, 1956; Monaghan et al., 2009). For example, glucocorticoid administration elevated reactive oxygen and nitrogen species in breast cancer cell lines (Flaherty et al., 2017) and suppressed antioxidant enzymes in the hippocampus of male Wistar rats, resulting in higher lipid hydroperoxides and protein carbonyls associated with cognitive decline (Sato et al., 2010).

Although glucocorticoids are often associated with oxidative damage, there is a large amount of individual variation in how the HPA axis responds to stressors that may activate different pathways to mitigate the damage incurred (Cockrem, 2013; Williams, 2008). For example, in house sparrows (*Passer domesticus*), individuals consistently differed in their HPA

axis response to multiple bouts of on-and-off again food restriction, but this stressor did not significantly increase oxidative stress or damage (Lendvai et al., 2014). The HPA axis can also be shaped during early development through epigenetic modifications, which may lead to individual differences in stress sensitivity and physiological consequences (Taff et al., 2024b; von Holdt et al., 2023; Crino et al., 2024). These studies emphasize large individual variation in HPA axis function across time, developmental periods, and various ecological contexts, suggesting that individuals differ in the magnitude of their HPA axis response for a given environment. The ability for an organism to modify its endocrine response to environmental variation is known as endocrine flexibility *(i.e.,* reversible changes in hormone responses), in which plasticity in HPA axis function may facilitate adaptive phenotypic responses (Grindstaff et al., 2022; Taff et al., 2024; Taff and Vitousek, 2016).

If endocrine flexibility is critical in buffering organismal responses to environmental challenges, flexibility must ultimately be linked to traits tied to fitness. Yet, changes in HPA responses, especially once the stressor is removed, is not well understood. Therefore, research targeting how flexibility in stress responses alter downstream, biologically linked processes and thus, manifest into alternative physiological outcomes (*i.e.,* cellular damage), may provide insight on how individuals cope in a changing world (Wada, 2019).

In this study, we used a constant light exposure regime as a stressor in diurnal zebra finches (*Taeniopygia guttata castanotis*) and examined consequences on persistent cellular damage throughout exposure and after a recovery period. Nighttime disturbances such as artificial lighting sources or night shifts can increase oxidative stress markers and glucocorticoids (Liu et al., 2022; Teixeira et al., 2019). For example, constant light decreased levels of the antioxidant glutathione, while simultaneously increasing levels of malondialdehyde, a marker of

lipid peroxidation, in the brain of Wistar rats (Sharma and Goyal, 2020). Early life exposure to altered light environments can also induce oxidative stress, with yellow-footed chickens reared under constant light showing persistent reduction in multiple antioxidant-related genes in addition to protein expression of nuclear factor erythroid 2-related factor 2 throughout development (Yang et al., 2022).

We took repeated measurements of DNA damage from zebra finches using a novel broad-spectrum damage detection assay (Gilat et al., 2021; Holton et al., 2018) from nucleated red blood cells collected before, during, and after recovery from constant light. Liver and pectoralis muscle were also collected after recovery to evaluate persistent markers of oxidative stress (protein carbonyls and 4-hydroxynonanel). Using these data, we tested the effects of constant light and recovery through two approaches: we 1) compared control and treatment groups for each damage variable and 2) examined the relationships among morphological and physiological variables previously collected (Pham et al., 2025) to test mechanisms related to the damage outcome. For the former approach, we predicted that constant light would increase DNA damage throughout treatment, but that damage would return to pretreatment levels after the recovery period, thereby indicating stress resilience. In contrast, under the assumption that constant light would lead to oxidative stress, we predicted that oxidative damage markers in the liver and muscle would persist after a recovery period and be higher in birds previously exposed to light compared to controls. For the latter approach, we used path analysis to assess how constant light altered the relationships between morphology, physiological mediators, and damage between experimental and control groups. In general, we predicted that stronger glucocorticoid responses to capture and restraint (*i.e.,* HPA axis reactivity) would be condition-dependent and positively related to liver GR density and the downstream glucose response, mediating the resulting

damage outcome. However, we predicted that exposure to constant light would uncouple the aforementioned relationships in treatment individuals, and would thus be different in terms of direction (positive/negative) or magnitude in comparison to control birds.

2. Materials and Methods

2.1 Animal husbandry

Briefly, 32 adult female zebra finches were individually housed in tower cages (38.10 cm width × 45.72 cm depth × 45.72 cm height) under a 14L:10D photoperiod, given ad libitum access to seed (Kaytee Supreme Finch food, Wilton, WI), water, and cuttlefish bone (Pham et al., 2025). Prior to light exposure, animals were given at least a two-month acclimation period. All experimental procedures were approved by the Institutional Animal Care and Use Committee (IACUC) at Auburn University (protocol #2020-3805). We used only females in this study because past research has shown that female zebra finches appear to be particularly sensitive to stressors such as high temperature and hormone manipulation relative to males (Spencer & Heidinger, 2010; Wada et al., 2018).

2.2 Experimental design

Zebra finches in this experiment were exposed to either constant light (24L:0D; n = 16) or a control light regime (14L:10D; n =16) for 23 days and allowed a recovery period in which individuals exposed to constant light returned to a photoperiod of 14L:10D as previously described (Pham et al., 2025, **Fig. 9**). Baseline (within 3 min of capture; average time = 2:02 ± 0.02 SD) and restraint-induced (30 min after capture and restraint; average time = 31:20 ± 0.04 SD) blood samples were collected to measure whole blood glucose levels using the ReliOn

Prime blood glucose monitoring system (Walmart Apollo LLC Bentonville, AR), a point-of-care device validated in zebra finches (Pham et al., 2025). The remaining blood was centrifuged at 14,600 *x g* to separate plasma and red blood cells. Corticosterone (Cort) levels were measured in plasma as previously described in Pham et al. (2025). Red blood cells were only collected from baseline blood samples and flash frozen in liquid nitrogen. Samples were then transported to the lab and stored in a -80°C freezer until DNA extraction. On Day 36, individuals were euthanized via overdose of isoflurane vapors. Liver tissue and right pectoralis muscle were collected to measure oxidative damage via immunoblotting. A broad-spectrum DNA damage assay, Repair Assisted Damage Detection (RADD), was used to quantify total DNA lesions in red blood cell DNA on Day -11, 3, 23, and 35 (Gilat et al., 2021; Holton et al., 2018). Protein carbonyls and 4-hydroxynonaneal were quantified in liver and pectoralis muscle. Note that while DNA damage was quantified on 12 days after treatment had ended (Day 35), oxidative damage metrics were quantified 13 days after treatment had ended (Day 36) to minimize confounding effects of prior sampling (handling, capture, and disturbance).

2.3 DNA extraction of red blood cells

DNA was isolated from baseline red blood cells across all four collection timepoints (Pretreatment, days 3 and 23 of Treatment, and Posttreatment). We chose to only include baseline blood samples for DNA damage analysis as DNA damage often increases with the standard capture and restraint protocol (Hoffman et al., In review). To extract DNA, we used Machery-Nagel NucleoSpin blood DNA extraction kits (Düren, Germany) following the manufacturer's protocol with slight modifications. Briefly, 25 µL of Proteinase K was added to 5 µL of red blood cells with 170 µL 0.1 M phosphate buffered saline (PBS). We added 200 µL of lysis buffer

(provided by the DNA extraction kit) and incubated all samples at 65°C for 30 min. To minimize variation in DNA damage that can be caused by vortexing (personal observation; unpublished data), we vortexed all samples for 5 sec only after incubation. All other steps followed the manufacturer's protocol. DNA concentration and purity (260/280 and 260/230 ratios) were determined using 2 µL of sample via a NanoDrop 2000 Spectrophotometer (Thermo Fisher Scientific), and samples were stored at -20°C. DNA was shipped on wet ice and analyzed at the University of Alabama, Birmingham using a DNA damage protocol, Repair Assisted Damage Detection (RADD).

2.4 Repair Assisted Damage Detection (RADD)

DNA lesions were measured using a modified Rapid RADD protocol (Gilat et al., 2021; Holton et al., 2018). First, 500 ng of extracted DNA was placed in a reaction tube with 1x Thermo Pol Buffer (New England Biolabs B9004), 1x NAD+ (New England Biolabs B9007), 0.5 µL of 200 mg/mL bovine serum albumin, and the lesion processing cocktail containing 2.5 U of UDG (NEB M0280), FPG (NEB M0240), T4PDG (NEB M0308), EndoIV (NEB M0304), and EndoVIII (NEB M0299). The reaction mixture was incubated for 1 h at 37°C. Then, a gap-filling cocktail containing 1x Thermo Pol Buffer, 2.5 U Klenow exo- (Thermo Fisher EP0422), and 0.1 µL fluorescent ATTO-550-UTP (Jena Biosciences GMBH) was added to the reaction tube and incubated for an additional 1 h at 37°C. Using an Oligo Clean and Concentrator kit for 96-well plates (Zymo Research), we purified the labeled DNA samples from excess fluorophores using the manufacturer's protocol and added two washing steps with the kit's DNA wash buffer.

To quantify the DNA lesion levels, positively charged Teflon-coated microscope slides (Tekdon, customized well formation, 2 mm diameter wells, 90 wells per slide) were incubated

for 1 h at 37°C at 25 rpm and overnight at 4°C. We then blocked slides by washing twice with PBS with tween (0.05% Tween 20) and PBS (Sigma) and immersing in a 5% w/v bovine serum albumin (Sigma) solution in PBS. The slides were then placed in a second incubation for 1 h at 37°C at 25 rpm and a second overnight incubation at 4°C. Lastly, we washed slides with water, dried them using nitrogen gas, and immediately proceeded to the next step.

A total of 1 μL of labeled DNA was placed in each well, with three replicates of each sample. Slides were incubated for 14 min at 42°C and then for 24 min at 30°C in humid conditions to avoid drying (RapidFISH slide hybridizer, Boekel Scientific). The slides were then washed with water and dried under nitrogen.

Slides were imaged using an Amersham Typhoon Biomolecular Imager using a 532 nm laser. After imaging the ATTO-550 fluorophore, the total DNA was stained with EvaGreen DNA binding dye (Biotium). A total of 1 μL of 20x EvaGreen Dye in water was added to each well containing the bound DNA. Wells containing only water and no DNA were also stained to obtain the background signal of the EvaGreen dye in the absence of DNA. Slides were incubated in the dark for 30 min at room temperature. The slides were then washed with water and dried under nitrogen. The DNA content was imaged again using the Typhoon with the 488 nm laser to image the EvaGreen stain.

The fluorescence intensity of each well was quantified using ImageQuant analysis software (GE Healthcare). The background signal was determined using unlabeled DNA wells and subtracted from the ATTO-550 channel, which reports the DNA damage, and EvaGreen channel, which reports the DNA content in the well. The background-corrected ATTO-550 signal in each well was divided by the corrected signal from the EvaGreen channel of the same well to normalize the signal to the amount of DNA in the well. The ATTO-550/EvaGreen ratio provides

the relative DNA damage in the DNA applied to the slide. These ratios were averaged, and the standard deviation for each sample calculated over three replicates.

2.5 Immunoblots

Lipid peroxidation (4-hydroxynonaneal) was measured in prepared liver samples that were also used to measure GR using a custom antibody as previously described (Hoffman et al., 2024; Hyatt et al., 2016; Pham et al., 2025). 4-hydroxynonaneal was also measured in the right pectoralis muscle following the same tissue preparation methodology. To measure protein oxidation (protein carbonyls), tissue homogenates of the liver and right pectoralis muscle were diluted to a concentration of 1.5 μg/μL using ultrapure water. Subsequently, 10 μL of the sample homogenate (15 μg of total protein lysate) was added to 10 μL of 12% SDS and 10 μL dinitrophenylhydrazine from the OxyBlot Protein Oxidation Detection Kit (S7150) to form detectable hydrazones, which are derivatives of protein carbonyls, and incubated for 15 min until the reaction was terminated using 7.5 μL of kit neutralization buffer (Hoffman et al., 2024; Yap et al., 2022).

Proteins were separated by polyacrylamide gel electrophoresis. After gel electrophoresis, proteins were transferred to a polyvinylidene difluoride (PVDF) membrane. Non-specific sites were blocked with 5% nonfat milk containing tris-buffered saline with tween (TBS-T). After three washes with TBS-T, each membrane was rocked and incubated in the primary antibody of interest. Primary antibodies included an anti-rabbit 4-hydroxynonaneal for lipid peroxidation (ab46545; 1:1000 dilution) and anti-rabbit dinitrophenylhydrazine (S7150; 1:250 dilution), both prepared with 5% bovine serum albumin with TBS-T. Secondary antibodies were an anti-rabbit horseradish peroxidase secondary antibody (Cell Signaling 7074; 1:2000 dilution) and anti-rabbit

horseradish peroxidase secondary antibody (S7150; 1:500 dilution) provided by the kit in 5% bovine serum albumin with TBS-T. Protein bands were visualized using UV chemiluminescence with ECL Prime (VWR 89238-012) and images were captured using ImageQuant LAS 4000 (GE Healthcare). Protein bands were all analyzed using Bio-Rad Image Lab (Bio-Rad, Hercules, CA). Ponceau staining of total protein was used as a normalizing and transfer control.

2.6 Statistical analysis

Linear mixed effects models

All statistical analyses were run in R (R version 4.5.0). To test for treatments effect on each of the damage variables across tissue types (DNA damage, protein carbonyls, and 4-hydroxynonaneal), we used packages "lme4" and "lmerTest" (Bates et al., 2015; Kuznetsova et al., 2017) to construct linear mixed effects models. For DNA damage, Treatment (a two level factor), and Timepoint (a four level factor) and the interaction between them (Treatment x Timepoint) were treated as fixed effects, with Bird ID/Room/Phase as a random intercept to account for non-independence and the hierarchical nature of the experimental design as previously described (Pham et al., 2025). For each tissue type (liver and skeletal muscle), we ran linear mixed effects models with protein and lipid oxidation markers (protein carbonyls and 4-hydroxynonaneal) as the response variable with Gel as a random effect and Treatment as a fixed factor. Two significant outliers were identified using Grubb's test (GraphPad) and excluded from analysis. Among these outliers, one value pertained to 4-hydroxynonaneal levels in the liver and one value pertained to DNA damage in red blood cells. Relative abundance of protein carbonyls, 4-hydroxynonaneal, and DNA damage were log transformed to meet model assumptions. Alpha values were set to $P < 0.05$.

Path analysis

To evaluate the interconnected relationships between physiological mediators and damage variables and how those relationships differed with light exposure, we utilized path analysis using the "Lavaan" package in R (Rosseel, 2012; 2014). Path analysis identifies causality and bidirectional covariation between dependent and response variables depending on the directionality of the arrows (single-headed or double-headed arrow). We used body mass, physiological mediators (HPA and glucose stress responses), relative abundance of liver GR measured in Pham et al. (2025), and damage variables (DNA damage, protein carbonyls, 4-hydroxynonaneal) to construct our models. HPA axis and glucose stress responses were calculated by subtracting post-restraint values from baseline values and indicated by a delta symbol in path analyses. We standardized all variables prior to analysis (mean of zero and standard deviation ±1). Standardizing all variables allows for direct comparisons between each relationship. To compare models, we ensured that each individual was represented equally across all models, such that no individual was included in the analysis if they were missing any measurement. For example, if a bird was missing a glucose response measurement, it was excluded from path analysis entirely. Out of the 32 birds in this experiment, this eliminated 12 individuals from the dataset, such that we had a total sample size of N = 20 for these analyses, comprised of n = 12 treatment birds and n = 8 control birds. We followed a statistical workflow further described below (Model selection criterion and statistical workflow) to ensure criteria were met for the generated models. We included a "group = treatment" argument in our models to generate standardized path coefficients for each relationship in both control and light-exposed birds to explain the damage outcome. An overall diagnostic report indicating model fit is described in **Table 1.**

Justification of *a priori* models

Four a priori models were tested on red blood cell and liver damage markers but not damage markers from pectoralis, because we did not have data on GR density of muscle (**Fig 10**). These a priori models were constructed under the assumption that body mass is a reliable indicator of individual condition in birds, even when not corrected for body size (e.g., tarsus length) (Labocha and Hayes, 2012; Ranta et al., 1994). Because we did not see differences between groups in body mass before the experiment, and all individuals were adult females from the same source population, we assumed that body size was relatively uniform.

Model A

In model A, HPA axis reactivity was a condition-dependent trait and integrator of the physiological regulatory network. Here, we expected three separate unidirectional relationships (**Fig. 10A**). First, one path explained the relationship between HPA axis reactivity and the damage variable of interest through an unexplained variable not directly measured in this study. Second, one path linked HPA axis reactivity to the downstream glucose stress response via a non-genomic pathway (e.g., internalization of glucose transporters), which directly affected the damage variable of interest. Third, one path linked HPA axis reactivity with the relative abundance of liver GR, which either 1) influenced the damage variable of interest via a GR-mediated genomic pathway not measured in this study, or 2) affected the damage variable of interest via the glucose stress response.

Model B

In model B, liver GR density was condition dependent and determined the capacity for HPA axis reactivity to affect downstream traits. Here, if GR was condition-dependent, we expected three separate unidirectional relationships (**Fig. 10B**). First, one path explained the relationship between liver GR and the damage variable of interest through an unexplained variable not directly measured in this study. Second, one path linked GR abundance to the glucose stress response via a genomic pathway that directly affected the damage variable of interest. Third, one path linked GR abundance with HPA axis reactivity, which either 1) directly affected the damage variable of interest or 2) mediated damage outcomes through changes in the glucose stress response.

Model C

In model C, HPA axis reactivity and abundance of liver GR were interconnected traits that covaried with each other and explained damage through the glucose stress response. Here, we expected three unidirectional relationships (**Fig. 10C**). First, we expected one relationship directly linking HPA axis reactivity with the damage variable of interest via an unexplained variable not measured in this study. Second, GR abundance should directly affect the damage variable of interest via an unexplained variable not measured in this study. Third, we expected HPA axis reactivity and GR abundance to covary, affecting the downstream glucose stress response and mediating changes in the damage variable of interest.

Model D

In model D, HPA axis reactivity, abundance of liver GR, and the glucose stress response were all condition-dependent traits that each covaried with each other. Here, we expected four

relationships (**Fig. 10D**). First, we expected one relationship directly linking HPA axis reactivity with the damage variable of interest via unexplained pathways or variables not measured in this study. Second, GR abundance should directly affect the damage variable of interest via unexplained pathways or variables not measured in this study. Third, we expected that HPA axis reactivity, liver GR abundance, and the glucose stress response to all covary to affect the da m-age outcome. Lastly, we expected changes in the damage variable of interest to be solely explained through changes in the glucose stress response.

Model selection criterion and statistical workflow

Because statistical power was low due to the relatively small sample size and number of parameter estimates, we used four different criteria to ensure proper model fit. These criteria included chi-square (χ^2), SRMR (square root mean residuals), CFI (Bentler's comparative fit index), and AICc (Akaike information criterion corrected for small sample sizes). SRMR and χ^2 are both absolute fit indexes. χ^2 assesses how well the hypothesized relationships compare to the observed data, while SRMR calculates model fit by comparing the observed data to a predicted perfect model, with lower values indicating a better fit. In contrast, Bentler's comparative fit index is a relative measure, in which a null baseline model is generated that is compared against the observed model, with higher values indicating a better fit. Lastly, AICc compares competing models, but penalizes multiple parameter estimates and small sample sizes to minimize committing a type I error, with lower values indicating a better model. To further ensure proper model fit, we used cut-off values of ≤ 0.08 for SRMR, 0.95 for CFI, and AICc scores with differences ≥ 2 to determine the best fit model, along with changing the directionality of relationships (casual or allowing for covariation) (McCollum et al., 2024; Vágási et al., 2020;

Streiner, 2006; Xia and Yang, 2019). If multiple competing models were deemed appropriate in all criteria, the model with the lowest AICc score was chosen and interpreted. Significant path relationships and χ^2 differences were determined using an alpha value of $P < 0.05$.

Following these criteria, we found that model A best explained traits related to damage markers. Once model A was chosen, to determine whether treatment groups differed in their path estimates overall, we used a difference in χ^2 test to compare the unconstrained complex model vs two separate simpler models that constrained the regression estimates and intercepts to the same value (**Table 2**). By constraining these values, the simpler model assumes that path estimates/intercepts are equal between groups, as opposed to the unconstrained complex model that allows relationships to freely vary in their estimates/intercepts (in our case, by treatment groups). Constrained and unconstrained models were then compared to assess data fit using the difference in χ^2 test. If a significant p-value was found, the null hypothesis was rejected, which assumes 1) path estimates do not vary between treatment groups and therefore are not different and 2) that the simpler constrained model fits the data better than the more complex unconstrained model.

After confirming that there was a difference between treatment groups in path estimates, we ran a difference in χ^2 test for each generated relationship to identify which specific paths were significantly different. If a significant p-value was found, the null hypothesis was rejected, which assumes that the specific path relationship tested was not significantly different between treatment groups.

3. Results

3.1 Effect of continuous light on damage variables

DNA damage in red blood cells

We did not detect significant main effects of Treatment ($F_{1,30}$; $P > 0.90$) or Timepoint ($F_{3,86}$; $P > 0.86$) on DNA damage in red blood cells. Furthermore, we did not detect a significant interaction between Treatment and Timepoint ($F_{3,86}$; $P > 0.46$), indicating that continuous light had no effect on DNA damage levels in red blood cells during the time course of the experiment (**Fig. S2; supplementary materials**).

Oxidative damage in liver and pectoralis muscle

We did not detect a main effect of Treatment on any oxidative damage markers in the liver (4-hydroxynonenal: $F_{1,29} = 1.45$; $P > 0.23$; Protein carbonyls: $F_{1,30} = 0.68$; $P > 0.41$) or in the pectoralis muscle (4-hydroxynonenal: $F_{1,28} = 0.50$; $P > 0.48$; Protein carbonyls: $F_{1,28} = 0.45$; $P > 0.50$) which were collected after the recovery period (**Fig. S3 A-D; supplementary materials**).

3.2 Path analyses of damage variables

Among all models, effects of body mass, physiological stress mediators, and liver GR abundance on red blood cell DNA damage and liver protein carbonyl damage were best explained by model A (**Table 1A; Fig. 10A**). Similarly, variation in liver 4-hydroxynonaneal was best explained by model A, although the fit of the data was poor and did not meet criterion for CFI (AICc = 53.91; CFI= 0.91). Allowing for bidirectional covariation between ΔCORT, GR density, and 4-hydroxynonaneal levels significantly improved the model fit (AICc = 51.67; CFI

= 0.995), however, this resulted in SRMR not meeting the criterion (SRMR = 0.118). Allowing for bidirectional covariation between ΔCORT and 4-hydroxynonaneal levels significantly improved the fit of the model, with the final model diagnostic shown that met all criteria (**Table 1A).**

We did not detect a significant difference in χ^2 for red blood cell DNA damage between the unconstrained and constrained models, indicating that none of the path estimates generated between treatment groups differed for this damage marker (**Table 2**). In contrast, for liver protein and lipid damage markers, we found a significant difference in χ^2 between the unconstrained and constrained models for regression estimates, indicating that there was a difference between treatment groups in their paths (**Table 2**). Thus, we further ran a difference in χ^2 test on specific generated paths between treatment groups.

Model A- HPA axis reactivity and liver protein carbonyls

Within control finches, there was a significant positive relationship between HPA and glucose reactivity (standardized beta estimate = 0.69; $P \leq 0.02$), indicating tight coupling between these two traits. Moreover, the difference in χ^2 test revealed that this specific path relationship significantly differed from birds recovering from constant light ($\chi^2 = 4.23$; $P = 0.039$). Liver GR abundance was strongly and negatively related to liver protein carbonyls, such that individuals with greater abundance of GR had lower damage (standardized beta estimate = -0.72; $P \leq 0.005$; **Fig. 11**). Furthermore, the difference in χ^2 test revealed that this specific path relationship was significantly different from birds recovering from constant light ($\chi^2 = 4.23$; $P = 0.045$). In birds recovering from constant light, liver GR density was strongly positively related

to glucose reactivity (standardized beta estimate = 0.71, $P \leq 0.001$), but did not mediate any relationship with protein carbonyl damage.

Model A – HPA axis reactivity and liver 4-hydroxynonaneal

Within control finches, body mass had a significant positive relationship with HPA reactivity (standardized beta estimate = 0.44; $P \leq 0.01$; **Fig. 12**), such that individuals with higher body mass exhibited stronger HPA axis responses to capture and restraint. Furthermore, this specific path relationship was significantly different in birds recovering from constant light (χ^2 = 6.74; $P = 0.009$). There was a trend for HPA reactivity to negatively covary with liver 4-hydroxynonaneal levels (standardized beta estimate = -0.80; $P \leq 0.08$), but this did not reach statistical significance.

In birds recovering from light treatment, there was no relationship mediated by HPA axis reactivity. Liver GR abundance was positively associated with glucose reactivity, but as opposed to liver protein carbonyls, glucose reactivity mediated a negative relationship with liver 4-hydroxynonaneal damage (standardized beta estimate = -0.49; $P \leq 0.05$). However, this specific path relationship was not significantly different from controls (χ^2 = 1.34; $P = 0.25$). Liver GR abundance positively covaried with liver 4-hydroxynonaneal levels (standardized beta estimate = 0.89; $P = 0.03$), but this specific path relationship also did not significantly differ in controls (χ^2 = 0.40; $P = 0.11$)

4. Discussion

We previously found that female zebra finches showed varying degrees of stress resilience in different physiological and morphological traits after recovery from constant light (Pham et al., 2025). In this study, constant light did not result in increased protein or lipid damage in the liver and pectoralis muscle after a recovery period, or in DNA damage in red blood cells during or after treatment, indicating that zebra finches escaped some potential physiological costs of an altered light environment. This is contrary to previous findings in which constant light increased oxidative damage across tissues (Sharma and Goyal, 2020; Yang et al., 2022). However, one limitation of our design is that we did not quantify all oxidative damage measures (i.e., protein carbonyls and 4-hydroxynonaneal) immediately after light exposure. Based on the literature, we expected constant light would lead to oxidative stress in the short term, and thus focused our efforts on persistent oxidative damage (i.e., damage after recovery). While we did not detect differences between light-exposed and control groups in damage variables, leveraging physiological and morphological data previously collected in combination with path analysis in the present study revealed possible causality and covariation among different traits.

HPA-driven hyperglycemia was not related to oxidative damage

The best fitting path model investigating the relationship between body mass, physiological stress mediators, and damage variables revealed distinctive patterns between control and light-exposed birds. In both path models describing damage markers, controls birds exhibited strong coupling between the HPA axis and glucose reactivity, such that stronger adrenocortical responses were positively associated with stronger glucose stress responses. Yet,

glucose reactivity was not related to liver protein or lipid damage, indicating that there was not a physiological cost associated with heightened stress responses. In contrast, the relationship between HPA axis and glucose reactivity disappeared from birds recovering from constant light. In fact, the relationship shifted from positive to negative, suggesting an uncoupling of the two traits. This uncoupling could be a temporary response to prevent co-expression between linked traits, enabling individuals to recover from stressors. However, to evaluate if coupling/uncoupling plays a significant role in stress resilience or recovery, we would need to remeasure traits after a longer period to see if the relationships converge or remain uncoupled. Nevertheless, the patterns detected in our study suggests that constant light can lead to persistent changes to the physiological regulatory network, even after cessation of the stressor.

Similarly to how reactive oxygen species can damage macromolecules, extracellular glucose can react with biomolecules under hyperglycemic conditions, a process known as glycation. Glycation results in accelerated glycated end products (AGEs) through binding to the amino acid side chains of proteins and altering protein function, or by forming cross-links with DNA bases, inhibiting replication, and risking cellular health (Hurben et al., 2024). Yet, avian species, unlike mammals, may have evolved different mechanisms to resist the glycation of biomolecules (Anthony-Regnitz et al., 2020; Szwergold and Miller 2014), potentially explaining why we did not detect significant paths connecting HPA axis and glucose reactivity with any damage markers. Future studies should investigate the potential role of glucose in glycating biomolecules, especially given that avian species seem able to resist these detrimental effects despite maintaining circulating glucose concentration much higher than similar-sized mammals (Braun and Sweazea, 2008; Sweazea, 2022).

HPA axis reactivity was condition-dependent and varied by damage marker

With regard to the path model describing liver 4-hydroxynonaneal damage, HPA axis reactivity was positively associated with body mass in control birds, indicating condition-dependency of this phenotype: birds with greater body mass mounted stronger HPA axis responses. Here, condition was defined as properly functioning cellular processes (Hill, 2014). In this context, control birds in better condition exhibited a negative relationship with 4-hydroxynonaeal damage, although this relationship did not reach statistical significance ($P = 0.08$). However, similar condition-dependency in HPA axis reactivity was found in a previous study, where house sparrows in better condition (body mass corrected for tarsus length) had stronger adrenocortical responses (Vagasai et al., 2020). Moreover, this relationship was slightly associated with lower malondialdehyde damage in the red blood cells (Vagasai et al., 2020). We did not detect similar condition-dependency of HPA axis reactivity in liver protein carbonyl damage. However, we observed the opposite pattern in birds recovering from constant light, where condition-dependency of HPA axis reactivity disappeared. These finding highlights that recovery from stressors such as constant light can not only uncouple physiological relationships (HPA and glucose reactivity), but also condition-dependent relationships that could result in differential costs depending on the context.

Mounting stronger HPA responses may lower fitness related traits, particularly during unfavorable environmental conditions or if individuals have already invested in reproduction (Vitousek et al., 2010; Wingfield and Kitaysky, 2002). However, heightened HPA axis reactivity may be beneficial depending on individual condition, breeding experience, or habitat quality (Jessop et al., 2013; Müller et al., 2010; Seltmann et al., 2012). Thus, whether HPA axis reactivity is adaptive will be context-dependent. Future studies should further evaluate if and

how condition-dependency of HPA axis reactivity shifts in its direction and magnitude after exposure and recovery from stressors.

Glucocorticoid receptors revealed nuanced relationships with downstream pathways

Interestingly, liver GR density was negatively associated with liver protein carbonyl damage in control birds, suggesting that a higher abundance of GR may increase and activate signaling pathways that mitigate protein oxidation. In contrast with the control group, birds recovering from light no longer had liver GR abundance associated with liver protein carbonyl damage. Instead, the positive relationship between liver GR abundance and glucose reactivity mediated a negative relationship with liver 4-hydroxynonaneal. Somewhat paradoxically, however, there was positive covariation between liver GR abundance and liver 4-hydroxynonaneal. Overall, these patterns indicate that recovery from stressors such as constant light can weaken or alter the relationship of GR-mediated pathways on oxidative damage, likely due to differential regulation of specific genes.

While we did not assess the role of liver GR in activating specific downstream pathways, GR is an essential transcription factor in multiple molecular pathways (Timmermans et al., 2019; Præstholm et al., 2021). Chromatin Immunoprecipitation Sequencing (ChIP-seq) is a technique that identifies which glucocorticoid response elements are activated in response to GR binding. While GR can activate the nuclear genome, it can also translocate into the mitochondria to stimulate or suppress mitochondrial gene expression, affecting oxidative phosphorylation and ATP output via the electron transport system (Lapp et al., 2019). In fact, an in vitro study utilizing human liver cell culture demonstrated that dexamethasone (a synthetic glucocorticoid) upregulated multiple genes involved in oxidative phosphorylation and altered ATP output (Psarra

and Sekeris, 2011). Mitochondria generate many reactive oxygen species and are vulnerable to oxidative damage through normal cellular respiration. Thus, the role of mitochondria in balancing oxidative phosphorylation, damage, and repair in response to GR-mediated transcription may partly determine physiological costs after exposure to stressors (Manoli et al., 2007). Indeed, dexamethasone suppressed oxidative phosphorylation and ATP production in microglia cell culture and elevated oxidative stress, and administration of a drug that inhibited GR translocation reduced oxidative stress and lowered cellular apoptosis (Dang et al., 2024). These studies indicate a mechanistic link between glucocorticoids, GR, and damage and repair processes involved in the mitochondrial response to stress. While we were unable to determine the specific cause of the different relationships between liver GR abundance and damage in our study, future studies should use techniques like ChIP-seq to identify which specific pathways are up or down regulated in response to GR-mediated transcription. Alternatively, measurements of GR expression and other physiological biomarkers may also clarify the changing role of GR in recovery from stressors. These approaches may reveal how exposure to and recovery from stressors impact molecular networks and their physiological consequences.

Limitations of the study

While path analysis revealed interesting associations between body mass, physiological stress mediators, and damage outcomes, the results of the study should be taken with caution. Although we followed criterion to ensure proper model fit and path-specific comparisons, sample sizes in our analysis were low (Treatment: n = 12; Control: n = 8). Thus, the main benefit of the associations found here is to be used to generate novel hypotheses. Moreover, this study was only conducted in female zebra finches, and patterns may differ in strength or direction in

males. While liver GR density and glucose reactivity showed interesting relationships with oxidative damage outcomes, GR can lead to changes in transcription of thousands of genes in a tissue-specific manner (Oakley and Cidlowski, 2013; Præstholm et al., 2021), and our dataset did not include transcription variables to determine how these parameters specifically affected damage. We assumed GR impacted gluconeogenic pathways in the liver, thereby affecting glucose levels and damage outcomes. However, with pathways not directly mediated by glucose reactivity, we are less certain of casual mechanisms that would explain damage outcomes.

Many patterns found here challenge our understanding of the role of HPA axis reactivity in driving damage outcomes. However, the main limitation of our study may be that we did not find any overall difference in damage markers between treatment groups. Additionally, while we found that exposure to constant light alters relationships between stress response variables and damage outcomes, there is a lack of performance measures after the 2-week recovery period. Thus, we are unable to determine if physiological network rewiring between treatment groups is adaptative, maladaptive, or even plays a central role at all in determining outcomes further related to damage. Nevertheless, the associations found in this study provide a basis to reevaluate our understanding of the mechanistic role of stress responses in activating downstream pathways that determine physiological outcomes, and how these relationships may change after recovery from stressors.

5. Conclusions

Recent work has geared towards a unifying framework to understand the consequences of stress, yet we know little about how shared biological pathways mediated by glucocorticoids shift under different ecological contexts, throughout time, and due to prior stress history. Here,

we found that female zebra finches escaped some long-term physiological costs of constant light, with no persistent changes in DNA, protein, or lipid damage in red blood cells, liver, and pectoralis. At the same time, path analysis revealed distinctive patterns between control and treatment birds, where relationships among morphological and physiological variables changed in direction or magnitude, or disappeared, after the recovery period from constant light. These changes in physiological network linkage may help animals cope with challenges, or they may be signs of ongoing physiological disruption due to light treatment (i.e., homeostatic overload) (Romero et al., 2009; Wada, 2019). While understanding how stressors cause damage is critical, we must combine it with fitness, performance, or health metrics (Wada, 2019; Wada & Heidinger, 2019). Furthermore, how individuals mitigate damage and recover from stress are also important aspects of organismal function. To elucidate how animals appropriately respond to environmental variation, we urge stress physiologists to examine how endocrine flexibility may alter relationships within the physiological regulatory network through studies integrating variation in physiological stress mediators, meaningful molecular endpoints, performance, and fitness-related measures.

Author Contributions:

Kevin Pham: Conceptualization, data curation, formal analysis, Investigation, funding acquisition, Investigation, methodology, project administration, visualization, writing – original draft, writing – review & editing

Madeline Lazenby: Conceptualization, data curation, Investigation, project administration, writing – review & editing

Dr. Natalie R. Gassman: Methodology, validation, formal analysis, data curation, writing – review & editing

Dr. Christine R. Lattin: Methodology, validation, writing – review & editing

Dr. Haruka Wada: Conceptualization, Investigation, funding acquisition, project administration, resources, supervision, writing – review & editing

Acknowledgments

The authors would like to thank the Wada lab for helpful comments on improving the manuscript. The authors would also like to thank Britt Heidinger, Gabrielle Names, Jennifer Grindstaff, and members of the symposium "Identifying the Physiological Mechanisms that Underlie Phenotypic Responses to Rapid Environmental Change" at the 2025 annual meeting for Integrative and Comparative Biology in Atlanta, Georgia. We also thank Ulrike Miller for her gracious invitation to submit to the Journal of Integrative and Comparative Biology. We thank two anonymous reviewers, the Associate Editor, Dr. Elizabeth Addis, and an ad hoc reviewer for comments and suggestions that enhanced the quality and clarity of the manuscript. Finally, we thank the Managing Editor, Dr. Suzanne Miller, for assistance in the preparation of the manuscript.

Funding

K.P was supported by a National Institutes of Health T-32 Training Grant (G-RISE; Grant number: 5T32GM141739) and two NSF IOS grants (IOS-1553657 and IOS-201580) awarded to H.W. N.R.G is supported by startup funding though the University of Alabama, Birmingham and C.R.L is supported by NSF grant IOS-2237423.

Supplementary data:

A supplementary data file is provided

Conflict of Interest:

The authors declare no conflict of interest

Data availability:

Raw data and code will be made available per the request to the corresponding author without due reservations.

References

Angelier, F., Wingfield, J.C., 2012. Importance of the glucocorticoid stress response in a changing world: Theory, hypotheses and perspectives. Gen. Comp. Endocrinol. 190, 118–128. https://doi.org/10.1016/j.ygcen.2013.05.022

Angelier, F., Wingfield, J.C., Weimerskirch, H., Chastel, O., 2010. Hormonal correlates of individual quality in a long-lived bird: A test of the "corticosterone-fitness hypothesis." Biol. Lett. 6, 846–849. https://doi.org/10.1098/rsbl.2010.0376

Anthony-Regnitz, C.M., Wilson, A.E., Sweazea, K.L., Braun, E.J., 2020. Fewer Exposed Lysine Residues May Explain Relative Resistance of Chicken Serum Albumin to In Vitro Protein Glycation in Comparison to Bovine Serum Albumin. J. Mol. Evol. 88, 653–661. https://doi.org/10.1007/s00239-020-09964-y

Bates, D., Mächler, M., Bolker, B.M., Walker, S.C., 2015. Fitting linear mixed-effects models using lme4. J. Stat. Softw. 67. https://doi.org/10.18637/jss.v067.i01

Braun, E.J., Sweazea, K.L., 2008. Glucose regulation in birds. Comp. Biochem. Physiol. - B Biochem. Mol. Biol. 151, 1–9. https://doi.org/10.1016/j.cbpb.2008.05.007

Breuner, C.W., Orchinik, M., Hahn, T.P., Meddle, S.L., Moore, I.T., Owen-Ashley, N.T., Sperry, T.S., Wingfield, J.C., 2003. Differential mechanisms for regulation of the stress response across latitudinal gradients. Am. J. Physiol. - Regul. Integr. Comp. Physiol. 285, 1–3. https://doi.org/10.1152/ajpregu.00748.2002

Cockrem, J.F., 2013. Individual variation in glucocorticoid stress responses in animals. Gen. Comp. Endocrinol. 181, 45–58. https://doi.org/10.1016/j.ygcen.2012.11.025

Cohen, A.A., Martin, L.B., Wingfield, J.C., McWilliams, S.R., Dunne, J.A., 2012. Physiological regulatory networks: Ecological roles and evolutionary constraints. Trends Ecol. Evol. 27, 428–435. https://doi.org/10.1016/j.tree.2012.04.008

Cohen, S., Janicki-Deverts, D., Doyle, W.J., Miller, G.E., Frank, E., Rabin, B.S., Turner, R.B., 2012. Chronic stress, glucocorticoid receptor resistance, inflammation, and disease risk. Proc. Natl. Acad. Sci. U. S. A. 109, 5995–5999. https://doi.org/10.1073/pnas.1118355109

Crespi, E.J., Williams, T.D., Jessop, T.S., Delehanty, B., 2013. Life history and the ecology of stress: How do glucocorticoid hormones influence life-history variation in animals? Funct. Ecol. 27, 93–106. https://doi.org/10.1111/1365-2435.12009

Crino, O.L., Bonduriansky, R., Martin, L.B., Noble, D.W.A., 2024. A conceptual framework for understanding stress-induced physiological and transgenerational effects on population responses to climate change. Evol. Lett. 8, 161–171. https://doi.org/10.1093/evlett/qrad037

Dang, R., Hou, X., Huang, X., Huang, C., Zhao, X., Wang, X., Zhang, N., Yang, Y., Li, N., Liu, S., Yan, P., Fan, P., Song, X., Zhang, S., Deng, Y., Cheng, X., Xia, X., 2024. Effects of the Glucocorticoid-Mediated Mitochondrial Translocation of Glucocorticoid Receptors on Oxidative Stress and Pyroptosis in BV-2 Microglia. J. Mol. Neurosci. 74, 1–15. https://doi.org/10.1007/s12031-024-02192-9

De Kloet, E.R., Reul, J.M.H.M., 1987. Feedback action and tonic influence of corticosteroids on brain function: A concept arising from the heterogeneity of brain receptor systems. Psychoneuroendocrinology 12, 83–105. https://doi.org/10.1016/0306-4530(87)90040-0

Flaherty, R.L., Owen, M., Fagan-Murphy, A., Intabli, H., Healy, D., Patel, A., Allen, M.C., Patel, B.A., Flint, M.S., 2017. Glucocorticoids induce production of reactive oxygen species/reactive nitrogen species and DNA damage through an iNOS mediated pathway in breast cancer. Breast Cancer Res. 19, 1–13. https://doi.org/10.1186/s13058-017-0823-8

Forget, H., Lacroix, A., Bourdeau, I., Cohen, H., 2016. Long-term cognitive effects of glucocorticoid excess in Cushing's syndrome. Psychoneuroendocrinology 65, 26–33. https://doi.org/10.1016/j.psyneuen.2015.11.020

Gilat, N., Fridman, D., Sharim, H., Margalit, S., Gassman, N.R., Michaeli, Y., Ebenstein, Y., 2021. From single-molecule to genome-wide mapping of DNA lesions: repair-assisted damage detection sequencing. Biophys. Reports 1, 100017. https://doi.org/10.1016/j.bpr.2021.100017

Grindstaff, J.L., Beaty, L.E., Ambardar, M., Luttbeg, B., 2022. Integrating theoretical and empirical approaches for a robust understanding of endocrine flexibility. J. Exp. Biol. 225. https://doi.org/10.1242/jeb.243408

Harman, D., 1956. Aging: a theory based on free radical and radiation chemistry. J. Gerontol. 11, 298–300. https://doi.org/10.1093/geronj/11.3.298

Hoffman, A.J., Jr, J.W.F., Kavazis, A.N., Wada, H., 2024. Developmental Thermal Conditioning Regulates Oxidative State and Beak Coloration in Response to Thermal Stressors in Adulthood 97.

Holton, N.W., Ebenstein, Y., Gassman, N.R., 2018. Broad spectrum detection of DNA damage by Repair Assisted Damage Detection (RADD). DNA Repair (Amst). 66–67, 42–49. https://doi.org/10.1016/j.dnarep.2018.04.007

Hurben, A.K., Zhang, Q., Galligan, J.J., Tretyakova, N., Erber, L., 2024. Endogenous Cellular Metabolite Methylglyoxal Induces DNA-Protein Cross-Links in Living Cells. ACS Chem. Biol. 19, 1291–1302. https://doi.org/10.1021/acschembio.4c00100

Hyatt, H.W., Kephart, W.C., Holland, A.M., Mumford, P., Brooks Mobley, C., Lowery, R.P., Roberts, M.D., Wilson, J.M., Kavazis, A.N., 2016. A ketogenic diet in rodents elicits improved mitochondrial adaptations in response to resistance exercise training compared

to an isocaloric western diet. Front. Physiol. 7, 1–9. https://doi.org/10.3389/fphys.2016.00533
Jessop, T.S., Letnic, M., Webb, J.K., Dempster, T., 2013. Adrenocortical stress responses influence an invasive vertebrate's fitness in an extreme environment. Proc. R. Soc. B Biol. Sci. 280. https://doi.org/10.1098/rspb.2013.1444
Khajali, F., Liyanage, R., Wideman, R.F., 2011. Methylglyoxal and pulmonary hypertension in broiler chickens. Poult. Sci. 90, 1287–1294. https://doi.org/10.3382/ps.2010-01120
Kuo, T., McQueen, A., Chen, T. C., and Wang, J. C. 2015. Regulation of Glucose Homeostasis by Glucocorticoids. Adv Exp Med Biol. 2015;872:99-126. doi:10.1007/978-1-4939-2895-8_5
Kuznetsova, A., Brockhoff, P.B., Christensen, R.H.B., 2017. lmerTest Package: Tests in Linear Mixed Effects Models. J. Stat. Softw. 82, 1–26. https://doi.org/10.18637/JSS.V082.I13
Labocha, M.K., Hayes, J.P., 2012. Morphometric indices of body condition in birds: A review. J. Ornithol. 153, 1–22. https://doi.org/10.1007/s10336-011-0706-1

Lapp, H.E., Bartlett, A.A., Hunter, R.G., 2019. Stress and glucocorticoid receptor regulation of mitochondrial gene expression. J. Mol. Endocrinol. 62, R121–R128. https://doi.org/10.1530/JME-18-0152
Lattin, C.R., Kelly, T.R., 2020. Glucocorticoid negative feedback as a potential mediator of trade-offs between reproduction and survival. Gen. Comp. Endocrinol. 286, 113301. https://doi.org/10.1016/j.ygcen.2019.113301
Lattin, C.R., Waldron-Francis, K., Richardson, J.W., de Bruijn, R., Bauer, C.M., Breuner, C.W., Michael Romero, L., 2012. Pharmacological characterization of intracellular glucocorticoid receptors in nine tissues from house sparrow (Passer domesticus). Gen. Comp. Endocrinol. 179, 214–220. https://doi.org/10.1016/j.ygcen.2012.08.007
Lendvai, Á.Z., Ouyang J.Q., Schoenle L.A., Fasanello, V, Haussmann M.F., Bonier, F., Moore I.T., 2014. Experimental Food Restriction Reveals Individual Differences in Corticosterone Reaction Norms with No Oxidative Costs. PLoS One 9(11): e110564. https://doi.org/10.1371/journal.pone.0110564
Liu, Q., Wang, Z., Cao, J., Dong, Y., Chen, Y., 2022. Dim Blue Light at Night Induces Spatial Memory Impairment in Mice by Hippocampal Neuroinflammation and Oxidative Stress. Antioxidants 11. https://doi.org/10.3390/antiox11071218
Manoli, I., Alesci, S., Blackman, M.R., Su, Y.A., Rennert, O.M., Chrousos, G.P., 2007. Mitochondria as key components of the stress response. Trends Endocrinol. Metab. 18, 190–198. https://doi.org/10.1016/j.tem.2007.04.004
McCollum, S.E., Canter, O., Fasanello, V.J., Gronsky, S., Haussmann, M.F., 2024. Birds of a feather age together: telomere dynamics and social behavior predict life span in female Japanese quail (Coturnix japonica). Front. Endocrinol. (Lausanne). 15, 1–13. https://doi.org/10.3389/fendo.2024.1363468
Monaghan, P., Metcalfe, N.B., Torres, R., 2009. Oxidative stress as a mediator of life history trade-offs: Mechanisms, measurements and interpretation. Ecol. Lett. 12, 75–92. https://doi.org/10.1111/j.1461-0248.2008.01258.x
Müller, C., Jenni-Eiermann, S., Jenni, L., 2010. Development of the adrenocortical response to stress in Eurasian kestrel nestlings: Defence ability, age, brood hierarchy and condition. Gen. Comp. Endocrinol. 168, 474–483. https://doi.org/10.1016/j.ygcen.2010.06.009

Murata-Kamiya N., Kamiya H. 2001 Methylglyoxal, an endogenous aldehyde, crosslinks DNA polymerase and the substrate DNA. Nucleic Acids Res. 2001;29(16):3433-3438. doi:10.1093/nar/29.16.3433

Oakley, R.H., Cidlowski, J.A., 2013. The biology of the glucocorticoid receptor: New signaling mechanisms in health and disease. J. Allergy Clin. Immunol. 132, 1033–1044. https://doi.org/10.1016/j.jaci.2013.09.007

Pham, K., Lazenby, M., Yamada, K.L., Lattin, C.R., Wada, H., 2025. Zebra finches (*Taeniopygia castanotis*) display varying degrees of stress resilience in response to constant light. Gen. Comp. Endocrinol. 361, 114644. https://doi.org/10.1016/j.ygcen.2024.114644

Præstholm, S.M., Correia, C.M., Goitea, V.E., Siersbæk, M.S., Jørgensen, M., Havelund, J.F., Pedersen, T., Færgeman, N.J., Grøntved, L., 2021. Impaired glucocorticoid receptor expression in liver disrupts feeding-induced gene expression, glucose uptake, and glycogen storage. Cell Rep. 37, 109938. https://doi.org/10.1016/j.celrep.2021.109938

Psarra, A.M.G., Sekeris, C.E., 2011. Glucocorticoids induce mitochondrial gene transcription in HepG2 cells. Role of the mitochondrial glucocorticoid receptor. Biochim. Biophys. Acta - Mol. Cell Res. 1813, 1814–1821. https://doi.org/10.1016/j.bbamcr.2011.05.014

Ranta, E., Laurila, A., Elmberg, J. 1994. Reinventing the Wheel: Analysis of Sexual Dimorphism in Body Size. Oikos, 70(3), 313–321. https://doi.org/10.2307/3545768

Rosseel, Y. 2012). lavaan: An R Package for Structural Equation Modeling. Journal of Statistical Software, 48(2), 1–36. https://doi.org/10.18637/jss.v048.i02

Rosseel, Y., 2014. The lavaan tutorial. lavaan Tutor. 37.

Sapolsky, R.M., Romero, L.M., Munck, A.U., 2000. How do glucocorticoids influence stress responses? Integrating permissive, suppressive, stimulatory, and preparative actions. Endocr. Rev. 21, 55–89. https://doi.org/10.1210/er.21.1.55

Sato, H., Takahashi, T., Sumitani, K., Takatsu, H., Urano, S., 2010. Glucocorticoid generates ROS to induce oxidative injury in the hippocampus, leading to impairment of cognitive function of rats. J. Clin. Biochem. Nutr. 47, 224–232. https://doi.org/10.3164/jcbn.10-58

Seltmann, M.W., Öst, M., Jaatinen, K., Atkinson, S., Mashburn, K., Hollmén, T., 2012. Stress responsiveness, age and body condition interactively affect flight initiation distance in breeding female eiders. Anim. Behav. 84, 889–896. https://doi.org/10.1016/j.anbehav.2012.07.012

Sharma, A., Goyal, R., 2020. Long-term exposure to constant light induces dementia, oxidative stress and promotes aggregation of sub-pathological Aβ42 in Wistar rats. Pharmacol. Biochem. Behav. 192, 172892. https://doi.org/10.1016/j.pbb.2020.172892

Rodnan, G. P., Ebaugh, F. G., Jr., Fox, M. R. 1957. The life span of the red blood cell and the red blood cell volume in the chicken, pigeon and duck as estimated by the use of Na2Cr51O4, with observations on red cell turnover rate in the mammal, bird and reptile. Blood, *12*(4), 355–366. https://doi.org/10.1182/blood.V12.4.355.355

Spencer, K.A., Heidinger, B.J., D'Alba, L.B., Evans, N.P., Monaghan, P., 2010. Then versus now: Effect of developmental and current environmental conditions on incubation effort in birds. Behav. Ecol. 21, 999–1004. https://doi.org/10.1093/beheco/arq090

Streiner, D.L., 2006. Building a better model: An introduction to structural equation modelling. Can. J. Psychiatry 51, 317–324. https://doi.org/10.1177/070674370605100507

Sweazea, K.L., 2022. Revisiting glucose regulation in birds – A negative model of diabetes complications. Comp. Biochem. Physiol. Part - B Biochem. Mol. Biol. 262, 23332973. https://doi.org/10.1016/j.cbpb.2022.110778

Szwergold B.S., Miller C.B., 2014. Potential of birds to serve as pathology-free models of type 2 diabetes, part 2: do high levels of carbonyl-scavenging amino acids (e.g., Taurine) and low concentrations of methylglyoxal limit the production of advanced glycation end products? Rejuvenation Res 17:347–358. https://doi.org/10.1089/rej.2014.1561

Taff, C.C., Baldan, D., Mentesana, L., Ouyang, J.Q., Vitousek, M.N., Hau, M., 2024a. Endocrine flexibility can facilitate or constrain the ability to cope with global change. Philos. Trans. R. Soc. B Biol. Sci. 379. https://doi.org/10.1098/rstb.2022.0502

Taff, C.C., McNew, S.M., Campagna, L., Vitousek, M.N., 2024b. Corticosterone exposure is associated with long-term changes in DNA methylation, physiology and breeding decisions in a wild bird. Mol. Ecol. 33, 1–13. https://doi.org/10.1111/mec.17456

Taff, C.C., Vitousek, M.N., 2016. Endocrine Flexibility: Optimizing Phenotypes in a Dynamic World? Trends Ecol. Evol. 31, 476–488. https://doi.org/10.1016/j.tree.2016.03.005

Teixeira, K.R.C., dos Santos, C.P., de Medeiros, L.A., Mendes, J.A., Cunha, T.M., De Angelis, K., Penha-Silva, N., de Oliveira, E.P., Crispim, C.A., 2019. Night workers have lower levels of antioxidant defenses and higher levels of oxidative stress damage when compared to day workers. Sci. Rep. 9, 1–11. https://doi.org/10.1038/s41598-019-40989-6

ter Heegde, F., De Rijk, R.H., Vinkers, C.H., 2015. The brain mineralocorticoid receptor and stress resilience. Psychoneuroendocrinology 52, 92–110. https://doi.org/10.1016/j.psyneuen.2014.10.022

Timmermans, S., Souffriau, J., Libert, C., 2019. A general introduction to glucocorticoid biology. Front. Immunol. 10. https://doi.org/10.3389/fimmu.2019.01545

Vágási, C.I., Tóth, Z., Pénzes, J., Pap, P.L., Ouyang, J.Q., Lendvai, Á.Z., 2020. The Relationship between Hormones, Glucose, and Oxidative Damage Is Condition and Stress Dependent in a Free-Living Passerine Bird. Physiol. Biochem. Zool. 93, 466–476. https://doi.org/10.1086/711957

Vitousek, M.N., Jenkins, B.R., Safran, R.J., 2014. Stress and success: Individual differences in the glucocorticoid stress response predict behavior and reproductive success under high predation risk. Horm. Behav. 66, 812–819. https://doi.org/10.1016/j.yhbeh.2014.11.004

von Holdt, B.M., Kartzinel, R.Y., van Oers, K., Verhoeven, K.J.F., Ouyang, J.Q., 2023. Changes in the rearing environment cause reorganization of molecular networks associated with DNA methylation. J. Anim. Ecol. 92, 648–664. https://doi.org/10.1111/1365-2656.13878

Wada, H., 2019. Damage-Fitness Model: the missing piece in integrative stress models. Stress 22, 548–562. https://doi.org/10.1080/10253890.2019.1614556

Wada, H., 2008. Glucocorticoids: Mediators of vertebrate ontogenetic transitions. Gen. Comp. Endocrinol. 156, 441–453. https://doi.org/10.1016/j.ygcen.2008.02.004

Wada, H., Kriengwatana, B.P., Steury, T.D., Macdougall-Shackleton, S.A., 2018. Incubation temperature influences sex ratio and offspring's body composition in Zebra finches (Taeniopygia guttata). Can. J. Zool. 96, 1010–1015. https://doi.org/10.1139/cjz-2017-0099

Wingfield, J.C., Kitaysky, A.S., 2002. Endocrine responses to unpredictable environmental events: Stress or anti-stress hormones? Integr. Comp. Biol. 42, 600–609. https://doi.org/10.1093/icb/42.3.600

Xia, Y., Yang, Y., 2019. RMSEA, CFI, and TLI in structural equation modeling with ordered categorical data: The story they tell depends on the estimation methods. Behav. Res. Methods 51, 409–428. https://doi.org/10.3758/s13428-018-1055-2

Yang, Y., Cong, W., Liu, J., Zhao, M., Xu, P., Han, W., Wang, D., Zhao, R., 2022. Constant light in early life induces fear-related behavior in chickens with suppressed melatonin secretion and disrupted hippocampal expression of clock- and BDNF-associated genes. J. Anim. Sci. Biotechnol. 13, 1–11. https://doi.org/10.1186/s40104-022-00720-4

Yap, K.N., Andreasen, V.A., Williams, A.S., Yamada, K.L.Y., Zikeli, S., Kavazis, A.N., Hood, W.R., 2022. The persistent effects of corticosterone administration during lactation on the physiology of maternal and offspring mitochondria. J. Exp. Biol. 225. https://doi.org/10.1242/jeb.244171

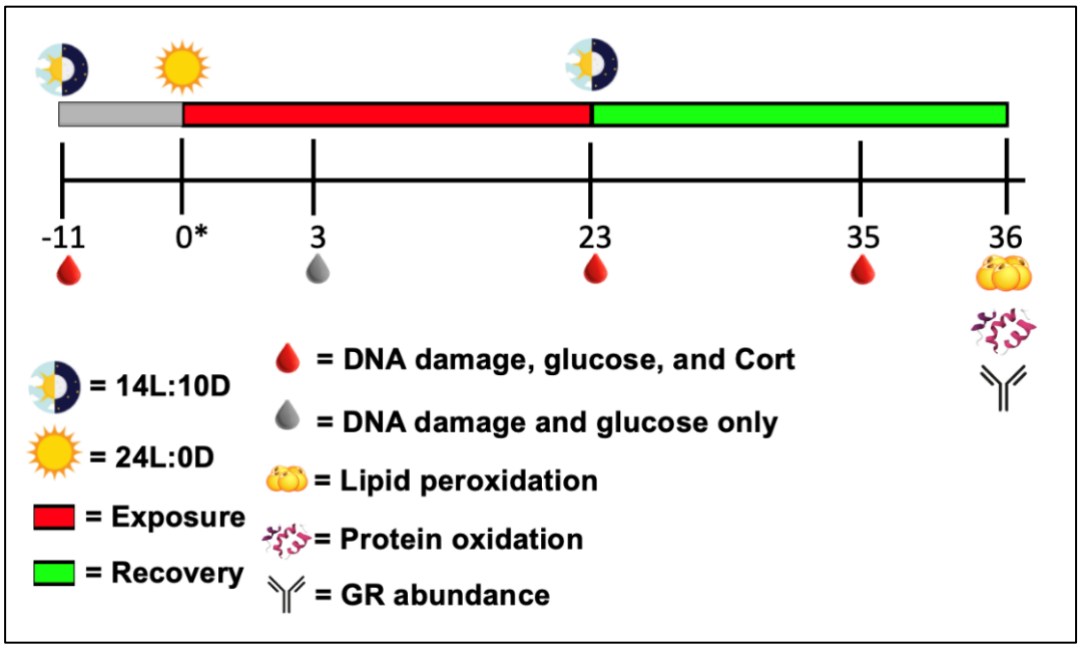

Figure 9. Illustration of the sampling timeline for treatment birds only. Slightly modified from Figure 1 from Pham et al., (2025). The numbers -11, 3, 23, 35, and 36 on the figure lines correspond to sampling collection timepoints in days: -11 = Pretreatment, 3 and 23 = during Treatment, and 35 and 36 = Posttreatment, respectively. The number 0* corresponds to the beginning of experimental treatment, in which treatment birds were exposed to 24 h of constant light. 24L:0D and 14L:10D photoperiods are illustrated by a full sun icon and a sun/moon icon, respectively. The red drop icon indicates when broad-spectrum DNA damage, glucose and Cort were quantified from blood samples. The grey drop icon indicates that only broad-spectrum DNA damage and glucose were quantified from blood samples. Broad-spectrum DNA damage was quantified after 12 days of recovery, while lipid and protein markers for oxidative damage and liver glucocorticoid receptor density were quantified when birds were euthanized the following day, indicated by lipid, protein, and receptor icons, to reduce effects of capture and restraint from the previous day of sampling. Thus, oxidative damage markers and liver

glucocorticoid receptor abundance are measured after 13 days of recovery, The same sampling schedule was simultaneously followed for the control group, without the constant light treatment.

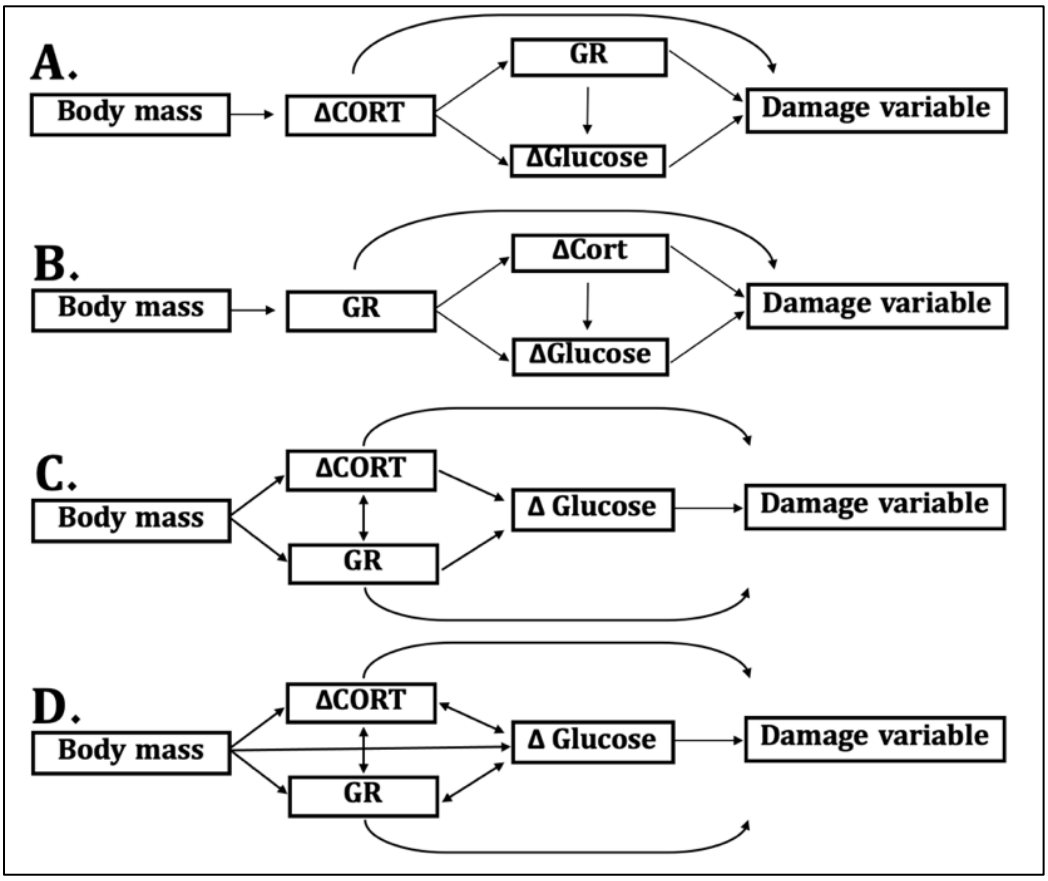

Figure 10: List of a priori path analysis model predictions (A-D). Single headed arrows indicate causal relationships, while double-headed arrows indicate bidirectional covariation. All models were tested for each damage metric; however, only the top model results are shown. The best fitting path model that explained all three damage variables was model A, in which HPA axis reactivity was the main condition-dependent trait. ΔCORT = change in glucocorticoid hormone concentrations from baseline to restraint-induced; ΔGlucose = change in circulating blood glucose levels from baseline to restraint-induced; GR = glucocorticoid receptor density measured in liver.

Mode	Damage Variable	X^2	SRMR	AICc	CFI
A – HPA axis reactivity as the main condition-dependent trait	Red blood cell DNA damage	2.7	0.051	54.87	1.0
	Liver protein carbonyls	2.4	0.040	40.63	1.0
	Liver 4-hydroxynonaneal	5.1	0.075	50.65	1.0
B – Liver glucocorticoid receptor density as the main condition-dependent trait	Red blood cell DNA damage	6.1	0.107	58.27	0.99
	Liver protein carbonyls	5.8	0.107	44.02	1.0
	Liver 4-hydroxynonaneal	11.8	0.099	57.31	0.79
C – HPA axis reactivity and liver glucocorticoid receptor density as two interconnected traits	Red blood cell DNA damage	1.6	0.058	64.37	1.0
	Liver protein carbonyls	1.2	0.061	50.12	1.0
	Liver 4-hydroxynonaneal	7.3	0.083	63.41	1.0
D – HPA axis reactivity, glucose reactivity, and liver glucocorticoid receptor density as three interconnected traits	Red blood cell DNA damage	1.0	0.036	71.58	1.0
	Liver protein carbonyls	0.64	0.018	57.33	1.0
	Liver 4-hydroxynonaneal	6.7	0.062	70.62	0.83

Table 1: List of model outputs (A-D) across three damage markers. Diagnostics were generated with data from all N = 20 birds included in the models (n = 12 treatment birds and n = 8 control birds). A "group = treatment" argument was included to assess standardized path coefficients in both control and treatment birds. To ensure proper model fit, we used a cut-off value of ≤ 0.08 for Square Root Mean Residuals (SRMR), 0.95 for Comparative Fit Index (CFI), and corrected Akaike Information Criterion (AICc) scores with differences ≥ 2 to determine the best fit model. We utilized AICc as the final determinant to select the best model fit, which designated model A.

Model A damage marker	Model constraints	χ^2	Difference in χ^2	P-value
Red blood cell DNA damage	Unconstrained	2.7	NA	NA
	Constrained regressions	12.7	9.99	0.19
	Constrained regressions and intercepts	16.1	3.4	0.48
Liver protein carbonyls	Unconstrained	2.4	NA	NA
	Constrained regressions	20.4	18.1	0.01
	Constrained regressions and intercepts	22.97	2.5	0.17
Liver 4-hydroxynonaneal	Unconstrained	5.1	NA	NA
	Constrained regressions	17.9	12.8	0.01
	Constrained regressions and intercepts	24.3	6.4	0.17

Table 2: Comparison of χ^2 differences between unconstrained and constrained models across three damage markers. The unconstrained model was first compared to the constrained regressions, and then the constrained regression model was further compared to constrained regressions and intercepts. Significant p-values (< 0.05) are bolded, indicate a significant difference in χ^2, and indicate that the unconstrained model is the best model.

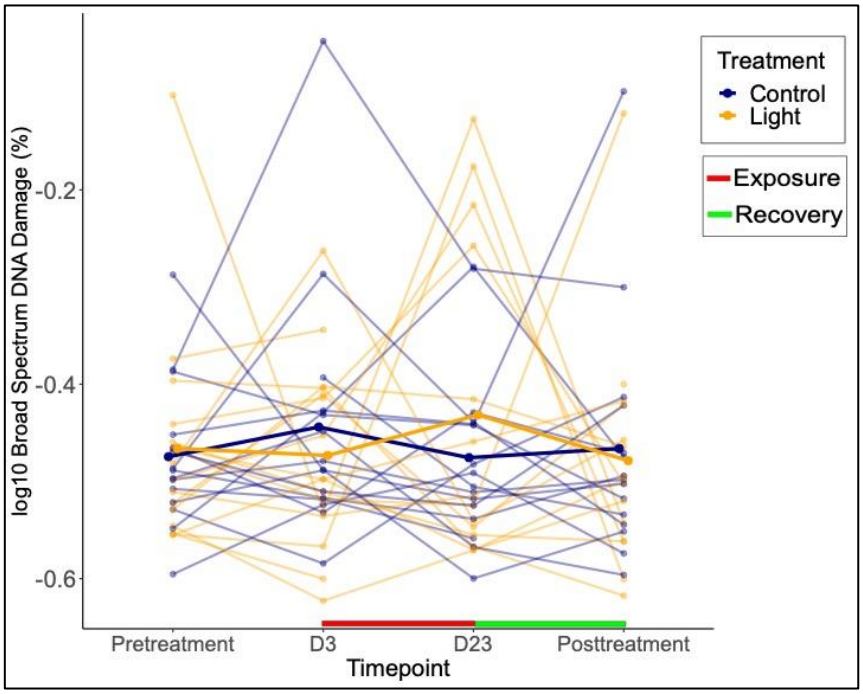

Figure S2: A spaghetti plot of red blood cell DNA damage of each individual over time using raw data. Timepoint is on the x-axis that spans across all collection timepoints (-11 = Pretreatment, D3 and D23 = Day 3 and 23 of treatment, and posttreatment = 12 day recovery). Log transformed Average %DNA damage is shown with raw data points with connecting lines and points representing one individual. Darker colored, solid lines indicate average DNA damage across timepoints.

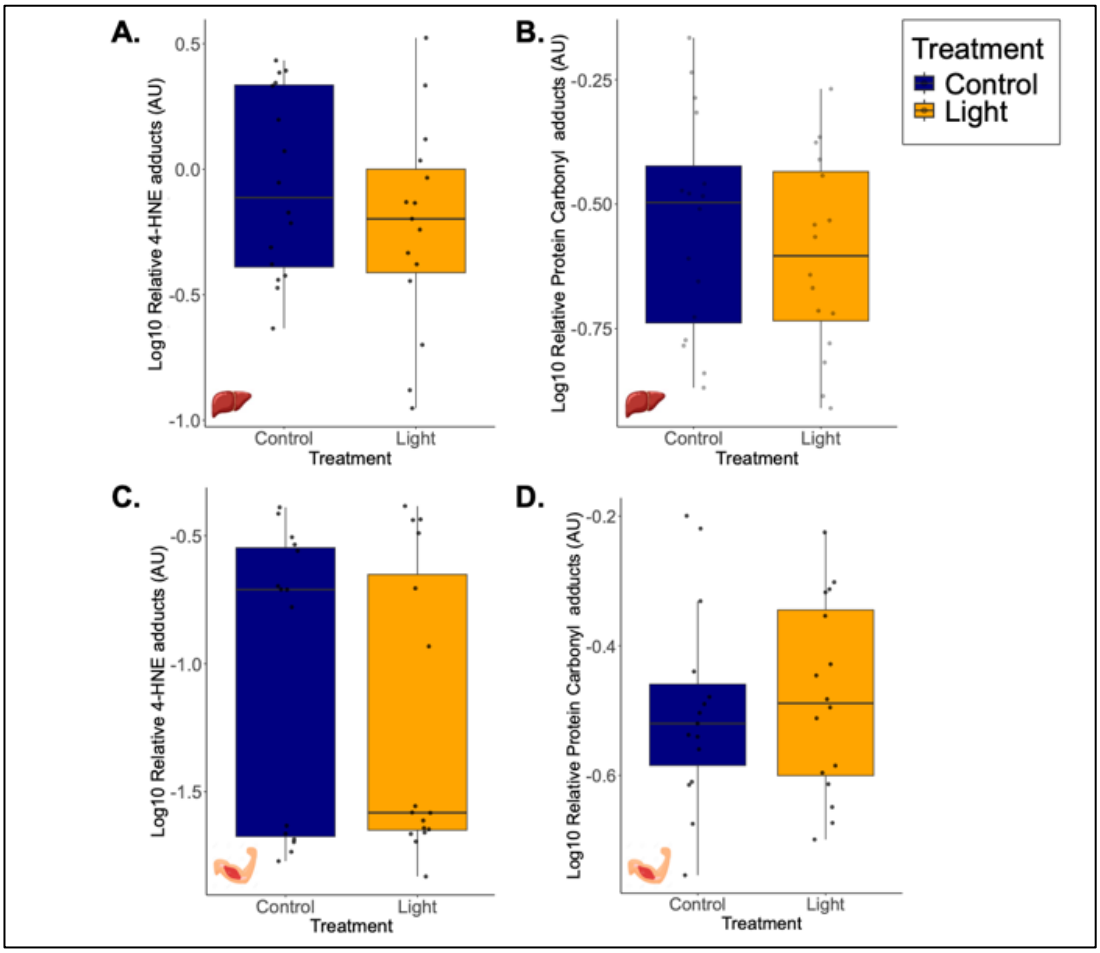

Figure S3 A-D: Oxidative damage in the liver (indicated with a liver icon) and pectoralis muscle (indicated by the flexing bicep icon) 13 days after treatment. Treatment groups are indicated on the x-axis (Control = blue; Treatment = orange), with log transformed relative abundance of each respective protein of interest on the y-axis. Box and violin plots are overlaid to indicate variance of data with solid lines indicating the median value. The solid black line indicates the median value, with the upper 75% quartile and lower 25% quartile depicted, and the interquartile representing 50% of the observed data.

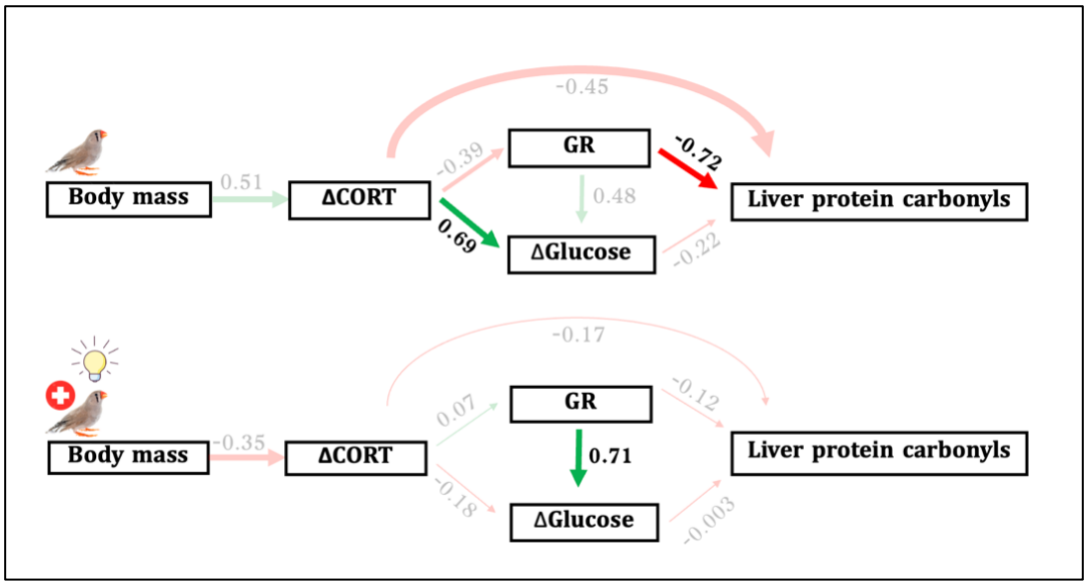

Figure 11. HPA axis reactivity as the main condition-dependent trait for liver protein carbonyls. Single-headed arrows indicate causal relationships, while double-headed arrows indicate covariation. Green arrows indicate positive relationships, while red arrows indicate negative relationships. Standardized beta estimates are listed, with the thickness of the arrows indicating the magnitude of the relationship. Significant relationships are bolded. Control birds are indicated on the top, while treatment birds (recovering from the light treatment) are indicated on the bottom. ΔCORT = change in glucocorticoid hormone concentrations from baseline to restraint-induced; ΔGlucose = change in glucose concentrations from baseline to restraint-induced. GR = glucocorticoid receptor density measured in liver.

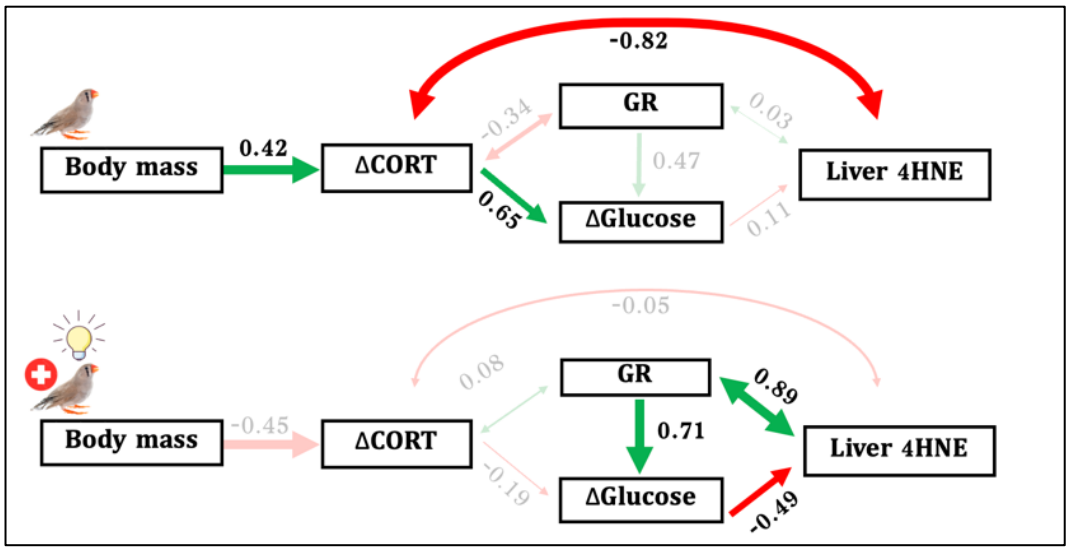

Figure 12. HPA axis reactivity as the main condition-dependent trait that explained liver 4-hydroxynonaneal damage. Single headed arrows indicate causal relationships, while double headed arrows indicate bidirectional covariation. Green arrows indicate positive relationships, while red arrows indicate negative relationships. Standardized beta estimates are listed, with the thickness of the arrows indicating the magnitude of the relationship. Significant ($p < 0.05$) and nearly significant ($p < 0.10$) relationships are bolded. Control birds are indicated on the top, while treatment birds (recovering from the light treatment) are indicated on the bottom. ΔCORT = change in glucocorticoid hormone concentrations from baseline to restraint-induced; ΔGlucose = change in glucose concentrations from baseline to restraint-induced. GR = glucocorticoid receptor density measured in liver.

Chapter 4: Continuous light, but not darkness, has sex and tissue-specific effects on mitochondrial physiology in house mice (*Mus musculus*)

*_In revision_ at the Journal of Experimental Zoology Part A: Ecological and Integrative Physiology

Authors: Kevin Pham[*1], KayLene YH Yamada[1], Emma M. Rhodes[1], Agata. M. Rudolf[1,2], and Wendy R. Hood[1]

[1]Department of Biological Sciences, Auburn University, Auburn, AL 36849, USA

[2]Space Technology Centre, AGH University of Krakow, Krakow, Poland

Key words: Light at night, house mouse, mitochondria, oxidative damage, sex, physiology

Abstract

Exposure to altered nighttime lighting conditions has become common in today's modern world. Circadian and circannual processes are at the core of all organisms across the tree of life, therefore identifying physiological consequences due to disruptive patterns of light at night at variable intensities and spectral compositions is essential. In this study, 36 male and female wild-derived house mice (*Mus musculus)* were exposed to continuous light, darkness, or a control light cycle for six weeks. We examined animals' bioenergetic capacity at the whole-organism and subcellular level, while also measuring morphological indicators of metabolic phenotypes and physiological trade-offs in oxidative damage. We found that six weeks of constant light increased maximum mitochondrial respiration via complex I in the livers of female mice. We did not detect a similar response in males or changes in any mitochondrial respiratory variables in the skeletal muscle of either sex under constant light or darkness. Furthermore, we did not detect any difference in mitochondrial volume or lipid peroxidation in the liver between treatment groups. Surprisingly, there were no differences in body mass or fat pads due to treatment, contrasting many other studies investigating the effects of light at night on mammalian physiology. Our data indicate that wild-derived mice, particularly females, are better able to cope to an altered light environment via changes in mitochondrial respiratory capacity in the liver.

Introduction:

Human-induced environmental change has dramatically modified the ecological landscape. One consequence of this disturbance is an altered nighttime environment, caused by increased prevalence of sensory pollutants, such as artificial light, at varying spectral compositions, intensities, and types (Bumgarner and Nelson, 2021; Navara and Nelson, 2007;

Ouyang et al., 2018). Appropriate timing of light exposure is critical to align biological processes such as foraging or sleep/wake cycles to the external environment, such that they are optimally timed to activity periods or when resources are present (Ouyang et al., 2018).

Numerous physiological and behavioral traits are vulnerable to altered lightning conditions, yet one trait that appears to be consistently impacted is metabolism, regardless of temporal niche, or lighting regime (Nelson and Chbeir, 2018). Moreover, pathologies induced by the subsequent metabolic disruption, such as hyperglycemia, insulin resistance, or oxidative damage are associated with the development of metabolic syndromes and even psychiatric disorders (Hohor et al., 2023; Sharma and Goyal, 2020).

While many studies have identified physiological indicators of metabolic diseases associated with exposure to light at night, further research is needed to clarify its impact on bioenergetics. Even just two weeks of dim light at night (< 5 lux) suppresses metabolic rate in lab mice and alters the respiratory exchange ratio (*i.e.,* respiratory quotient; RQ). This change biases energy production towards carbohydrates rather than fat, potentially leading to greater fat storage, and consequently, weight gain (Borniger et al., 2014). Furthermore, lighting intensities as little as 0.3 lux at night reduces energy expenditure in great tits *(Parus major)*, but this may be an indirect effect that reflects a reduction in foraging effort in a resource rich environment, rather than metabolic disruption (Welbers et al., 2017). Given that other factors such as body size, age, or sex contributes to variation in bioenergetic capacity, the physiological mechanisms driving shifts in metabolic demands are still largely unresolved (Koch et al., 2021; Metcalfe et al., 2023). This is especially important to consider as shift work and light at unnatural times become ubiquitous components of modern-day life and are inexplicitly linked to metabolic disruption. One possibility is that the range or capacity of mitochondrial respiration across tissues may

constrain or contribute to the impact of light at night on whole-organism respiration (Casagrande; 2023; Metcalfe et al., 2023; Salin et al., 2016).

Mitochondria are essential organelles that fuel metabolic processes by producing 90% of the body's adenosine-triphosphate (ATP) (Pizzorno, 2014). As mitochondria are major sites for generating reactive oxygen species (ROS) through normal cellular respiration, exogenous challenges could affect efficiency in mitochondrial machinery through changes in morphology, abundance, or size across tissues that translate into whole organismal costs or benefits (Heine and Hood, 2020; Hood et al., 2018).

Mitochondria respond readily to exogenous challenges, showing phenotypic flexibility in morphology and respiratory capacity to seasonality, life-history, and environmental perturbation in a tissue-specific manner (Rhodes et al., 2024; Treidel et al., 2023; Sokolova 2018). Mitochondrial respiratory function can also be enhanced through moderate stressors, or extended activity that is mediated by multiple signaling molecules, known as mitochondrial hormesis (Hood et al., 2018; Palmeira, 2019). From an exercise perspective, a single brief bout of high intensity interval training resulted in concomitate increases in mRNA gene expression of *PGC*-1α (a marker of mitochondria biogenesis) three hours post exercise and protein expression within 24 hours in human skeletal muscle (Granata et al., 2018). Moreover, extended high intensity interval training (at least up to six bouts) enhanced cytochrome C oxidase enzymatic activity, resulting in significantly higher state 3 maximum respiratory function in skeletal muscle (Jacobs et al., 2013). However, chronic challenges can suppress mitochondrial respiratory function and increase oxidative damage across tissues, which are both implicated in metabolic and age-related diseases (Manoli et al., 2007; Natarajan et al., 2020; Picard et al., 2014; Picard and McEwen, 2018). Therefore, how mitochondria balance between adaptive responses and physiological

consequences across tissues may provide critical insights into the mechanisms that facilitate or constrain their role in driving whole-organismal metabolic rates.

Although the link between light at night and metabolic disruption have clearly been demonstrated, most studies primarily focus on laboratory strains of mice (Fleury et al., 2020). This is important to highlight, as many laboratory strains of mice display phenotypic differences from wild and wild-derived mice as an artifact of artificial selection and maintenance in environments that are virtually invariable (Abolins et al., 2017; Chalfin et al., 2014; Dohm et al., 1994). For example, lab mice are larger than their natural or wild-derived counterpart (Abolins et al., 2017). Moreover, within a commonly utilized lab strain (C57BL/6), a meta-analysis points to 73% of phenotypic traits showing sexual dimorphism (Wilson et al., 2022). These phenotypic differences are critical to acknowledge, especially as more research regarding sleep loss and circadian rhythm disruption highlights the role of sex in determining vulnerability or susceptibility to detrimental health outcomes, particularly in females (Qian et al., 2019; Rångtell et al., 2019; Santhi et al., 2016). Therefore, relying on laboratory mice strains' responses to inform public health, without consideration of how other populations may react to the same challenge, may paint an incomplete picture that neglects alternative responses through phenotypic plasticity or flexibility.

It is often difficult to obtain repeated measures in a natural population or control for confounding variables such as age that is known to play a role in magnifying the effects of circadian disruption (Panagiotou and Deboer, 2020). Thus, leveraging a wild-derived rodent model that retains sensitivity to stressors, coupled with a tightly controlled laboratory study, provides a unique opportunity to disentangle the complex nature of how animals combat an altered nighttime environment.

In this study, both male and female wild-derived house mice (*Mus musculus)* were exposed to constant light or darkness for a total of six weeks, with controls maintained under normal lighting conditions. We measured resting metabolic rate (RMR) before exposure to light treatments and after five weeks of exposure, while monitoring changes in body mass weekly. At the end of the six-week treatment period, we measured mitochondrial respiration in the liver and hindlimb skeletal muscles. The liver is the main site of metabolism, and multiple physiological traits point to the liver being the prime target underlying disease outcomes. Moreover, skeletal muscle may be a prime target to evaluate changes in respiration, as activity levels are commonly seen to be disrupted due to altered lighting conditions.

We hypothesized that chronic, aperiodic lighting conditions would result in physiological disruption, leading to suppression of mitochondrial function and resting metabolic rate, therefore resulting in common indicators of metabolic phenotypes such as weight gain and fat accumulation. Specifically, we predicted that constant light would increase body mass over time and result in heavier fat pads compared to controls and constant darkness. Furthermore, we predicted that constant light would suppress respiratory capacity, indicating metabolic inefficiency and resulting in higher oxidative damage compared to constant darkness and controls. Because sexes may differ in their sensitivity to light at night, we predicted that females would display more pronounced changes in all variables measured.

2. Methods and Materials

2.1 Animal husbandry

Adult male and female wild-derived house mice (Mus musculus) were the model system used in this experiment. Wild-derived animals are shown to capture natural variation in

physiological responses that are absent in lab mice. Mice were born at Auburn University and descended from individuals originally obtained by Wayne Potts in Gainesville, FL. Genetic diversity was maintained by crossing with mice collected from the Farallon Islands, USA (John Godwin, NCSU) in 2019. Mice utilized in this study were approximately 22 generations removed from the wild. Animals were held in standard polypropylene rodent boxes (29cm x 19cm x 13cm) with a mouse wheel for enrichment and ad lib access to water and rodent chow (Teklad Global Rodent Chow 2019). Animals were housed at Auburn University, Auburn, AL. Female mice were housed as pairs, while males were housed individually according to IACUC standards. This experiment was conducted in January 2022, with animals maintained under a standardized photoperiod of 10L:14D to mimic sunrise and sunset conditions. All animal husbandry and experimental procedures were approved by the Auburn University Institutional Animal Care and Use Committee (PRN 2022-4042).

2.2 Experimental Design

Male (n = 18) and female (n = 18) mice (N= 36) were weight and age-matched into three groups (n = 6/treatment/sex), constant light (LL; 24L:0D; 160.74 lux ± 14.17 SD), constant darkness (DD; 0L:24D; 0 lux), or a control group under a normal light cycle (LD; 10L:14D; 159.68 lux ± 17.56 SD) (**Fig. 13)**. Average age for each group at the beginning of the experiment is as follows: constant light (4.3 months ± 0.65 SD), constant darkness (4.4 months ± 0.52 SD), and controls (4.25 months ± 0.62 SD). Each treatment group comprised of six males and six females. All individuals were given at least one month to acclimatize to a consistent 10L:14D light cycle provided with light emitting diodes (LEDs) at a color temperature of 5000K. Start dates were staggered to accommodate constraints on the number of animals that could be held in

the metabolic chambers and the number of animals that could be processed for mitochondrial respiration on any given day. Six animals entered the experiment each week. On each start date, two animals were randomly selected from each group, baseline resting metabolic rate (RMR) was measured, and then after two days of recovery, mice were moved into the room associated with their assigned light/dark cycle. This pattern followed for six weeks, resulting in a total of six cohorts of mice that followed a staggard experimental start-to-finish timeline. Animal husbandry tasks and the amount of disturbance was kept consistent with the addition of each cohort into respective treatment groups. A red headlamp was utilized at all times during animal husbandry of mice held in constant darkness. Treatment lasted for a total of six weeks (42 days), with body mass measures obtained to the nearest 0.1 (g) obtained every week (7 days). RMR was remeasured after five weeks (35 days) of treatment. After six weeks (42 days) of treatment, animals were quickly euthanized via decapitation utilizing a rodent guillotine. We collected small portions of the liver and hindlimb muscles to the nearest 0.01 (mg) to measure mitochondrial physiology and oxidative damage by Hansatech Oxytherm and Western blot, respectively. Lastly, we collected fat pads to the nearest 0.01mg, specifically, subcutaneous, retroperitoneal, and gonadal (epididymal/parametrial) adipose tissue. Two mice died during the acclimation period; the cause of their deaths was unclear. The limited data collected from these mice was removed from analysis.

2.3 Resting metabolic rate (RMR)

Resting metabolic rate (RMR) was quantified using standard push flow-through respirometry, with animal held in plastic chambers maintained at 30°C (thermoneutrality) (Sable Systems International, Las Vegas, NV). Individuals were measured for a total of 11 hours

between the hours of ~0600-1700 following methods described in (Yamada et al., in review). Each chamber (6 animals and 1 blank chamber) was fed oxygen dried using Drierite at a flow rate of approximately 500ml/min. Oxygen levels were measured by subsampling (250ml/min) between each chamber every ten minutes, with oxygen consumption values normalized to the blank chamber with no animal using a FoxBox Gas Analysis System (Sable Systems International, Las Vegas, NV). The first three hours of data collection were excluded from the analysis, as animals were acclimating to the chambers, decreasing activity levels, and switching to a fasted state (respiratory quotient <0.7 for all animals). At the end of the 11-hour sampling, each mouse had several ten-minute oxygen consumption readings. Readings in which the oxygen consumption spiked were thrown out, as this indicates measurement error due to external factors (e.g., door shutting). After excluding 3 hours towards the beginning of measurement, as well as spiked readings, each individual had a range of 1-5 total readings. The lowest sixty seconds of oxygen consumption from each ten minute reading was averaged for each individual using ExpeData software (version 1.9.27, Sable Systems International, Las Vegas, NV). After 35 days of treatment, we remeasured individuals' oxygen consumption following the same methodology.

2.4 Mitochondrial Physiology

We measured mitochondrial function using methods previously described in (Yap et al., 2022) and Yamada et. al., (*in review*). Briefly, approximately 0.5 g of liver tissue was placed in 10mL of ice-cold liver isolation buffer (250mmol/L sucrose, 5 mmol/L 2-(4-(2-hydroxyethyl)-1-piperazinyl) ethanesulfonic acid (HEPES), and 1 mmol/L ethylene glycol-bis(2-aminoethyl ether)-N,N,N',N'-tetraacetic acid (EGTA)). Approximately 0.8-1g of muscle tissue from both hindlimbs were placed in 10 mL of ice-cold muscle isolation buffer at a pH of 7.4 (100mmol/L

KCl, 40 mmol/L Tris-HCl, 10 mmol/L Tris base, 1 mmol/L MgSO4, 0.1 mmol/L Ethylenediaminetetraacetic acid (EDTA), 0.2 mmol/L ATP, and 0.2% free fatty acid bovine serum albumin (BSA)). Both tissues were minced with scissors before going through separate homogenization and centrifugation processes. For the liver, we used a Potter-Elvehjem PTFE pestle and glass tube to homogenize tissue, while we used a handheld Polytron at half power for 5 seconds for muscle tissue. A protease was added to muscle tissue and continuously mixed for 7 minutes, before terminating the digestion by adding 10 mL of muscle isolation buffer. Both homogenates were then centrifuged in a prechilled 4°C at 500 *x g* for 10 minutes and passed through double-layered cheesecloth. Both homogenates were spun again at 3500 *x g* for a total of 10 minutes. The supernatant was discarded, and the mitochondrial pellet was collected for both tissues. Another 10 mL of liver and muscle isolation buffer were added to the respective mitochondrial pellets and spun again for 10 minutes at 3500 *x g*. For the liver, the final mitochondrial pellet was resuspended in mannitol sucrose at a pH of 7.4 (220 mmol/L mannitol, 70 mmol/L sucrose, 10 mmol/L Tris-HCl, and 1 mmol/L EGTA) and placed on ice. For the muscle, there was one additional centrifugation process, in which 10 mL of muscle isolation buffer (without BSA) was added to the mitochondrial pellet and spun at 3500 *x g* for 10 minutes. The supernatant was discarded, resuspended in mannitol sucrose, and placed on ice before oxygen consumption was measured.

Oxygen consumption was measured from each isolated mitochondrial sample from the liver and skeletal muscle in a respiration chamber (Hansatech Instruments, Lynn, United Kingdom). A standardized 20 µL of isolated mitochondria was pipetted into the chamber containing respiration buffer at a pH of 7.0 (100mmol/L KCl, 50 mmol/L MOPS, 10 mmol/L KH2PO4, 20 mmol/L glucose, 10 mmol/L MgCl2, 1 mmol/L EGTA, and 0.2% BSA). We

stimulated maximum mitochondrial respiration (state 3) by adding substrates pyruvate (2 mmol/L), malate (2 mmol/L), and glutamate (2 mmol/L) responsible for donating elections through complex I and substrates rotenone (0.5 mmol/L) and succinate (5 mmol/L) responsible for donating elections through complex II, in addition to adenosine diphosphate (0.25 mmol/L; ADP) to each chamber. Basal mitochondrial respiration (state 4) was determined after all ADP was phosphorylated and leak respiration (state 4_{leak}) was determined by adding oligomycin as an inhibitor of ATP synthase. State 4leak measures the basal oxygen requirements necessary to maintain the proton motive force by recycling proteins that are not utilized by ATP synthase. The respiratory control ratio (RCR), a relative measure describing mitochondrial function, was calculated as the ratio between state 3 and state 4_{leak} (state 3/state 4_{leak}). To normalize mitochondrial respiration variables (state 3, 4, 4_{leak}), we measured total protein content of each isolated mitochondrial sample against a standard linear curve using Bradford assay (VWR Cat# 97065-020).

2.5 Citrate synthase (CS) activity

After obtaining protein concentration, small aliquots of isolated liver mitochondria were diluted using ultra-pure water to obtain a final concentration of 0.5 µg/µL across all samples. To quantify citrate synthase enzymatic reaction, a reaction mixture was prepared (0.125 M Tris-HCL, 3mM Acetyl CoA, and 10mM 5,5'-dithiobis-2-nitrobenzoic acid; DTNB). A standardized 20 µL of sample (10 µg of total mitochondrial protein) was added to a 96-well plate with 250 µL reaction mixture and the reaction was initiated by adding 5 µL of oxaloacetate (50 mM). The acid reduction of 5,5'-dithiobis-2-nitrobenzoic acid was measured every 10 seconds for a total of one minute at 412 nm using a plate reader.

2.6 Western blot

Western blots were conducted on liver tissue to evaluate lipid peroxidation using a polyclonal anti-rabbit 4-hyroxynoneal antibody (4-HNE; cat# ab46545; Abcam) following methods described in (Parry et al., 2021) and (Yamada et. al., 2024; *in review*). Briefly, approximately 50-100 mg of raw liver tissue was homogenized in a lysis buffer with a protease inhibitor cocktail. Total protein concentration of the homogenate was calculated through Bradford assay. Equal volumes of sample homogenate and Laemmli tracking dye with β-mercaptoethanol was added to a 1.7mL Eppendorf tube and raised to a total volume of 200µL using ultrapure water to achieve a standardized final protein concentration of 2.0 µg/µL across all samples. Subsequently, samples were denatured for 5 minutes to release proteins from their conformations at 100°C. Proteins were separated by polyacrylamide gel electrophoresis using 4-15% Criterion TGX precast at 200 V (Bio-Rad, Hercules, CA). Proteins were transferred to a polyvinylidene difluoride (PVDF) membrane via Bio-Rad Transfer box ran at 200 mA in cold transfer buffer for 2 hours (Bio-Rad, Hercules, CA). The membrane's non-specific sites were blocked for 2 hours at room temperature while rocking in 5% nonfat milk containing tris-buffered saline with tween (TBS-T). After 3 washes of TBS-T, the membrane was rocked and incubated in a the 4-HNE antibody prepared at a 1:1000 concentration with 5% BSA with tween for one hour at room temperature. Membranes were washed 3 more times with TBS-T then rocked and incubated with an anti-rabbit horseradish peroxidase secondary antibody (Cell Signaling Cat# 7074) prepped at 1:2000 concentration with 5% BSA with tween at room temperature. Protein bands were visualized by adding ECL prime (VWR cat # 89238-012) under UV chemiluminescence using ImageQuant LAS 4000. Protein bands were analyzed using Bio-

Rad Image Lab (Bio-Rad, Hercules, CA). Total protein via ponceau staining was used as a normalizing and transfer control.

2.7 Statistical analysis

All statistical analyses were run in R (Version 4.5.0). Statistical significance was determined using an alpha value of ($P \leq 0.05$). Linear mixed effects models were generated with Treatment (three level factor) and Sex (two level factor) treated as fixed effects for mitochondrial respiration variables. We included an interaction term between Treatment and Sex as well as organ mass as a fixed covariate, as mitochondrial abundance may differ between tissue sizes. For repeated measures of body mass and RMR, an addition of Timepoint (seven and two level factor, respectively) was included as a fixed factor, as well as pretreatment and five week body mass measures for RMR.

Because dividing oxygen consumption by body mass does not allometrically scale to account for variation, we extracted the residuals to eliminate the role of sex in driving RMR. For both body mass and RMR response variables (which we used residuals as the response variable), we included individual mouse ID as a random intercept, as well as 2-way and 3-way interactions between Treatment, Sex, and Timepoint. If a significant or nearly significant interaction term that was deemed to have biological significance was detected, Tukey's post-hoc test followed using the "emmeans" package in R for pair-wise comparisons to maintain a type I error. Non-significant interaction terms were removed from the final model and the main effects are interpreted. Assumptions of the linear model (linearity and homoscedasticity) were tested using histograms and residual plots. Grub's test was used to identify any significant outliers (± 2 standard deviations from the mean; GraphPad) and were removed from the final analysis. We

detected one outlier for state 3 and state 4_{leak} respiration in the skeletal muscle, resulting in the inability to calculate two RCR values. Furthermore, there was one outlier detected for the RCR that was subsequently removed.

3. Results:

Body mass:

We detected a main effect of sex on body mass ($F_{1,30} = 26.92$, $P < 0.0001$), indicating that males were significantly heavier than females ($\beta = 5.32$; 95% CI = 3.38- 7.27; t = 5.19; $P < 0.0001$; **Fig. 14**). Additionally, there was a main effect of timepoint ($F_{6,186} = 22.85$; $P < 0.0001$) in which body mass increased in comparison to pretreatment levels, but this was not related to treatment as we did not detect an interaction between treatment and timepoint ($F_{12,168} = 0.99$; $P > 0.46$; **Fig. S4**). Moreover, we did not detect an interaction between treatment and sex ($F_{2,28} = 0.032$; $P > 0.96$) or a 3-way interaction between treatment, timepoint, and sex ($F_{12,168} = 0.78$; $P > 0.67$).

Fat pads

There was a significant main effect of sex across all three measures of the fat pads, in which males had significantly greater amount of fat (Subcutaneous: $F_{1,30} = 11.90$, $P = 0.002$; Gonadal: $F_{1,30} = 15.33$; $P = 0.0005$; Retroperitoneal: $F_{1,30} = 5.7$; $P = 0.02$; **Fig. 15**) compared to females, but this was regardless of treatment as there was no significant interaction between sex and treatment across all three fat pads ($P > 0.53$).

Liver mitochondrial physiology measures

For complex I, we found a near significant interaction between treatment and sex on state 3 respiration ($F_{2,26} = 2.97$, $P = 0.069$), thus we continued with post-hoc analysis. Post-hoc test revealed that after six weeks of constant light, female mice had higher state 3 mitochondrial respiration in the liver compared to control females ($\beta = 0.83$, ± 95% CI 0.023-1.64; $t = 2.56$; $P < 0.04$; **Fig. 16A**), but not females under constant darkness ($P > 0.26$). We did not detect a similar treatment*sex interaction on state 4 leak respiration ($P > 0.42$; **Fig. 16B**) or the respiration control ratio (RCR; $P > 0.25$; **Fig. 16C**). For complex II, we did not detect a significant treatment*sex interaction on state 3, state 4 leak, or RCR (**Supplementary materials; Fig. S5D-F**).

Skeletal muscle mitochondrial physiology measures

We did not detect significant main effects of treatment or sex or their interaction on any mitochondrial physiology variables in the skeletal muscle (**supplementary materials; Figure S6A-F)**.

Resting Metabolic Rate (RMR)

We did not detect significant interactions between treatment and sex ($F_{2,27} = 2.08$, $P = 0.14$) or sex and timepoint ($F_{1,31} = 2.38$, $P = 0.13$) on RMR. Furthermore, we did not detect a 3-way interaction between treatment, sex, and timepoint on RMR (**Fig. 17**).

CS (Citrate synthase) activity

We did not detect a significant main effect of treatment ($F_{2,25} = 0.94$; $P \geq 0.40$), sex ($F_{1,25} = 0.14$; $P \geq 0.62$), or their interaction ($F_{2,25} = 1.96$; $P > 0.16$) on CS activity in the liver (**Supplementary materials; Figure S7**)

Liver 4-HNE adducts

We did not detect a significant effect of treatment ($F_{2,27} = 2.4$; $P > 0.10$), Sex ($F_{1,27} = 0.14$; $P \geq 0.70$), or the interaction between treatment and sex ($F_{2,27} = 1.4$; $P \geq 0.25$) on relative abundance of 4-HNE adducts in the liver (**Supplementary materials; Figure S8**).

Discussion

In this study, male and female wild-derived house mice were exposed to continuous light or darkness for six weeks. Contrary to our predictions, rather than constant light suppressing mitochondrial respiratory function, we found a sex and tissue-specific response. Specifically, we detected an increase in maximum mitochondrial respiratory function in female mice via complex I in the liver compared to control females after six weeks of exposure to constant light. A similar response was not detected in the male livers, or skeletal muscle of both sexes under constant light or darkness. While an increase mitochondrial function and oxidative stress are often observed and associated with stress (Picard et al., 2014), aperiodic light did not affect lipid peroxidation in wild-derived house mice. Furthermore, there were no differences between treatment groups in mitochondrial volume. While maximum mitochondrial respiratory function increased in the liver of mice under constant light, we did not detect this at the whole-organism

level. Most surprisingly, our light treatments did not result in differences in body mass or fat accumulation, contrasting other studies.

We expected that mitochondria would be vulnerable to the deleterious effects of light at night given that mitochondrial dynamics such as fission and fusion and respiratory function are under circadian control (Rajput et al., 2023; De Goede et al., 2018). However, this was not the case at all. In similar designs using shorter durations of constant light at a higher light intensity, glucocorticoid rhythms were lost along with elevated oxidative stress markers in mice and rats (Ashkenazi and Haim, 2013; Claustrat et al., 2008). Importantly, these observed patterns are commonly associated with pathologies and diseases thought to have a bioenergetic underpinning (Bedrosian et al., 2016; Fishbein et al., 2021; Picard et al., 2014). Thus, it is surprising in our study to find that an even longer exposure time did not suppress mitochondrial function but enhanced it exclusively in the livers of female mice. In contrast, brief exposure to constant light (3 days) resulted in an increase in the respiratory control ratio in the pineal gland of adult male Wistar rats (Bitzer-Quintero et al., 2010).

Enhancement in liver respiratory function may be associated with matching energetic demands of the current environment (Manoli et al., 2007). However, considering that mice are nocturnal, constant light is predicted to decrease energy and activity, with a concomitate match in metabolic rates and mitochondrial respiratory function (Rajput et al., 2023; De Goede et al., 2018; Aschoff, 1960). Thus, the rise in respiration in female livers may point to potential differences in behavioral patterns, or sex-specific physiological responses not commonly seen in laboratory strains under constant light. While we did not measure behavioral patterns or circulating hormones in our study of wild-derived mice, we can speculate on the mechanisms

that may have driven a change in respiratory function or the role of sex in determining physiological outcomes to disruptions in the nighttime environment.

Behavioral phenotypes differ between wild and lab rodents (Chalfin et al., 2014). Thus, it is likely exogenous challenges, such as constant light, result in different behavioral outcomes. Behavioral flexibility is a critical component in mediating organismal responses to environmental variation. Lizards can escape lethal thermal temperatures by preferentially choosing shady eras, and birds could choose nesting sites shielded with foliage and natural structures to block ambient light. Mice build complex nests and burrows that alleviate costs of thermoregulation, especially in colder environments (Gaskill et al., 2013). Thus, in an environment with unpredictable changes in lighting intensity or duration, mice may build more complex nesting structures to shield themselves from ambient light, thereby escaping or minimizing physiological costs related to an altered light environment. In this context, it is possible in our study that females under constant light built bigger or more complex nests to mitigate costs related to a constant light environment; especially given that wild-derived females tend to be less territorial, display cooperative social networks (König and Lindholm et al., 2012), and were housed as pairs in our study. While we cannot confirm the role of behavior in driving females' response to constant light, it is evident they were able enhance liver mitochondrial respiratory function and minimize physiological costs. Future studies should investigate how behavioral flexibility allows animals to escape the physiological consequences to environmental variation such as light at night.

Alternatively, there may be sex-specific differences in how mitochondrial respiration is modulated (Karakelides et al., 2010; Guevara et al., 2009). One mechanism may be sex-specific regulation of circulating hormone levels. Accumulating evidence has identified thyroid hormone,

glucocorticoids, or sex steroids in driving mitochondrial respiratory capacity (Oefele et al., 2024; Yap et al., 2022; Verlarde, 2014). Similarly to an exercise response, hormones serve as important signaling molecules and program numerous sex-specific physiological or behavioral responses (Manoli et al., 2007). For example, glucocorticoid elevation and translocation of their hormone receptors into nuclear and mitochondrial genomes activate metabolic and oxidative pathways, highlighting their role in facilitating the mitochondrial response to stressors (Picard et al., 2014; Manoli et al., 2007;Webber, 2002). Although we did not measure hormones such as circulating thyroid or glucocorticoids in our mice, light at night alters the hypothalamic-pituitary-adrenal axis, among others endocrine axes (Ouyang et al., 2018; Bedrosian et al., 2016). Moreover, because of the role of glucocorticoids in the mitochondrial response to stressors, they may be important facilitators to mitochondrial adaptions that translate into functional differences (Manoli et al., 2007). Further research should identify sex differences in hormone regulation and how exposure to light at night alters circulating concentrations that translate into downstream modifications to mitochondrial function.

It is important to note, however, that constant, aperiodic conditions are not common in temperate environments, where human population densities are greatest and animals are most specious (Bernhardt et al., 2020). Thus, the ecological importance of using relevant experimental lighting regimes that is reflective of common conditions wildlife or shift workers experience will be critical to reveal consequences on physiology and behavior. A study investigating wild-derived populations of nocturnal or diurnal mammals exposed to ecologically relevant levels of light at night would be particularly valuable.

Together, our findings should encourage researchers to diversify model systems, especially in rodents, to understand phenotypic flexibility in response to environmental variation,

such as changes in the light environment. Moreover, the importance of individual variation and sensitivity to stressors is important to highlight. While metabolic impacts due to altered light environments are clearly supported in numerous studies, the underlying physiological mechanism(s) associated with health outcomes remains to be identified. Investigation of the mitochondria, and how animals modify their phenotypes to maintain function under altered light environment will be critical in a rapidly changing world.

Acknowledgements:

We would like to thank LouAnn Crosby for her assistance in setting up the experiment, as well as Caitlin McIlwain, Lauren Sharpe, and Su-Min Cho, for providing excellent animal husbandry care. We would also like to thank the Hood/Hill/Wada lab groups for their helpful comments on a previous draft of the paper. Lastly, we thank the two anonymous reviewers for their comments.

Author contributions:

Kevin Pham: Conceptualization, data curation, formal analysis, funding acquisition, Investigation, methodology, project administration, visualization, writing – original draft, writing – review & editing

Dr. KayLene YH. Yamada: Investigation, methodology, data curation, project administration, validation, writing – review & editing

Emma M. Rhodes: Investigation, methodology, data curation, writing – review & editing

Dr. Agata M. Rudolf: Investigation, methodology, data curation, writing – review & editing

Dr. Wendy R. Hood: Conceptualization, funding acquisition, project administration, resources, supervision, validation, visualization, writing – review & editing

Funding:

This study was supported by an Alabama EPSCoR grant (OIA1736150) awarded to W.R.H and a National Institutes of Health (NIH) T-32 Graduate Research Training Initiative for Student Enhancement (G-RISE; 5T32GM141739) Fellowship awarded to K.P.

Conflict of Interest:

The authors declare that there is no conflict of interest.

Data availability:

Raw data and code will be made available upon request to the corresponding author without reservations.

References

Abolins, S., King, E.C., Lazarou, L., Weldon, L., Hughes, L., Drescher, P., Raynes, J.G., Hafalla, J.C.R., Viney, M.E., Rile, E.M., 2017. The comparative immunology of wild and laboratory mice, Mus musculus domesticus. Nat. Commun. 8, 1–13. https://doi.org/10.1038/ncomms14811

Aschoff, J., 1960. Exogenous and endogenous components in circadian rhythms. Cold Spring Harb. Symposia Quantitative Biol. 25, 11–28.

Ashkenazi, L., Haim, A., 2013. Effect of Light at Night on oxidative stress markers in Golden spiny mice (Acomys russatus) liver. Comp. Biochem. Physiol. - A Mol. Integr. Physiol. 165, 353–357. https://doi.org/10.1016/j.cbpa.2013.04.013

Bedrosian, T.A., Fonken, L.K., Nelson, R.J., 2016. Endocrine Effects of Circadian Disruption. Annu. Rev. Physiol. 78, 109–131. https://doi.org/10.1146/annurev-physiol-021115-105102

Bernhardt, J.R., O'Connor, M.I., Sunday, J.M., Gonzalez, A., 2020. Life in fluctuating environments: Adaptation to changing environments. Philos. Trans. R. Soc. B Biol. Sci. 375. https://doi.org/10.1098/rstb.2019.0454

Bitzer-Quintero, O.K., Marín, A.J.D., Pacheco-Moises, F.P., Torres-Sánchez, E.D., Ortíz, G.G., 2010. Effect of brief constant darkness and illumination on mitochondrial respiratory control of the pineal gland, Harderian gland, spleen and thymus of adult rat. Sleep Sci. 3, 53–55.

Bumgarner, J.R., Nelson, R.J., 2021. Light at Night and Disrupted Circadian Rhythms Alter Physiology and Behavior. Integr. Comp. Biol. 61, 1160–1169. https://doi.org/10.1093/icb/icab017

Casagrande, S., Dzialo, M., Trost, L., Malkoc, K., Sadowska, E.T., Hau, M., Pierce, B., McWilliams, S., Bauchinger, U., 2023. Mitochondrial metabolism in blood more reliably predicts whole-animal energy needs compared to other tissues. iScience 26, 108321. https://doi.org/10.1016/j.isci.2023.108321

Chalfin, L., Dayan, M., Levy, D.R., Austad, S.N., Miller, R.A., Iraqi, F.A., Dulac, C., Kimchi, T., 2014. Mapping ecologically relevant social behaviours by gene knockout in wild mice. Nat. Commun. 5, 1–10. https://doi.org/10.1038/ncomms5569

Claustrat, B., Valatx, J.L., Harthé, C., Brun, J., 2008. Effect of constant light on prolactin and corticosterone rhythms evaluated using a noninvasive urine sampling protocol in the rat. Horm. Metab. Res. 40, 398–403. https://doi.org/10.1055/s-2008-1065330

De Goede, P., Wefers, J., Brombacher, E.C., Schrauwen, P., Kalsbeek, A., 2018. Circadian rhythms in mitochondrial respiration. J. Mol. Endocrinol. 60, R115–R130. https://doi.org/10.1530/JME-17-0196

Dohm, M.R., Richardson, C.S., Garland, T. Jr., 1994. Exercise physiology of wild and random-bred laboratory house mice and their reciprocal hybrids. Am J Physiol. 267(4 Pt 2):R1098-R1108. https://doi:10.1152/ajpregu.1994.267.4.R1098

Fishbein, A.B., Knutson, K.L., Zee, P.C., 2021. Circadian disruption and human health. J. Clin. Invest. 131, 1–12. https://doi.org/10.1172/JCI148286

Fleury, G., Masís-Vargas, A., Kalsbeek, A., 2020. Metabolic Implications of Exposure to Light at Night: Lessons from Animal and Human Studies. Obesity 28, S18–S28. https://doi.org/10.1002/oby.22807

Gaskill, B.N., Gordon, C.J., Pajor, E.A., Lucas, J.R., Davis, J.K., Garner, J.P., 2013. Impact of nesting material on mouse body temperature and physiology. Physiol. Behav. 110–111, 87–95. https://doi.org/10.1016/j.physbeh.2012.12.018

Granata, C., Jamnick, N.A., Bishop, D.J., 2018. Training-Induced Changes in Mitochondrial Content and Respiratory Function in Human Skeletal Muscle. Sport. Med. 48, 1809–1828. https://doi.org/10.1007/s40279-018-0936-y

Guevara, R., Santandreu, F.M., Valle, A., Gianotti, M., Oliver, J., Roca, P., 2009. Sex-dependent differences in aged rat brain mitochondrial function and oxidative stress. Free Radic. Biol. Med. 46, 169–175. https://doi.org/10.1016/j.freeradbiomed.2008.09.035

Heine, K.B., Hood, W.R., 2020. Mitochondrial behaviour, morphology, and animal performance. Biol. Rev. 95, 730–737. https://doi.org/10.1111/brv.12584

Hohor, S., Mandanach, C., Maftei, A., Zugravu, C.A., Oțelea, M.R., 2023. Impaired Melatonin Secretion, Oxidative Stress and Metabolic Syndrome in Night Shift Work. Antioxidants 12. https://doi.org/10.3390/antiox12040959

Hood, W.R., Zhang, Y., Mowry, A. V., Hyatt, H.W., Kavazis, A.N., 2018. Life history trade-offs within the context of mitochondrial hormesis. Integr. Comp. Biol. 58, 567–577. https://doi.org/10.1093/icb/icy073

Jacobs, R.A., Flück, D., Bonne, T.C., Bürgi, S., Christensen, P.M., Toigo, M., Lundby, C., 2013.

Improvements in exercise performance with high-intensity interval training coincide with an increase in skeletal muscle mitochondrial content and function. J. Appl. Physiol. 115, 785–793. https://doi.org/10.1152/japplphysiol.00445.2013

Karakelides, H., Irving, B.A., Short, K.R., O'Brien, P., Sreekumaran Nair, K., 2010. Age, obesity, and sex effects on insulin sensitivity and skeletal muscle mitochondrial function. Diabetes 59, 89–97. https://doi.org/10.2337/db09-0591

Koch, R.E., Buchanan, K.L., Casagrande, S., Crino, O., Dowling, D.K., Hill, G.E., Hood, W.R., McKenzie, M., Mariette, M.M., Noble, D.W.A., Pavlova, A., Seebacher, F., Sunnucks, P., Udino, E., White, C.R., Salin, K., Stier, A., 2021. Integrating Mitochondrial Aerobic Metabolism into Ecology and Evolution. Trends Ecol. Evol. 36, 321–332. https://doi.org/10.1016/j.tree.2020.12.006

König, B., Lindholm, A. K., Macholán, M., Baird, S. J., Munclinger, P., Piálek, J., 2012. Evolution of the house mouse. *Chap. The complex social environment of female house mice*, 114-134.

Manoli, I., Alesci, S., Blackman, M.R., Su, Y.A., Rennert, O.M., Chrousos, G.P., 2007. Mitochondria as key components of the stress response. Trends Endocrinol. Metab. 18, 190–198. https://doi.org/10.1016/j.tem.2007.04.004

Metcalfe, N.B., Bellman, J., Bize, P., Blier, P.U., Crespel, A., Dawson, N.J., Dunn, R.E., Halsey, L.G., Hood, W.R., Hopkins, M., Killen, S.S., McLennan, D., Nadler, L.E., Nati, J.J.H., Noakes, M.J., Norin, T., Ozanne, S.E., Peaker, M., Pettersen, A.K., Przybylska-Piech, A., Rathery, A., Récapet, C., Rodríguez, E., Salin, K., Stier, A., Thoral, E., Westerterp, K.R., Westerterp-Plantenga, M.S., Wojciechowski, M.S., Monaghan, P., 2023. Solving the conundrum of intra-specific variation in metabolic rate: A multidisciplinary conceptual and methodological toolkit: New technical developments are opening the door to an understanding of why metabolic rate varies among individual animals of a species. BioEssays 45. https://doi.org/10.1002/bies.202300026

Natarajan, V., Chawla, R., Mah, T., Vivekanandan, R., Tan, S.Y., Sato, P.Y., Mallilankaraman, K., 2020. Mitochondrial Dysfunction in Age-Related Metabolic Disorders. Proteomics 20, 1–11. https://doi.org/10.1002/pmic.201800404

Navara, K.J., Nelson, R.J., 2007. The dark side of light at night: Physiological, epidemiological, and ecological consequences. J. Pineal Res. 43, 215–224. https://doi.org/10.1111/j.1600-079X.2007.00473.x

Nelson, R.J., Chbeir, S., 2018. Dark matters: Effects of light at night on metabolism. Proc. Nutr. Soc. 77, 223–229. https://doi.org/10.1017/S0029665118000198

Oefele, M., Hau, M., Ruuskanen, S., Casagrande, S., 2024. Mitochondrial function is enhanced by thyroid hormones during zebra finch development. R. Soc. Open Sci. 11. https://doi.org/10.1098/rsos.240417

Ouyang, J.Q., Davies, S., Dominoni, D., 2018. Hormonally mediated effects of artificial light at night on behavior and fitness: Linking endocrine mechanisms with function. J. Exp. Biol. 221. https://doi.org/10.1242/jeb.156893

Palmeira, C.M., Teodoro, J.S., Amorim, J.A., Steegborn, C., Sinclair, D.A., Rolo, A.P., 2019. Mitohormesis and metabolic health: The interplay between ROS, cAMP and sirtuins. Free Radic. Biol. Med. 141, 483–491. https://doi.org/10.1016/j.freeradbiomed.2019.07.017

Panagiotou, M., Deboer, T., 2020. Effects of Chronic Dim-light-at-night Exposure on Sleep in Young and Aged Mice. Neuroscience 426, 154–167. https://doi.org/10.1016/j.neuroscience.2019.11.033

Parry, H.A., Randall, R.B., Hyatt, H.W., Hood, W.R., Kavazis, A.N., 2021. Short and long-term effect of reproduction on mitochondrial dynamics and autophagy in rats. Heliyon 7, e08070. https://doi.org/10.1016/j.heliyon.2021.e08070

Picard, M., Juster, R.P., McEwen, B.S., 2014. Mitochondrial allostatic load puts the "gluc" back in glucocorticoids. Nat. Rev. Endocrinol. 10, 303–310. https://doi.org/10.1038/nrendo.2014.22

Picard, M., McEwen, B.S., 2018. Psychological Stress and Mitochondria: A Systematic Review. Psychosom. Med. 80, 141–153. https://doi.org/10.1097/PSY.0000000000000545

Pizzorno, J., 2014. Mitochondria—Fundamental to Life and Health THE PATH AHEAD. Integr. Med. A Clin. J. 13, 8–15.

Qian, J., Morris, C.J., Caputo, R., Wang, W., Garaulet, M., Scheer, F.A.J.L., 2019. Sex differences in the circadian misalignment effects on energy regulation. Proc. Natl. Acad. Sci. U. S. A. 116, 23806–23812. https://doi.org/10.1073/pnas.1914003116

Rajput, P., Kumar, D., Krishnamurthy, S., 2023. Chronic exposure to dim artificial light disrupts the daily rhythm in mitochondrial respiration in mouse suprachiasmatic nucleus. *Chronobiol Int*. 40(7):938-951. doi:10.1080/07420528.2023.2236708

Rångtell, F. H., Karamchedu, S., Andersson, P., Liethof, L., Olaya Búcaro, M., Lampola, L., Schiöth, H. B., Cedernaes, J., Benedict, C., 2019. A single night of sleep loss impairs objective but not subjective working memory performance in a sex-dependent manner. *J Sleep Res*. 28(1):e12651. https://doi:10.1111/jsr.12651

Salin, K., Auer, S.K., Rudolf, A.M., Anderson, G.J., Selman, C., Metcalfe, N.B., 2016. Variation in metabolic rate among individuals is related to tissue-specific differences in mitochondrial leak respiration. Physiol. Biochem. Zool. 89, 511–523. https://doi.org/10.1086/688769

Santhi, N., Lazar, A. S., McCabe, P. J., Lo, J. C., Groeger, J. A., Dijk, D. J., 2016. Sex differences in the circadian regulation of sleep and waking cognition in humans. *Proc Natl Acad Sci U S A*. 2016;113(19):E2730-E2739. https://doi:10.1073/pnas.1521637113

Sharma, A., Goyal, R., 2020. Long-term exposure to constant light induces dementia, oxidative stress and promotes aggregation of sub-pathological Aβ42 in Wistar rats. Pharmacol. Biochem. Behav. 192, 172892. https://doi.org/10.1016/j.pbb.2020.172892

Sokolova, I., 2018. Mitochondrial Adaptations to Variable Environments and Their Role in Animals' Stress Tolerance. Integr. Comp. Biol. 58, 519–531. https://doi.org/10.1093/icb/icy017

Treidel, L.A., Goswami, P., Williams, C.M., Changes in mitochondrial function parallel life history transitions between flight and reproduction in wing polymorphic field crickets. *Am J Physiol Regul Integr Comp Physiol*. 2023;324(6):R735-R746. https://doi:10.1152/ajpregu.00191.2022

Velarde, M.C., 2014. Mitochondrial and sex steroid hormone crosstalk during aging. Longev. Heal. 3, 1–10. https://doi.org/10.1186/2046-2395-3-2

Weber, K., Brück, P., Mikes, Z., Küpper, J.H., Klingenspor, M., Wiesner, R.J., 2002. Glucocorticoid hormone stimulates mitochondrial biogenesis specifically in skeletal muscle. *Endocrinology*. 143(1):177-184. https://doi:10.1210/endo.143.1.8600

Welbers, A.A.M.H., van Dis, N.E., Kolvoort, A.M., Ouyang, J., Visser, M.E., Spoelstra, K., Dominoni, D.M., 2017. Artificial light at night reduces daily energy expenditure in breeding great tits (Parus major). Front. Ecol. Evol. 5, 1–10. https://doi.org/10.3389/fevo.2017.00055

Wilson, L.A.B., Zajitschek, S.R.K., Lagisz, M., Mason, J., Haselimashhadi, H., Nakagawa, S., 2022. Sex differences in allometry for phenotypic traits in mice indicate that females are not

scaled males. Nat. Commun. 13. https://doi.org/10.1038/s41467-022-35266-6
Yap, K.N., Andreasen, V.A., Williams, A.S., Yamada, K.L.Y., Zikeli, S., Kavazis, A.N., Hood, W.R., 2022. The persistent effects of corticosterone administration during lactation on the physiology of maternal and offspring mitochondria. J. Exp. Biol. 225. https://doi.org/10.1242/jeb.244171

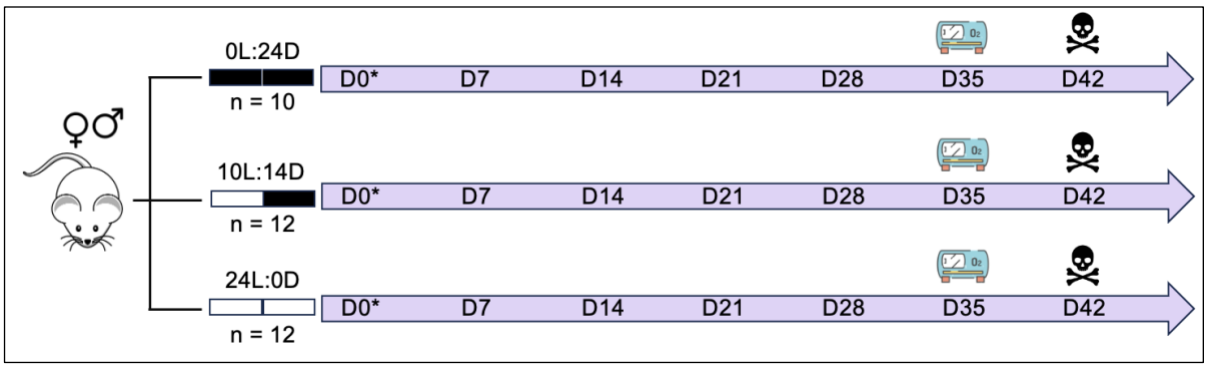

Figure 13: Schematic of experimental design. A total of 36 male and female mice were distributed across three treatment groups. These groups included a constant light group (24L:0D), constant darkness group (0L:24D), and a control group on a 10L:14D light cycle each comprised of 12 mice (six male and six female). Individuals were measured for baseline RMR before beginning treatment, which is indicated as D0* and were exposed to their respective lighting condition for a total of six weeks (D42; i.e., 42 days). We remeasured RMR at D35 (five weeks exposure) and then mice were euthanized one week later (D42) to measure mitochondrial physiology. Note that the full sample size by the end of the experiment included 34 mice due to removal of data belonging to mice that died during the acclimation period.

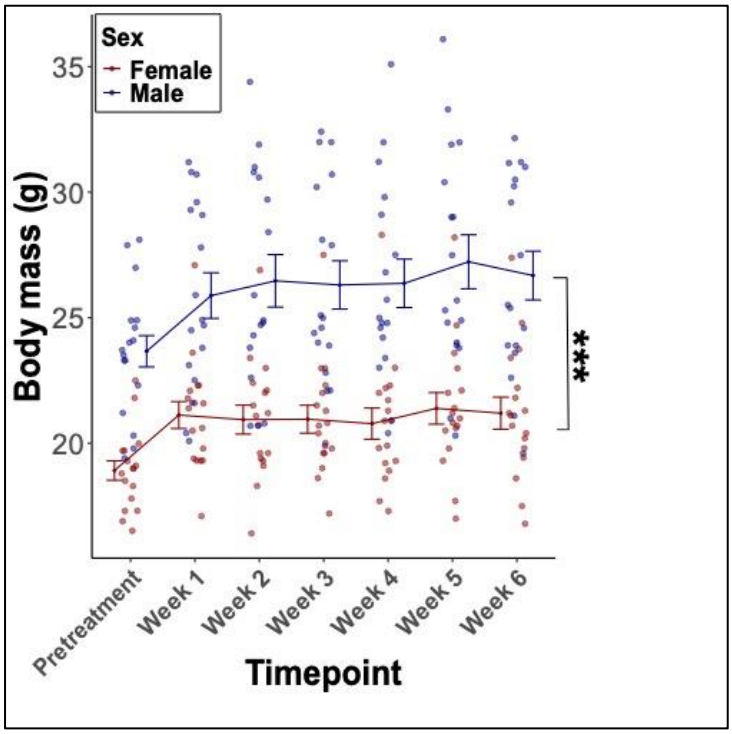

Figure 14. Body mass over the duration of the experiment between sex. Females (N = 17) are depicted with the dark red line, while males (N=17) are indicated by the dark navy line The x-axis represents different timepoints in the experiment when mice were measured, with the y-axis indicating body mass (g). Average body mass (g) of females and males is plotted across timepoints using raw data with error bars indicating ± the standard error of the mean (SEM). Statistical significance is indicated with a bracket with asterisks denoting associated p values (***$p \leq 0.001$).

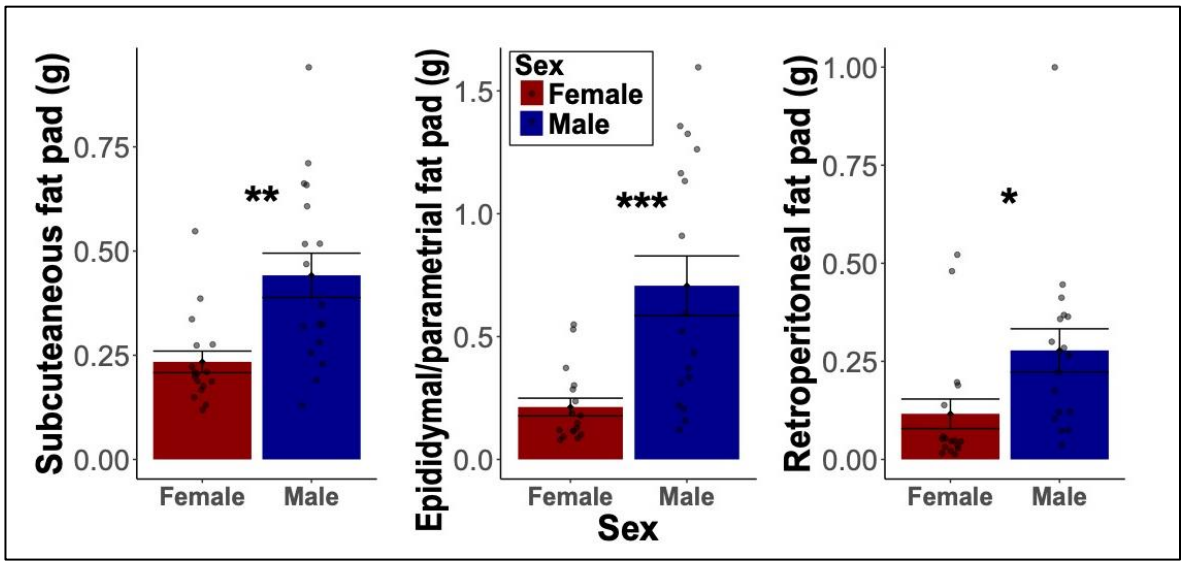

Figure 15. Fat pad weight between sex at euthanasia. Females (N = 17) are depicted with the dark red bar, while males (N=17) are indicated by the dark navy bar. The x-axis represents sex, with the y-axis indicating respective fat pad (subcutaneous, gonadal, and retroperitoneal) mass (g). Average fat pad mass (g) of females and males is plotted using raw data with error bars indicating ± the standard error of the mean (SEM). Statistical significance between sexes is denoted with asterisks (*$P \leq 0.05$; **$P \leq 0.01$; ***$P \leq 0.001$).

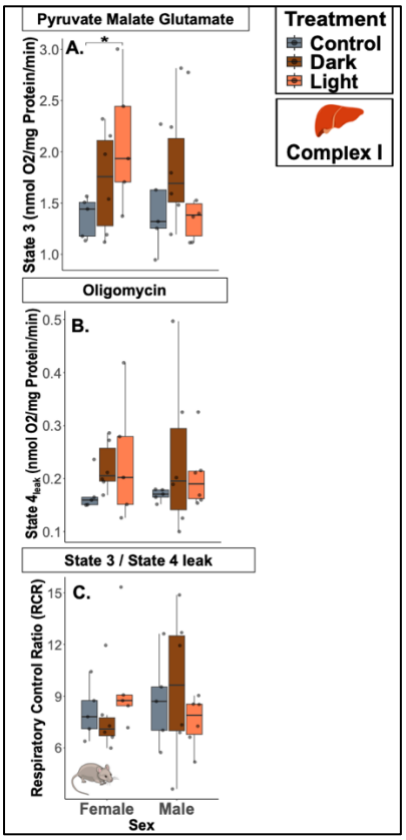

Figure 16A-C: Mitochondrial respiration variables via liver complex I between Sex and Treatment. Box and whisker plots are depicted, with control mice (n = 10) indicated by the slate grey box, mice under constant darkness (n = 12) indicated by saddle brown box, and mice under constant light (n = 12) are indicated by the coral box. The X-axis, indicates male and female mice separated between treatment groups, with the Y-axis indicating the mitochondrial respiration variable of interest in nmol O2/mg protein/min. The solid black line in between the box and whisker plots depicts the median value, with the black diamond indicating the mean value and gray dots indicating raw data. The upper 75% quartile and lower 25% quartile are depicted, with interquartile representing 50% of the observed data. Statistical significance is shown with a solid black line with asterisks denoting associated p values after correction for multiple comparisons using Tukey's (post hoc analysis; $*P \leq 0.05$).

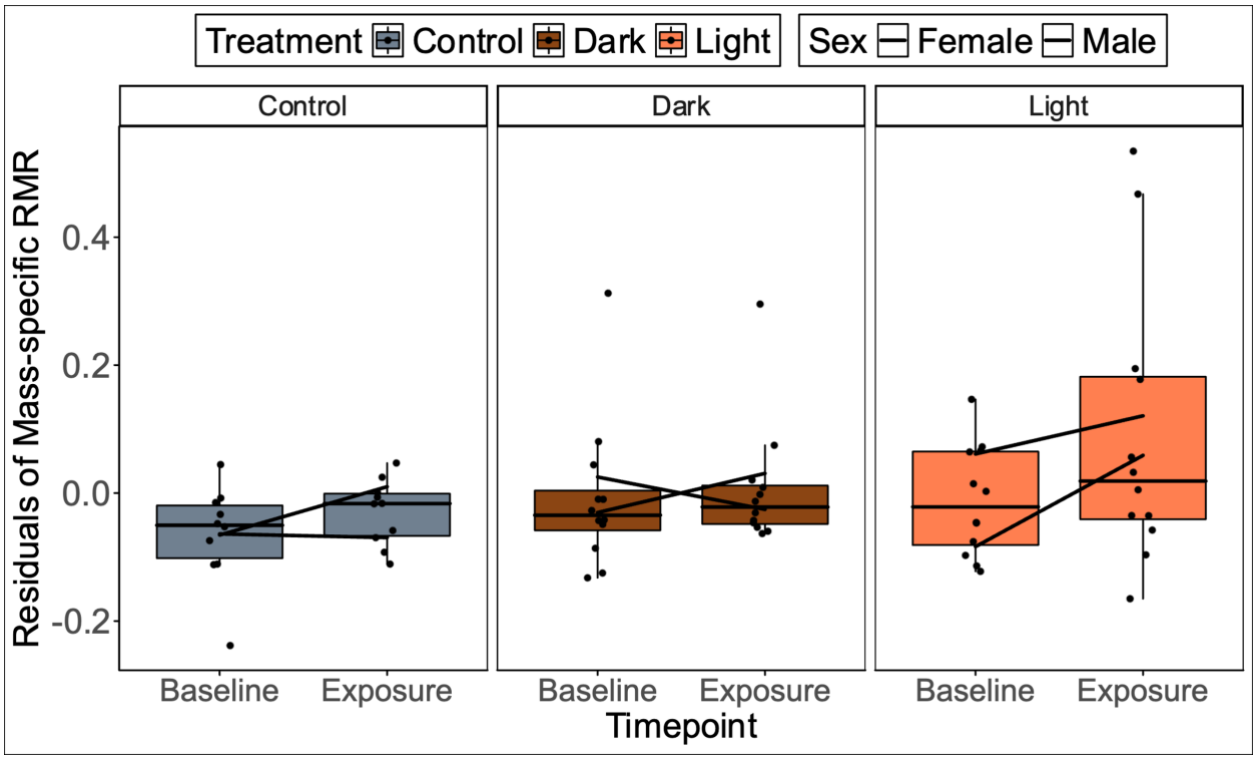

Figure 17: Residuals of mass-specific resting metabolic rates between Treatments. Box and whisker plots are depicted, with control mice (n = 10) indicated by the slate grey box, mice under constant darkness (n = 12) indicated by saddle brown box, and mice under constant light (n = 12) are indicated by the coral box. The X-axis indicates timepoints in which RMR was measured, with the Y-axis indicating residuals of mass-specific resting metabolic rates. The solid black line in between the box and whisker plots depicts the median value, with the black diamond indicating the mean value and gray dots indicating raw data. The upper 75% quartile and lower 25% quartile are depicted, with interquartile representing 50% of the observed data. Solid and dotted lines represent the slope between baseline and exposure measurements between female and male mice, respectively.

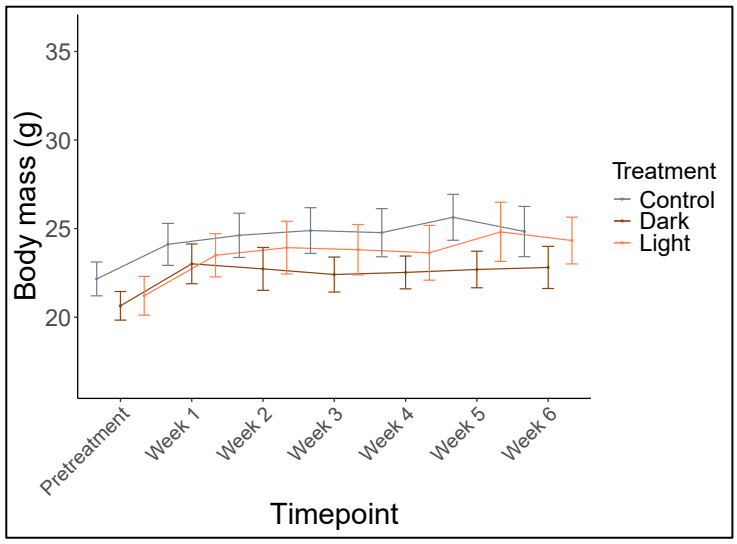

Figure S4. Body mass over the duration of the experiment between treatment groups. Control mice (n = 10) are indicated by slate gray line, mice under constant darkness (n = 12) are indicated by saddle brown line, and mice under constant light (n = 12) are indicated by the coral line. The x-axis represents different timepoints in the experiment when mice were measured, with the y-axis indicating body mass (g). Average body mass (g) of the three groups is plotted across timepoints using raw data with error bars indicating ± the standard error of the mean (SEM).

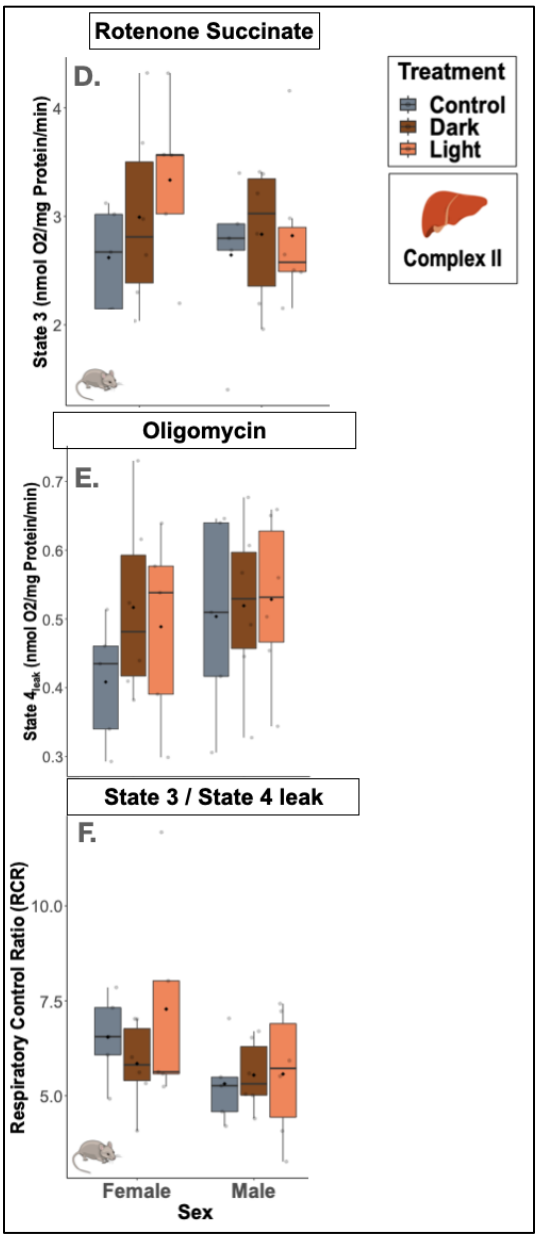

Figure S5 D-F: Mitochondrial respiration variables via liver complex II between sex and treatment. Box and whisker plots are depicted, with control mice (n = 10) indicated by the slate grey box, mice under constant darkness (n = 12) indicated by saddle brown box, and mice under constant light (n = 12) are indicated by the coral box. The X-axis, indicates male and female mice separated between treatment groups, with the Y-axis indicating the mitochondrial

respiration variable of interest in nmol O2/mg protein/min. The solid black line in between the box and whisker plots depicts the median value. The upper 75% quartile and lower 25% quartile are depicted, with interquartile representing 50% of the observed data.

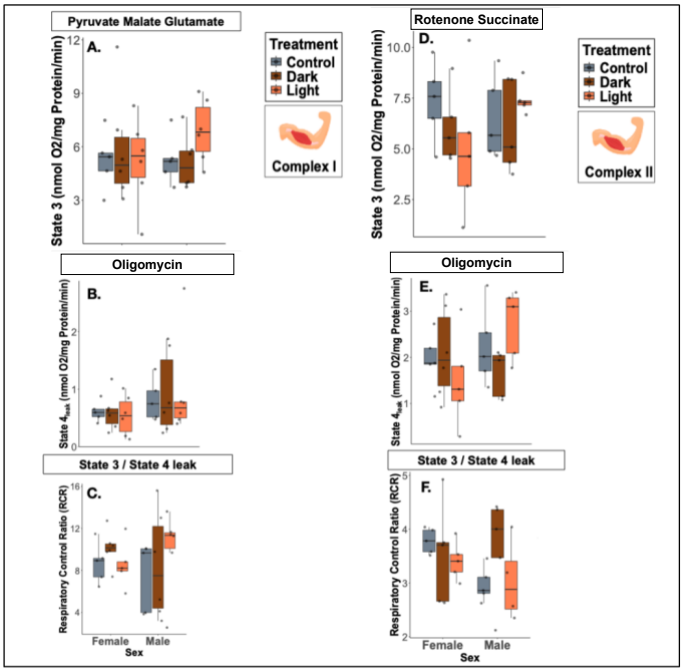

Figure S6 A-F: Mitochondrial respiration variables via skeletal muscle in complex I and II between sex and treatment groups. Box and whisker plots are depicted, with control mice (n = 10) indicated by the slate grey box, mice under constant darkness (n = 12) indicated by saddle brown box, and mice under constant light (n = 12) are indicated by the coral box. The X-axis, indicates male and female mice separated between treatment groups, with the Y-axis indicating the mitochondrial respiration variable of interest in nmol O_2/mg protein/min. The solid black line in between the box and whisker plots depicts the median value. The upper 75% quartile and lower 25% quartile are depicted, with interquartile representing 50% of the observed data.

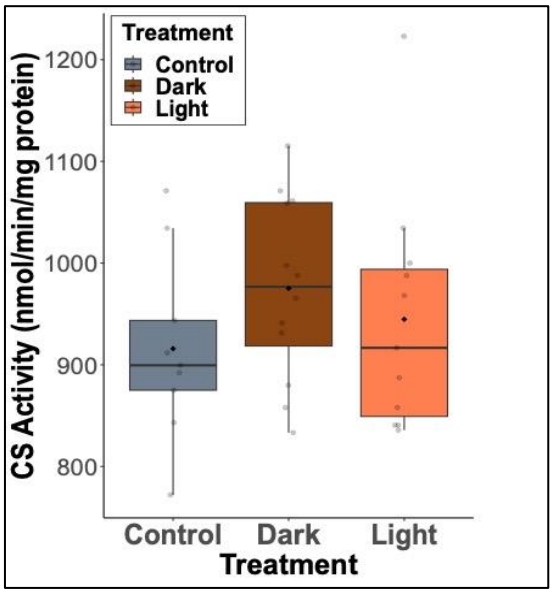

Figure S7: Citrate synthase across treatment groups. Box and whisker plots are depicted, with control mice (n = 10) indicated by the slate grey box, mice under constant darkness (n = 12) indicated by saddle brown box, and mice under constant light (n = 12) are indicated by the coral box. The X-axis indicates treatment groups, with the Y-axis indicating citrate synthase activity measured per nmol/min/mg protein. The solid black line in between the box and whisker plots depicts the median value. The upper 75% quartile and lower 25% quartile are depicted, with interquartile representing 50% of the observed data.

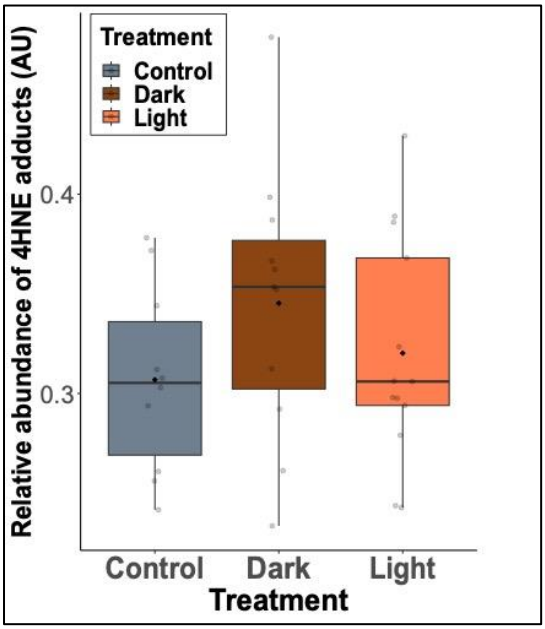

Figure S8: Relative abundance of 4-HNE adducts across treatment groups. Box and whisker plots are depicted, with control mice (n = 10) indicated by the slate grey box, mice under constant darkness (n = 12) indicated by saddle brown box, and mice under constant light (n = 12) are indicated by the coral box. The X-axis indicates treatment groups, with the Y-axis indicating relative 4-HNE adducts. The solid black line in between the box and whisker plots depicts the median value. The upper 75% quartile and lower 25% quartile are depicted, with interquartile representing 50% of the observed data.

Chapter 5: Mimicking the night shift: Hypothalamic-pituitary-adrenal (HPA) axis regulation, energy homeostasis, and oxidative stress in a model diurnal songbird

In preparation to submit to the Proceedings for Royal Society B

Kevin Pham*[1], Victoria M. Coutts[2], Alexander J. Hoffman[1], and Haruka Wada[1]

[1]Department of Biological Sciences, Auburn University, Auburn, AL 36849, USA

[2]Department of Biological Sciences, Loussiana State University, Baton Rouge, LS 36849, USA

Key words: Night shift work, circadian rhythms, hormones, glucocorticoids, melatonin, metabolism, HPA axis, birds, oxidative damage

Abstract:

Everchanging socioeconomic demands, coupled with modern day technological advancements, have lifted constraints on human activity patterns and enabled us to take advantage of the nighttime environment. Society has benefited from the essential duties that night shift workers perform, from maintaining infrastructures to providing around the clock medical care. At the same time, these individuals may be at higher risk of developing pathological diseases due to circadian rhythm disruption, revealing an important cost to extended nighttime activities. However, experimental manipulation is limited to rodent models and epidemiological studies in humans are unable to control for a variety of confounding factors. To this end, we exposed zebra finches (*Taeniopygia guttata castanotis*), a diurnal songbird, to a consistent light/dark cycle of 12L:12D or alternating lighting patterns of 12D:12L and 12L:12D every three days for 66 days to mimic conditions similar to what night shift workers may experience. We found that simulated night shift work suppressed the reactivity of the hypothalamic-pituitary-adrenal (HPA) axis and inverted the acrophase of corticosterone expression compared to controls. Yet, melatonin profiles remained robust, albeit slight evidence suggesting a similar inversion. Relative protein abundance of superoxide dismutase 1 was lower in the brain of treatment birds, but there was no elevated oxidative damage to lipids. Our study underscores the need to capitalize on unique model organisms to evaluate the role of simulated night shift work on physiology to inform public health decisions, given that the nighttime environment has become permanently altered, with both humans and wildlife exposed to light at unnatural times.

Introduction:

Loss of adequate sleep quality and duration has become one of the most prominent drivers of circadian rhythm disruption in today's industrialized world. Sleep disturbance results from a variety of sources, including social jetlag or prolonged exposure to bright light prior to sleep onset, or shift work during the dark phase (Guindon et al., 2024; James et al., 2017). Exposure to distinct light spectra can differentially stimulate photoreceptors/pigments in the retina, pineal gland, or suprachiasmatic nucleus (SCN), causing signaling cascades that activate or inhibit multiple endocrine axes (Ouyang et al., 2018). Consequently, conflicting patterns of light at night can result in temporal mismatch between master and peripheral oscillators that phase shift core clock genes, alter gene expression profiles across the transcriptome, and disrupt hormone regulation (Husse et al., 2017; Kervezee et al., 2019).

There are multiple scenarios where an individual is exposed to light at unnatural times or experiences wakefulness during the dark phase. One scenario is through shift work, defined as any shift outside 7am-6pm (Caruso, 2014). Consistent or rotating night shifts encompass hours outside common day shift hours at various patterns, resulting in alterations between the number of days on and off shift work or the switch to a completely different type of shift work (Pilcher et al., 2000). During this time, tasks and recreational activities can greatly vary between individuals that consist of different psychosocial pressures that result in sleep loss, among other mental strains such as anxiety or irritation (Costa, 2003; Pilcher et al., 2000).

Night shift workers span across multiple sectors such as healthcare or transportation. In fact, epidemiological studies in health care workers show increased signs of pathologies associated with insulin resistance or obesity that predispose them to developing metabolic syndromes (Caruso, 2014; James et al., 2017). Yet, one critical gap in our knowledge stems from

the fact that there are inconsistencies in cross-sectional and observational epidemiological studies that link night shift work (among other things) to disease outcomes due to confounding variables, lack of statistical power, or occupation bias in meta-analyses (Asiamah et al., 2021; Hansen and Pedersen, 2025; Van et al., 2021). Indeed, because night shift work spans across multiple sectors, interpersonal social interactions or differences in work intensity could magnify the burden of night shift work or mask its effects.

Perhaps one of the main limitations regarding manipulative night shift studies is that it primary focuses on rodent models (Opperhuizen et al., 2015). Although these studies have proven useful in linking similar and clear patterns regarding glucose intolerance (e.g., hyperglycemia) and melatonin suppression between mammalian species, there are some studies that show differential effects between mice and rodents under the same circadian rhythm disruption paradigm (Summarized in Opperhuizen et al., 2015). Additionally, rodents have opposing phase relationships compared to humans such as glucocorticoid secretion, activity on/offset, and sleep/wake cycles. Therefore, translating findings from nocturnal rodents to diurnal humans may not be fully representative and should be done with caution (Mendoza, 2021; Opperhuizen et al., 2015).

Nevertheless, longitudinal, cross-sectional, or cohort based epidemiological studies have provided a solid foundation of evidence clarifying that night shift work is indeed a detrimental stressor (Guindon et al., 2024; James et al., 2017; Walker et al., 2020). Such associations with the development of diseases have even prompted researchers and the medical community to redefine night shift work as a carcinogen, given its link to the development of multiple cancers even after controlling for biases and confounding factors (World Health Organization monographs, 2019; Moon et al., 2024). However, there are likely alternative physiological outcomes and patterns in

response to night shift work based on sex, chronotype, individual sensitivity, and temporal niche, given that manipulative studies in other model systems are lacking, especially in diurnal animals (but see Mendoza, 2021).

Birds provide a unique opportunity to explore the effects of shift work and circadian misalignment. Songbirds have phase relationships that closely mimic human sleep/wake cycles and similar rhythms in glucocorticoid and melatonin secretion (Bahammam, 2025; Cassone, 2015, 2014). In contrast to mammals of similar body size, birds have a substantially higher resting metabolic rates, which reflect almost a 2-3 fold difference in fasted glucose levels and the capacity to mount glucose responses that exceed point-of-care device detection limits (600 mg/dL) (personal observations) (Braun and Sweazea, 2008; Sweazea, 2022). Yet, these extreme levels of glycemia show little to no association with oxidative stress or the glycation of biomolecules in birds (Brun et al., 2022; Sweazea, 2022). This is in direct opposition to rodent and human models, that are unable to sustain hyperglycemic conditions, known to be a driver in the development chronic health diseases, longevity, and cellular damage (Sweazea, 2022). Thus, a bird's natural evolutionary resistance to hyperglycemia and cellular damage provides an interesting avenue to investigate the mechanisms that may underlie their resilience to metabolic effects in response to night shift work, with the perspective of the evolutionary pressures that have shaped their life-history.

Zebra finches (*Taeniopygia guttata castanotis*) are an arid-adapted, diurnal songbird native to Australia. For decades, they have been the prime candidate model to evaluate endocrine axes, such as the hypothalamic-pituitary-adrenal (HPA) axis, which regulates physiological stress responses that mediate plastic responses to environmental variation, among other endocrine axes that underlie the neurobiology of learning and cognition (Perfito, 2010; Spierings and Cate,

2016). Unlike other diurnal birds that show flexibility in their nighttime activity (and possibly their physiology), zebra finches are strictly diurnal, showing little to no activity during the dark phase (Wang et al., 2012). Zebra finches are also opportunistic songbirds, meaning that photoperiodism is generally not the ultimate cue to time crucial life history events such as reproduction (Perfito et al., 2008). Thus, they provide the perfect opportunity to disentangle how shifting patterns of light at night underpin specific neuroendocrine pathways and their downstream consequences, without activating or confounding other pathways sensitive to photoperiodism and associated with life-history variation (gonadal stimulation).

To fill critical gaps in both rodent and human night shift literature, we leveraged the unique biology of the zebra finch to investigate how simulated night shift work altered regulation of two key hormones: glucocorticoids and melatonin. Glucocorticoids and melatonin are both under circadian control, and reflect circadian alignment, albeit downstream from the master clock. The zenith of glucocorticoids prior to activity onset or the early morning primes the body for wakefulness by increasing blood pressure, alertness, and heart rate, while simultaneously increasing appetite and promoting catabolism. Conversely, the nadir of glucocorticoids is thought to depress the body for the predicted resting phase by decreasing blood pressure and slowing down heart rate, while suppressing appetite and promoting anabolism (Oster et al., 2017; Rao and Androulakis, 2019). While melatonin is critical in biological timekeeping, it also acts as an antioxidant (Bonnefont-Rousselot and Collin, 2010). The melatonin antioxidant cascade integrates this hormone as well as its metabolites to reduce the superoxide anion (O_2^-), a normal byproduct of cellular metabolism, prior to or after chemical reactions with other reactive species such as hydroxyl and peroxyl groups (Tan et al., 2007). Thus, in combination with other

endogenous antioxidants (*e.g.,* superoxide dismutase) melatonin serves as a multifunctional hormone to prevent oxidative stress and accumulation of damage.

In this study, we exposed 24 female adult zebra finches to alternating light cycles of 12D:12L and 12L:12D to mimic rotating night shift work conditions for a total of 66 days, with 3 days on the simulated night shift protocol and 3 days off (while another group of 24 female zebra finches remained on 12L:12D; N=48). We hypothesized that simulated night shift work would alter regulation of the hypothalamic-pituitary-adrenal (HPA) axis and melatonin rhythms, resulting in downstream physiological consequences on energy metabolism, morphometrics, and oxidative stress.

We predicted that chronic exposure to our treatment paradigm would blunt the adrenocortical response and reduce their ability to facilitate negative feedback, resulting in poor efficiency in the breakdown of energy substrates (glucose and β-hydroxybutyrate). Furthermore, we predicted that the resulting disruption in energy homeostasis would lead to a rise in body mass and subcutaneous fat deposits. We also predicted that simulated night shift work would suppress the diurnal peak of glucocorticoids and the nocturnal peak of melatonin. Although we expected a suppression of these hormone peaks, we predicted that treatment birds would sustain higher levels of glucocorticoids and lower levels of melatonin compared to controls, therefore increasing the prevalence of oxidative damage in the liver and brain.

Materials and Methods:

Animal husbandry

Adult female zebra finches (N = 48) (all <1 year old) in this study originated from a captive breeding colony at Auburn University with known hatch date and history as well as from a local breeder located in Georgia, USA (~2 hours away from AU) and have never previously experienced light at night. Zebra finches were housed in in tower cages (38.10 cm width × 45.72 cm depth × 45.72 cm height) and maintained under a 14L:10D photoperiod at Avian Research Laboratory II at Auburn University. Average temperature and humidity levels ranged between 21.92°C (± 2.18 SD) and 58% (± 22 SD), respectively. A mixture of finch seeds (Kaytee supreme) and water was provided ad libitum.

Finches from both origins (20 birds from our breeding colony and 28 birds from the local breeder) were weight-matched and randomly distributed into two experimental groups. Animals were then transported from Avian Research Laboratory II to the Biological Research Facility on AU's campus (<1.2 miles) and housed there for the remainder of the experiment.
Once at the Biological Research Facility, zebra finches were further distributed and housed across four identical, temperature and humidity controlled animal housing rooms (2 rooms/treatment; n = 12/room). To account for potential differences due to Origin, birds from both sources were equally distributed across treatment groups and the animal housing room, with five AU birds and seven from the local breeder in each. Birds were singly housed in Prevue Pet Products black wire cages (24 in. L x 16 in. W x 16 in. H with 3/8 in. wire spacing) separated by a cage divider and situated on secured metal racks. Animals were within sight of one another,

and we followed the same animal husbandry regimen that was conducted at Aviary Research Laboratory II.

Birds were able to acclimatize to their new environment and photoperiod set at 12L:12D (lights on 6am; lights off at 6pm) for at least three weeks before pretreatment samples were collected. The lighting source provided were PLT Solutions 17-Watt 5000K white LED lights which consists of shorter wavelengths of light known to disrupt glucocorticoid levels at low-level light intensities and activate deep brain photoreceptors in avian species (Alaasam et al., 2018). Control birds experienced an average of 34.83 lux/ft2 (± 19.17 SD), while treatment birds experienced an average of 36.51 lux/ft2 (± 15.29 SD), measured using Hobologgers (HOBO onset product # UA-002-64 and U12-006). Low ambient white noise (<10 decibels) was played throughout the entirety of the experiment to eliminate unwanted outside noise. All animal handling, training, and care procedures were approved by the Institutional Animal Care and Use Committee (IACUC) protocol #2023-5154 at Auburn University.

Experimental design and sampling scheme

All birds were acclimatized to a 12L:12D light cycle with lights turning on at 6am (ZT0) and lights turning off at 6pm (ZT12). To simulate night shift work conditions, the treatment group (n = 24) switched between a 12D:12L and 12L:12D light cycle every three days when experimental treatment began (**Fig. 18**). This resulted in treatment birds experiencing "dark hours" starting at 6am and "light hours" starting at 6pm. After three days of the night shift protocol, treatment birds switched back to a 12L:12D light cycle to mimic "off shift" conditions, in which they experienced the same light cycle as controls and were previously acclimated to, and this pattern persisted for the duration for the experiment (66 days). Animal husbandry was

completed only when animals experienced light hours. Moreover, sampling for our variables of interest only occurred when all animals experienced the same light cycle.

Per IACUC regulations (Protocol #2024-5154), to not exceed 140 µL of blood sample collection every 2 weeks (i.e., 1% of an average 14g zebra finch's body mass), blood sampling for different metrics occurred on different days. We measured HPA axis dynamics after 3 and 21 night shifts, which were on days 4 and 40 of the experiment, respectively, (**Fig. 18**). HPA axis dynamics included baseline, post-restraint, and post-dexamethasone regulation of circulating corticosterone (the main avian glucocorticoid and hereby referred to as Cort) levels. Blood samples (50µL) were collected within 3 min of disturbance via the brachial vein using a 26 gauge needle. Birds were subsequently restrained in a brown opaque bag as a standardized inducer of the glucocorticoid stress response. After 30 min, a post-restraint blood sample (30 µL) was collected from finches. Immediately after the post-restraint blood sample was taken, feathers covering the left pectoral muscle were gently pushed aside and the area was sterilized with a 70% ethanol-soaked cotton ball. After allowing the ethanol to evaporate (< 15 seconds), dexamethasone (a synthetic glucocorticoid) was administered to individuals intramuscularly using a 0.3 mm insulin syringe, prepared at a dosage of 1000 µg/kg of body weight (Jimeno et al., 2018; Kriengwatana et al., 2014). Finches were returned to their home cages to initiate negative feedback. After 30 min, we obtained a final blood sample (50 µL) to evaluate glucocorticoid negative feedback efficiency. All blood samples were spun at 14,800 *x g* for 10 min to separate plasma and red blood cells, snap frozen in liquid nitrogen, and subsequently stored in a -80°C freezer until analysis.

Fasted levels of blood metabolites (glucose and β-hydroxybutyrate) were measured after 6 and 24 night shifts on the morning of experimental days 11 and 47, respectively, following a brief fast from the night prior (**Fig. 18**).

Intraindividual variation in circulating hormone levels were measured prior to experimental manipulation and after 64 days of chronic simulated night shift work. Blood samples were collected from different individuals (n= 4/treatment) within 3 min of disturbance across six collection timepoints every four hours (ZT0, ZT4, ZT8, ZT12, ZT16, ZT20). ZT0 corresponds to 6:00am. Between ZT12-ZT20, finches were bled in under red light in total darkness to prevent melatonin suppression. After blood collection, samples were immediately spun down at 14,800 *x g* for 10 min to separate plasma and red blood cells, snap frozen in liquid nitrogen, and subsequently stored in a -80°C freezer. Birds were euthanized via isoflurane two days later on day 66 and we collected the right hemisphere of the brain and liver all within ten minutes of death.

Due to unknown reasons, two individuals from the control group died during the experiment. Therefore, the limited data collected from these birds were excluded from all analyses.

Morphometrics

Body mass (to the nearest 0.01 g) and a visual score (scale of 0-5) of the subcutaneous fat deposits over the tracheal pit (furculum fat) was obtained seven days prior to HPA axis dynamics sampling days. This ensured as accurate as possible a weight measurement to adjust injection volumes for correct dosage of dexamethasone across all birds, while also minimizing disturbance too close to the sampling timepoint. Body mass measurements were obtained using a scientific

scale and fat was scored by a single observer. To account for variance in body size, we measured the left and right tarsus length to the nearest 0.01 mm using calipers by a single observer.

HPA axis dynamics

We measured HPA dynamics across three collection timepoints (Pretreatment, 3, and 21 night shifts) using Arbor Assay Corticosterone Assay kit (Ann Arbor, MI cat # K014-H5). Following validations in our lab, we diluted plasma samples 1:10 with 8% disassociation reagent and ran samples in duplicate such that each unique individual measured across all collection timepoints were represented on a singular plate. A nine-point standard curve was generated in triplicate from 10,000 pg/mL to 39.06 pg/mL. A known concentration of corticosterone standard was prepared at 625 pg/mL and aliquoted across all plates to assess interplate variation. Due to unexpectedly low levels of Cort, all baseline samples (n = 136) fell off the standard curve and were undetectable; therefore, we excluded them from the further analysis. Negative feedback efficiency was calculated as the relative reduction or percent change from restraint-induced Cort to post-dexamethasone (Post-dex) Cort using the following equation below (Lattin et al., 2020). Positive values indicate that individuals suppressed Cort, with 100% indicating complete inhibition, while negative values indicate individuals secreted Cort, even after the dexamethasone injection. A total of 15 plates were ran across two days. Intraplate variation was 7.1% while interplate variation was 9.1%.

$$\frac{Restraint\text{-}induced\ Cort - Post\text{-dex}\ Cort}{Restraint\text{-}induced\ Cort} * 100\%$$

Equation (1)

Metabolites

Following a brief fast from the night prior, blood was collected within 3 min of disturbance the subjective morning to measure circulating metabolites. Blood glucose (mg/dL) and β-hydroxybutyrate (mmol/L) levels were measured in duplicate using the ReliOn prime blood glucose monitoring device (Walmart Apollo LLC Bentonville, AR) validated in our lab (Pham et al., 2025) and the PrecisionXtra ketone monitoring device (Abbott; product # 9881465), respectively.

To validate the PrecisionXtra ketone monitoring device for use in zebra finches, we compared β-hydroxybutyrate levels measured between the point-of-care device and a bench assay to ensure values collected by the meter were reflective of values from the bench assay. Male and female zebra finches (N = 13), which were not part of this study, were briefly fasted the night prior to sampling and randomized into various timepoints between 0-45 minutes post-room disturbance to create a range of β-hydroxybutyrate levels. We collected two blood samples per individual (~140uL total) via the brachial vein using a 26-guage needle. A drop of whole blood was used to measure circulating β-hydroxybutyrate levels in duplicate for all individuals. Blood samples were subsequently centrifuged, and plasma was collected to measure β-hydroxybutyrate levels using a commercial kit (Sigma Aldrich) following manufacture instructions. Due to sampling error (*e.g.,* hematocrit tube breaking), we had a total of 17 data points in which β-hydroxybutyrate levels were quantified both with the point-of-care device and benchtop assay (**supplementary materials; Fig. S9**).

24-h circulating hormone level

Because we expected low levels of circulating corticosterone throughout a 24-h period, we utilized an alcohol extraction method to extract corticosterone from plasma following (Parks et al., 2023) with slight modifications. Rather than 5 µL of starting plasma, we used 10 µL to increase our precision and ability to detect low levels of corticosterone with 40 µL of assay buffer provided by the Arbor Assay Corticosterone Assay kit (Ann Arbor, MI cat # K014-H5). Afterwards, 250 µL of ethyl-acetate was added to tube and was vortexed for 30 s at 1800 RPM. Samples were allowed to incubate for 5 mins at room temperature to allow for phase separation. Samples were then placed in the -80°C freezer for 10 minutes. After 10 min, samples were taken out, allowed to thaw, and the alcohol layer was collected. We repeated this process two more times for a total of 600-700 µL of the alcohol layer collected. To calculate extraction efficiency, a plasma pool from non-experimental bird samples was stripped of hormone and spiked with a corticosterone standard (100,000 pg/mL) to a known concentration of 10,000 pg/mL. We followed the same extraction method for this spiked sample. All samples were allowed to fully evaporate overnight under a fume hood.

After evaporation, tubes were reconstituted with 125 µL of assay buffer and placed in the -20°C freezer until assayed two days later using Arbor Assay Corticosterone kit (Ann Arbor, MI cat # K014-H5). A total of four plates were ran, with each unique individual measured across the two collections timepoints represented on a singular plate. Because we recovered 96% of the corticosterone from the spiked sample, we adjusted raw values based on 100% extraction efficiency to be comparable to other studies measuring 24-h corticosterone, and thus, report data based on 100% efficiency. Intraplate variation was 1.3% while interplate variation was 2.6%.

To measure 24-h melatonin, we used a Melatonin ELISA Kit (OKEH02566) previously validated in zebra finches (Mishra et al., 2019). We diluted plasma samples 1:1 with the sample dilutant provided by the kit and ran the assay according to the manufacturer instructions. A 7-point standard curve was generated in triplicate from 1,000 pg/mL to 15.63 pg/mL. Due to plasma limitations, we ran our samples as singlets, however, our values are reflective of previously published literature using the same kit in zebra finches across similar ZT collection timepoints (Alaasam et al., 2021). Intraplate variation was 9.8%.

Immunoblots

To prepare samples for immunoblotting, we utilized the right lobe of the liver and the right hemisphere of the brain, after removing the cerebellum, optic tectum, and a small portion of the frontal lobe, such that the majority of the brain tissue utilized was the diencephalon. Liver tissue was prepared in the same manner as previously described (Pham et al., *in press*; Hoffman et al., 2024), but due to low protein abundance in the brain, we standardized protein concentration to 0.5µg/µL across all brain samples. Primary antibodies included an anti-rabbit polyclonal 4-hydroxynonaneal antibody (Abcam; ab46545; 1:1000 dilution) and anti-rabbit polyclonal SOD1 antibody (GeneTex; GTX100554; 1:500). The secondary antibody was an anti-rabbit horse radish peroxidase antibody (Cell Signaling 7074) prepared at 1:2000 for 4-hydroxynonaneal and 1:1000 for SOD 1. Protein bands were visualized via chemiluminescence using ECL prime (VWR 89238-012) and images were captured using ImageQuant LAS 4000 (GE Healthcare). We used Image Analysis (Bio-Rad) to perform densitometry. We used ponceau staining to normalize values to total protein.

Statistical analysis

All statistical analyses were run in R (Version 4.5.0). Statistical significance was determined using an alpha value of $P \leq 0.05$. Global Linear mixed effects models using the "lme4" and "lmertest" package were generated with Treatment (two level factor) and Timepoint (three level factor) treated as fixed effects as well an interaction term between the two variables (Treatment * Timepoint). Fixed covariates included body mass and tarsus length to control for variation in body size and fluctuations in body mass. For β-hydroxybutyrate and glucose response variables, we also included a fixed covariate of order to control for the sequence in which we entered animal housing rooms during the metabolite measurement days. A fixed factor of origin was also included in all global models in order to determine whether patterns of our response variables were associated with the source population of our birds. To evaluate changes in fat score, we used the "Ordinal" package in R, as each incremental value in the score represents a change in the amount of subcutaneous fat. We included individual Bird ID as a random intercept in all models that had response variables that were sampled across multiple timepoints to account for repeated measures. For immunoblots, gel was included as a random effect. Protein abundance of SOD and 4-HNE were log-transformed to meet assumptions of the linear model. If a significant interaction term was detected on any of the response variables, Tukey's post-hoc test followed using the "emmeans" package in R for pair-wise comparisons. Non-significant interactions and covariates were removed from global models, and thus, the final model with results reported is the simplest model.

We used the "GLMMcosinor" package in R to fit models on 24-h hormone variables. This package combines the power of generalized linear models to fit multiple types of data distributions in addition to rhythmic data that often violate the assumptions of linearity and

normality. Furthermore, because we had birds measured at the same ZT time before and after exposure to treatment, we examined within-individual differences using linear mixed effects models at specific ZT times. In regard to the cosinor analysis, the response variables included circulating plasma corticosterone and melatonin collected across six sampling timepoints, and dependent variables ZT time, Treatment, and a family = Gamma or Gaussian distribution for corticosterone and melatonin, respectively. Shapiro-wilks test indicated non-normality of 24-h corticosterone and we chose a gamma distribution based on the best fit theoretical distribution using simulated data (n = 1000 iterations) that was generated from raw data via the "thefitdistrplus" package in R. Residuals of melatonin were normally distributed, and thus a Gaussian distribution was sufficient. We tested for group differences based on treatment on the acrophase (the peak of the hormone), amplitude (peak hormone level subtracted from average hormone levels), and mesor (the average rhythm of hormone). The acrophase of corticosterone and melatonin was calculated by extracting the beta estimate measured in radians divided by 2π multiplied by the period (24) following the below equation.

In regard to the linear mixed effects models, we had specific *a priori* predictions that individuals under night shift work would have a suppression in their corticosterone peak that coincides with ZT0, the predicted zenith for corticosterone release and at ZT12, the predicted nadir. Thus, we ran our models by subsetting data by specific ZT times. The response variable included 24-h corticosterone with the interaction of treatment and collection timepoint (pretreatment/exposure; 2 level factor). Bird ID was included as a random effect to account for non-independence and repeated measures. Because we had data points missing for pretreatment 24-h melatonin profiles, we lacked statistical power to investigate this hormone in a similar manner.

$$\frac{1.15\ radians}{2\pi} * 24 = Peak\ Cort\ for\ controls$$

$$\frac{-2.03\ radians}{2\pi} * 24 = Peak\ Cort\ for\ treatment$$

Equation (2)

$$\frac{-2.61\ radians}{2\pi} * 24 = Peak\ melatonin\ for\ controls$$

$$\frac{-0.17\ radians}{2\pi} * 24 = Peak\ melatonin\ for\ treatment$$

Equation (3)

Results:

Circadian variation in hormone levels

Linear mixed effects model indicated a significant interaction between collection timepoint and treatment ($F_{1,5} = 6.55$; $P = 0.05$) on corticosterone levels specifically collected at ZT0. Post-hoc analysis found that birds under chronic night shift work had an average suppression of -1.93 ng/mL in their corticosterone levels between the two collection timepoints (Tukey's Post hoc: β = -1.93; 95% CI = -4.21 to -0.65; t = -2.69; $P = 0.04$; **Fig. 19A**). We found that 87% of the overall variance in 24-h corticosterone levels at ZT0 was due to within-individual variation, while only 13% was due to between-individual differences.

We found that both groups had significant corticosterone rhythms, indicated by the mesor (Control: GLMMcosinor: β = 0.30, 95% CI = 0.03 to 0.56; $P = 0.03$; Night shift: GLMMcosinor: β = 0.31, 95% CI = 0.07 to 0.56; $P = 0.01$; **Fig. 19B**). Moreover, both groups had relatively the same amplitude (Control: β = 0.19; Night shift: β = 0.22), with no statistical difference (GLMMcosinor: β = 0.03; P = 0.92) and no average difference in corticosterone levels (**Fig. 19C**). We found that the acrophase of Cort peaked for control birds 4.49 hours from ZT0, resulting in the maximal level of Cort secreted approximately ~ZT4-5 (10am-11am) (GLMMcosinor: β = 1.15 radians). In contrast, birds under night shift had their peak in Cort -7.76 hours from ZT24, resulting in the highest level of Cort approximately ~ZT 16-17 (10pm-

11pm) (GLMMcosinor: β = -2.03). Furthermore, there was statistically significant difference in the acrophase between groups due to simulated night shift treatment (GLMMcosinor: β = 3.09; 95% CI = 0.62 to 5.56; P = 0.01; **Fig. 19B**).

Both groups had significant melatonin rhythms, indicated by the mesor (Control: GLMMcosinor: β = 157.43; 95% CI = 140.08 to 174.77; $P < 0.0001$; Night shift: GLMMcosinor: β = 171.57, 95% CI = 153.17 to 189.97; $P < 0.0001$; **Fig. 20A**). Both groups had similar amplitude estimates (Control: β = 17.31; Night shift: β = 10.72), with no statistically significant difference (GLMMcosinor: β = -6.58; $P > 0.72$) and no average difference in melatonin levels (**Fig. 20B**). We found that the acrophase of melatonin release for control birds was -8.25 hours from ZT 24, resulting in the highest level of melatonin approximately ~ZT 15-16 (9pm-10pm) (GLMMcosinor: β = -2.61). In contrast, the acrophase of melatonin for night shift birds was -0.65 hours from ZT 24, resulting in the highest level of melatonin observed approximately ~ZT 23-24 (5am-6am) (GLMMcosinor: β = -0.18). We detected a slight trend indicating that the acrophase was different between groups, but this did not reach statistical significance (GLMMcosinor: β = 2.44; 95% CI = -0.38 to 5.26 ± 95% CI; $P = 0.09$)

HPA axis reactivity

We did not detect a significant interaction between treatment and timepoint on post-restraint corticosterone levels (Treatment*Timepoint: $F_{2,75} = 0.57$; $P = 0.57$). However, there was an overall, significant main effect of treatment ($F_{1,38} = 12.72$; $P < 0.001$) in which post-restraint corticosterone levels in birds undergoing simulated night shift work were on average 2.53 ng/mL lower than those under a consistent light/dark cycle. (LMM: β = -2.53; 95% CI = -4.63 to -0.43; $t = -2.29$; $P = 0.02$; **Fig. 21**). There was no main effect of treatment ($F_{1,42} = 0.84$; $P = 0.36$) or its

interaction with timepoint ($F_{2,63} = 1.06$; $P = 0.35$) on negative feedback efficiency. There was strong evidence indicating that there was an overall main effect of timepoint ($F_{2,63} = 5.15$; $P \leq 0.008$) on negative feedback efficiency, however corticosterone levels did not differ when comparing between timepoints of interest (Pretreatment vs Acute: $P = 0.21$; Pretreatment vs Chronic: $P = 0.34$; **Fig. S9**)

Morphometrics

We did not detect an overall main effect of treatment ($F_{1,41} = 0.33$; $P = 0.57$) or its interaction with timepoint ($F_{3,126} = 1.65$; $P = 0.18$) on body mass (**Fig. S10**). There was no main effect of timepoint ($\chi^2 = 1.9$; $P = 0.59$), nor the interaction between treatment or timepoint ($\chi^2 = 2.7$; $P = 0.44$).

Metabolites

We detected a significant interaction between Treatment and Timepoint, in which β-hydroxybutyrate levels differed between treatment groups but was dependent on the duration of treatment ($F_{2,83} = 7.78$; $P = 0.0008$). Post hoc tests revealed that there was no initial average difference between control and night shift groups in circulating β-hydroxybutyrate levels (Tukey's Post hoc: β = 0.07; 95% CI = -0.70 to 0.83; t = 0.71; P = 0.86; **Fig. 22A**). However, after acute exposure to night shift work (6 night shifts), treatment birds had on average 1.28 mmol/L greater amount of β-hydroxybutyrate than controls (Tukey's Post hoc: β = 1.28; 95% CI = 0.53 to 2.04; $t = 3.38$; $P = 0.0011$; **Fig. 22A**) and remained elevated until day 47 of the simulated night shift (Tukey's Post hoc: β = 1.14; 95% CI = 0.39 to 1.9; $t = 3.02$; $P = 0.004$; **Fig. 22A**).

We detected a significant main effect of Timepoint, in which glucose levels increased over the duration of the experiment ($F_{2,85} = 11.8$; $P < 0.0001$), however this was regardless of treatment, as there was no significant Treatment*Timepoint interaction ($F_{2,83} = 0.10$; $P = 0.90$). Specifically, glucose levels increased on average 13.24 mg/dL between Pretreatment and when birds were remeasured on day 11 of the experiment (acute timepoint) (LMM: β = 13.24; 95% CI = 3.10 to 23.32; $t = 2.56$; $P < 0.01$; **Fig. 22B**). Moreover, when comparing Pretreatment to day 47 of the experiment (chronic timepoint), we found that glucose increased on average 25.40 mg/dL more between the two timepoints (LMM: β = 25.40; 95% CI = 15.13 to 35.63; $t = 4.85$; $P < 0.0001$; **Fig. 22B**).

Oxidative stress markers in the brain and liver

In the brain, there was a significant effect of treatment ($F_{1,29} = 17.41$; $P = 0.0002$) in which birds under night shift work had lower relative protein abundance of SOD1 compared to controls (LMM: β = -0.16; 95% CI = -0.24 to -0.08; $t = -4.17$; $P = 0.0002$; **Fig. 23A**). Although birds under night shift work had a reduction in SOD1 protein levels in the brain, this did not result in greater oxidative damage to lipids measured through 4-HNE adducts ($F_{1,30} = 0.71$; $P = 0.41$; **Fig 23B**). In the liver, there was no effect of treatment ($F_{1,37} = 2.16$; $P = 0.15$; **Fig. S11A**) on SOD1 levels or 4-HNE ($F_{1,36} = 1.08$; $P = 0.31$; **Fig. S11B**).

Discussion:

In this study, we examined how simulated night shift work altered corticosterone and melatonin rhythms, resulting in changes in HPA axis dynamics and downstream consequences on energy metabolism, body condition, and oxidative balance. We found that simulated night shift

inverted corticosterone profiles, with peak levels detected during the dark phase between 10-11pm, rather than during the light phase. Similarly, there was a slight trend indicating a shift in the acrophase of melatonin towards the early morning hours, rather than at night. Plasma constraints limited our ability to measure melatonin from samples collected towards the beginning of the light phase (ZT0) and the middle of the night (ZT16), likely contributing to inadequate variation to detect a stronger (or weaker) shift in the acrophase. Nevertheless, we still found significant melatonin and corticosterone rhythms in birds undergoing simulated night shift work, suggesting that they were able to tolerate the treatment paradigm and maintain circadian alignment, albeit inverted from their natural diurnal rhythm.

The inversion of corticosterone profiles may be a plastic response to alternating patterns of light at night, in which circadian oscillators resynchronize to predictable nighttime conditions to prevent a mismatch between endogenous rhythms - yet may not be without some cost. In our study, the inversion of corticosterone profiles altered physiological responses and energy homeostasis. Birds under simulated night shift work had a dampened glucocorticoid response to capture and restraint, indicating poor HPA axis reactivity. Furthermore, there was a significant reduction in corticosterone profiles at ZT0 (lights on; "awakening") after exposure to treatment. Poor sleep quality, a common outcome due to consistent/rotating night shift work in humans, show conflicting patterns on stress responsiveness, with studies indicating a suppressed or heightened response (van Dalfsen and Markus, 2018). This variation may stem from the fact that different aspects of sleep (i.e., duration, disturbance, or architecture) can differentially affect neuroendocrine responses, along with other factors such as sex (Bassett et al., 2015). However, the strongest predictor that seems to be associated with the blunting of stress responsiveness in humans is daytime sleepiness (van Dalfsen and Markus, 2018). In our study, it is possible that

birds under night shift work were unable to respond strongly to capture and restraint due to the fact that they were previously under the treatment paradigm the morning that we tested reactivity of the HPA axis (i.e., altered activity levels or loss of sleep). Given that corticosterone profiles were inverted and strongly rhythmic, it is possible behavioral rhythms followed in parallel, as there is tight coupling between both types of rhythms (Oster et al., 2017; Rao and Androulakis, 2019). However, we are unable to confirm this speculation as we did not measure behavioral rhythms or sleep patterns and it is possible for glucocorticoid and behavioral rhythms to disassociate through masking effects.

Although stress responsiveness was not tested, a similar inversion of glucocorticoids profiles (higher levels at night, rather than the morning) measured in saliva was found in female nurses working consistent night shifts (Niu et al., 2015). Moreover, several studies corroborate that salivary cortisol levels at the time of awakening are significantly lower in individuals working night shifts (Andreadi et al., 2025; Hennig et al., 1998; Niu et al., 2015). Interestingly, Niu et al., 2015 found that salivary cortisol levels remained lower in night shift nurses, even on the first day off the shift schedule, indicating a lingering effect. However, cortisol levels rebounded and were not significantly different from day shift nurses by the 2nd day off night shift. This finding further suggests plasticity of the circadian system to quickly realign to a newly imposed pattern of wakefulness/rest in a relatively short amount of time. In our study, we measured 24-h corticosterone profiles on the first day after three simulated night shifts to capture the strongest effect of our treatment paradigm. Our results may have produced similar results as Niu et al., 2015 if we had sampled 24-h hormone profiles on the second day off simulated night shift after allowing birds the opportunity to readjust to a different pattern (12L:12D). This reorganization between circadian oscillators suggests high flexibility to disrupting patterns of

light at night. Yet, there are likely species-specific differences in the time it takes to re-entrain to a light/dark cycle based on sensitivity to photoperiodism or the presence of supplementary environmental cues.

For birds (and mammals) within temperate zones that heavily rely on photoperiodism as an ultimate cue, circadian oscillators may be slower or more inflexible in their response to phase changes (i.e., days getting longer/shorter) given that they need to subsequently finetune downstream responses with proximal cues (e.g., food availability/temperature) to prevent mismatches (Tolla and Stevenson, 2020). One study found significantly more variation in the photoperiodic response of opportunistic breeders compared to seasonal breeders (measured through gonadal stimulation/growth), indicating that seasonal breeders, to some extent, lack flexibility in response to photoperiodism and is more of a fixed response (Watts et al., 2015). A study in Siberian hamster (seasonal breeder) found that supplementary cues (food availability and population size) became more important to time reproductive events when they were placed in a photoperiod unable to activate reproductive pathways, indicating flexibility when photoperiod is no longer sufficient or predictable (Paul et al., 2009). However, circadian genes or hormone profiles were not measured in either study. Nevertheless, our finding on inverted corticosterone profiles in response to simulated night shift work suggests that a diurnal, opportunistic songbird, can quickly adapt to unnatural patterns of light at night and could affect how they coordinate peripheral or master oscillators to maintain function.

Glucose metabolism is tightly regulated such that animals do not exceed or fall short of optimal ranges that risks hyper/hypoglycemia. Elevated blood glucose levels glycate biomolecules, increase oxidative stress markers, and damage epithelial lining of blood vessels in most animals (Preiser et al., 2016). Consequently, hyperglycemia is strongly associated with the

development of atherosclerosis, hypertension, and insulin insensitivity, all of which are risk factors underlying the increased prevalence of cardiovascular diseases in night shift workers (Briançon-Marjollet et al., 2015; James et al., 2017). Rodent models of shift work, and other perturbations in the nighttime light environment, show similar metabolic consequences as humans, such as elevated fasted blood glucose levels, and a reduction in insulin sensitivity (Opperhuizen et al., 2015). In our study, we did not detect changes in fasted blood glucose levels due to night shift work. This is likely due to the fact that avian species are able to withstand a wide range of glucose values, which reflect variation in environmental pressures, nutritional state, life-history, or seasons (Beattie et al., 2022; Remage-Healey and Romero, 2000). However, we did see an interesting overall increase in fasted glucose values throughout the duration of the experiment, which may be an indicator of repeated sampling and handling stress. Montoya et al., (2020) found that glucose levels increased due to successive handling to administer intraperitoneal injections within a much shorter timeframe (0-40 minutes) in zebra finches (Montoya et al., 2020). In a previous experiment using a constant light paradigm in zebra finches, we found a similar increase in baseline glucose levels in control birds' overtime, however, it was not statistically significant (Pham et al., 2025). In the current study, we sampled over a much longer duration (days), yet found an increase of glucose levels over time in both groups. This could be a plastic response to modify the setpoint of circulating glucose levels to appropriately respond to predictable stressors, such as repeated handling/injections. While baseline glucose levels were unaltered in response to inclement weather, adult tree swallows that previously experienced colder temperatures mounted a stronger glucose response to restraint stress compared to swallows that experienced warmer temperatures (Ryan et al., 2023). Thus,

changes in glucose regulation could prime individuals to adaptively respond to predictable challenges they may encounter in the future.

Birds under night shift lighting patterns had significantly higher β-hydroxybutyrate metabolites compared to controls. This finding suggests that they were under a greater energetic demand to metabolize fats for fuel, rather than for storage. Given that we found inverted corticosterone rhythms, this is somewhat paradoxical as anabolism should be favored in parallel to corticosterone rhythms. β-hydroxybutyrate levels are generally only detected when glucose is no longer the primary substrate for energy production (i.e., fasting conditions) (Tabatabaei Dakhili et al., 2025). Within the context of our study, we fasted our birds to eliminate sources of variation due to food consumption prior to sampling, but also to evaluate if night shift work differentially affected metabolic pathways. Indeed, the higher β-hydroxybutyrate levels detected in night shift birds could be suggestive of a compensatory mechanism to maintain sufficient energy and activate cellular pathways in costly tissues, such as the brain or cardiac muscle (Tabatabaei Dakhili et al., 2025). Ketone bodies activate antioxidant pathways (among others), suggesting that under greater energetic demands or fasting conditions, higher breakdown of lipids (i.e., higher ketone bodies) may preserve or enhance brain and cardiac function through activating cellular stress response pathways (Rojas-Morales et al., 2020; Tabatabaei Dakhili et al., 2025).

This perspective and our finding of higher β-hydroxybutyrate levels could explain the patterns detected regarding our oxidative stress markers. Simulated night shift work decreased SOD1 protein levels in the brain, but birds did not display elevated oxidative damage to lipids. Furthermore, there were no changes in SOD or 4-HNE in the liver, indicating a tissue-specific response of oxidative stress under night shift work. The decrease in SOD1 levels in the brain

could suggest a utilization, in which SOD1 was depleted in order to convert superoxide into hydrogen peroxide, a less reactive molecule that can be reduced to water through glutathione peroxidase or catalase activity. Because β-hydroxybutyrate can activate antioxidant pathways, we would expect to see greater levels of SOD1 in the brain given that β-hydroxybutyrate was elevated throughout the duration of our experiment, but this was not the case. Perhaps there was a counter-balancing effect, in which SOD1 levels were continuously depleted and replenished via β-hydroxybutyrate signaling to prevent the accumulation of damage.

Contrary to our predictions, birds under night shift work did not have a suppression in their melatonin levels. This finding may further explain why we did not detect elevated oxidative damage, given that melatonin can quench reactive species. However, we only measured one antioxidant and oxidative damage marker. It is possible night shift work differentially affects biomolecules, with some more vulnerable than others or repaired at different rates. In other studies, melatonin supplementation can realign circadian oscillators after jet lag conditions and reduce accumulation of oxidative damage, likely by quenching a wide range of reactive intermediates (Bonnefont-Rousselot and Collin, 2010; Zisapel, 2018).

While circadian misalignment is detrimental in many cases, through masking, diurnal and nocturnal animals may be able to unlock temporal niches that do not override circadian-gated mechanisms. For example, although zebra finches exposed to ecologically relevant levels of artificial light at night displayed higher activity bouts at night (indicating some loss of sleep), circadian gene regulation was maintained in the brain (Alaasam et al., 2021). Moreover, after 6 months of light at night, zebra finches were able to habituate and did not exhibit severe levels of oxidative stress (Alaasam et al., 2024). Therefore, this is an example of positive behavioral masking, with seemingly little physiological costs associated with the masking response.

In a mammalian model, *Octodon degus* are able to leverage both temporal niches. While degus are mainly diurnal, they can display inverted phases in activity and body temperatures compared to diurnal chronotypes (Otalora et al., 2010). Yet, other parameters such as neuropeptides associated with awakening, and core clock genes are invariable between diurnal and nocturnal degus (Otalora et al., 2010). Therefore, the ability to leverage the changes in the nighttime environment through behavioral or physiological masking, without overriding circadian-gated mechanisms may be an important plastic response in the face of modified ecological landscapes and modern lifestyles (Bahammam, 2025; Helm et al., 2017).

Conclusions

Both Corticosterone and melatonin are reliable indicators of circadian alignment. Thus, it is interesting to see that birds maintained significant rhythms after 66 days of simulated night shift lighting patterns. Such minimal effects of our treatment paradigm on body condition and oxidative damage suggests that birds may have been able to predict and habituate to the switches in lighting patterns by quickly realigning themselves to the imposed change through plastic mechanisms. These explanations seem plausible, especially because of the aforementioned study in nurses demonstrating that by the second day off night shift, cortisol patterns returned to levels similar to those working day shifts (Niu et al., 2015). This is the first study to our knowledge to describe similar corticosterone profile changes in human night shift workers using a diurnal songbird as the model system. Moreover, we extend upon previous findings, by showing that zebra finches display even more circadian plasticity through sustained, albeit inverted, hormone profiles in response to chronic, simulated night shift work.

Future directions

While we found interesting patterns in response to simulated night shift lighting patterns, we failed to identify the presence of cellular damage and body condition metrics commonly detected in human and rodent models of night shift work. Perhaps there were compensatory mechanisms at play that masked the effect of our simulated night shift work paradigm, or simply that our treatment was irreflective of actual night shift work patterns.

Overall, our results underscore the need to extend upon commonly used model systems used to investigate circadian rhythm disruption. Birds are a unique diurnal model system that shows similar plasticity as humans to realign circadian rhythm. Yet, our study brings up other questions. Because our study focused on females, futures studies should examine possible sex differences in the degree of plasticity, the cost of repeated realignment to new rhythms, and incorporate unpredictability in the timing of light disruption. Given that birds have a unique resistance to metabolic disruptions, they offer an insightful path to explore the mechanisms as to how and why birds seem to resist commonly observed effects of circadian rhythm disruption to inform chronotherapies options (Bahammam, 2025). This is the first study and step towards evaluating how simulated night shift work affects diurnal bird models with similar phase relationships to humans.

Acknowledgments:

The authors would like to thank the Wada/Hood/Hill labs for helpful comments on improving the manuscript. The authors would also like to thank the undergraduate researchers, Yeojin Joo, Darielys Diez, Jordan Shapach, and Katie Gross as well as graduate students in the Wada lab for their assistance with animal husbandry, experimental setup, and sample collection.

Lastly, the authors would like to thank Dr.'s Jenny Ouyang and Valentina Alaasam for helpful comments, suggestions, and sharing their melatonin assay protocol.

Author Contributions:

Kevin Pham: Conceptualization, data curation, formal analysis, funding acquisition, Investigation, methodology, project administration, visualization, writing – original draft, writing – review & editing

Dr. Victoria M. Coutts: Investigation, methodology, data curation, writing – review & editing

Dr. Alexander J. Hoffman: Investigation, methodology, data curation, writing – review & editing

Dr. Haruka Wada: Conceptualization, funding acquisition, project administration, resources, supervision, validation, visualization, writing – review & editing

Funding sources:

K.P was supported by a National Institutes of Health T-32 Training Grant (G-RISE; Grant number: 5T32GM141739) and two NSF IOS grants (IOS-1553657 and IOS-201580) awarded to H.W.

Data availability:

Raw data and code will be deposited to an open source data repository upon submission to Proc B

References:

Alaasam, V.J., Duncan, R., Casagrande, S., Davies, S., Sidher, A., Seymoure, B., Shen, Y., Zhang, Y., Ouyang, J.Q., 2018. Light at night disrupts nocturnal rest and elevates glucocorticoids at cool color temperatures. J. Exp. Zool. Part A Ecol. Integr. Physiol. 329, 465–472. https://doi.org/10.1002/jez.2168

Alaasam, V.J., Hui, C., Lomas, J., Ferguson, S.M., Zhang, Y., Yim, W.C., Ouyang, J.Q., 2024. What happens when the lights are left on? Transcriptomic and phenotypic habituation to light pollution. iScience 27, 108864. https://doi.org/10.1016/j.isci.2024.108864

Alaasam, V.J., Liu, X., Niu, Y., Habibian, J.S., Pieraut, S., Ferguson, B.S., Zhang, Y., Ouyang, J.Q., 2021. Effects of dim artificial light at night on locomotor activity, cardiovascular physiology, and circadian clock genes in a diurnal songbird. Environ. Pollut. 282, 117036. https://doi.org/10.1016/j.envpol.2021.117036

Andreadi, A., Andreadi, S., Todaro, F., Ippoliti, L., Bellia, A., Magrini, A., Chrousos, G.P., Lauro, D., 2025. Modified Cortisol Circadian Rhythm: The Hidden Toll of Night-Shift Work. Int. J. Mol. Sci. 26, 1–16. https://doi.org/10.3390/ijms26052090

Asiamah, N., Mends-Brew, E., Boison, B.K.T., 2021. A spotlight on cross-sectional research: Addressing the issues of confounding and adjustment. Int. J. Healthc. Manag. 14, 183–196. https://doi.org/10.1080/20479700.2019.1621022

Bahammam, A.S., 2025. From Wings to Wellness: A Research Agenda Inspired by Migratory Bird Adaptations for Sleep and Circadian Medicine. Nat. Sci. Sleep 17, 583–595. https://doi.org/10.2147/NSS.S519493

Bassett, S.M., Lupis, S.B., Gianferante, D., Rohleder, N., Wolf, J.M., 2015. Sleep quality but not sleep quantity effects on cortisol responses to acute psychosocial stress. Stress 18, 638–644. https://doi.org/10.3109/10253890.2015.1087503

Beattie, U.K., Ysrael, M.C., Lok, S.E., Romero, L.M., 2022. The Effect of a Combined Fast and Chronic Stress on Body Mass, Blood Metabolites, Corticosterone, and Behavior in House Sparrows (Passer domesticus). Yale J. Biol. Med. 95, 19–31.

Bedrosian, T.A., Fonken, L.K., Nelson, R.J., 2016. Endocrine Effects of Circadian Disruption. Annu. Rev. Physiol. 78, 109–131. https://doi.org/10.1146/annurev-physiol-021115-105102

Bonnefont-Rousselot, D., Collin, F., 2010. Melatonin: Action as antioxidant and potential applications in human disease and aging. Toxicology 278, 55–67. https://doi.org/10.1016/j.tox.2010.04.008

Braun, E.J., Sweazea, K.L., 2008. Glucose regulation in birds. Comp. Biochem. Physiol. - B Biochem. Mol. Biol. 151, 1–9. https://doi.org/10.1016/j.cbpb.2008.05.007

Briançon-Marjollet, A., Weiszenstein, M., Henri, M., Thomas, A., Godin-Ribuot, D., Polak, J., 2015. The impact of sleep disorders on glucose metabolism: Endocrine and molecular mechanisms. Diabetol. Metab. Syndr. 7, 1–16. https://doi.org/10.1186/s13098-015-0018-3

Brun, C., Hernandez-Alba, O., Hovasse, A., Criscuolo, F., Schaeffer-Reiss, C., Bertile, F., 2022. Resistance to glycation in the zebra finch: Mass spectrometry-based analysis and its perspectives for evolutionary studies of aging. Exp. Gerontol. 164. https://doi.org/10.1016/j.exger.2022.111811

Caruso, C.C., 2014. Negative impacts of shiftwork and long work hours. Rehabil. Nurs. 39, 16–25. https://doi.org/10.1002/rnj.107

Cassone, V.M., 2015. Avian circadian organization. Mech. Circadian Syst. Anim. Their Clin. Relev. 35, 69–94. https://doi.org/10.1007/978-3-319-08945-4_5
Cassone, V.M., 2014. Avian circadian organization: A chorus of clocks. Front. Neuroendocrinol. 35, 76–88. https://doi.org/10.1016/j.yfrne.2013.10.002
Costa, G., 2003. Shift work and occupational medicine: An overview. Occup. Med. (Chic. Ill). 53, 83–88. https://doi.org/10.1093/occmed/kqg045
Cox, D.T.C., Gaston, K.J., 2024. Cathemerality: a key temporal niche. Biol. Rev. 99, 329–347. https://doi.org/10.1111/brv.13024
Guindon, G.E., Murphy, C.A., Milano, M.E., Seggio, J.A., 2024. Turn off that night light! Light-at-night as a stressor for adolescents. Front. Neurosci. 18, 1–8. https://doi.org/10.3389/fnins.2024.1451219
Hansen, J., Pedersen, J.E., 2025. Night shift work and breast cancer risk – 2023 update of epidemiologic evidence. J. Natl. Cancer Cent. 5, 94–103. https://doi.org/10.1016/j.jncc.2024.07.004
Helm, B., Visser, M.E., Schwartz, W., Kronfeld-Schor, N., Gerkema, M., Piersma, T., Bloch, G., 2017. Two sides of a coin: Ecological and chronobiological perspectives of timing in the wild. Philos. Trans. R. Soc. B Biol. Sci. 372. https://doi.org/10.1098/rstb.2016.0246
Hennig, J., Kieferdorf, P., Moritz, C., Huwe, S., Netter, P., 1998. Changes in cortisol secretion during shiftwork: Implications for tolerance to shiftwork? Ergonomics 41, 610–621. https://doi.org/10.1080/001401398186784
Husse, J., Kiehn, J.T., Barclay, J.L., Naujokat, N., Meyer-Kovac, J., Lehnert, H., Oster, H., 2017. Tissue-specific dissociation of diurnal transcriptome rhythms during sleep restriction in mice. Sleep 40. https://doi.org/10.1093/sleep/zsx068
James, S.M., Honn, K.A., Gaddameedhi, S., Van Dongen, H.P.A., 2017. Shift Work: Disrupted Circadian Rhythms and Sleep—Implications for Health and Well-being. Curr. Sleep Med. Reports 3, 104–112. https://doi.org/10.1007/s40675-017-0071-6
Jimeno, B., Briga, M., Hau, M., Verhulst, S., 2018. Male but not female zebra finches with high plasma corticosterone have lower survival. Funct. Ecol. 32, 713–721. https://doi.org/10.1111/1365-2435.13021
Kervezee, L., Cuesta, M., Cermakian, N., Boivin, D.B., 2019. The Phase-Shifting Effect of Bright Light Exposure on Circadian Rhythmicity in the Human Transcriptome. J. Biol. Rhythms 34, 84–97. https://doi.org/10.1177/0748730418821776
Kriengwatana, B., Wada, H., Schmidt, K.L., Taves, M.D., Soma, K.K., MacDougall-Shackleton, S.A., 2014. Effects of nutritional stress during different developmental periods on song and the hypothalamic-pituitary-adrenal axis in zebra finches. Horm. Behav. 65, 285–293. https://doi.org/10.1016/j.yhbeh.2013.12.013
Mendoza, J., 2021. Nighttime Light Hurts Mammalian Physiology: What Diurnal Rodent Models Are Telling Us. Clocks and Sleep 3, 236–250. https://doi.org/10.3390/clockssleep3020014
Mishra, I., Knerr, R.M., Stewart, A.A., Payette, W.I., Richter, M.M., Ashley, N.T., 2019. Light at night disrupts diel patterns of cytokine gene expression and endocrine profiles in zebra finch (Taeniopygia guttata). Sci. Rep. 9, 1–12. https://doi.org/10.1038/s41598-019-51791-9
Monographs, I., Identification, O.N.T.H.E., Hazards, O.F.C., Humans, T.O., 2019. Carcinogenicity of night shift work, The Lancet. Oncology. https://doi.org/10.1016/S1470-2045(19)30455-3

Montoya, B., Briga, M., Jimeno, B., Verhulst, S., 2020. Glucose regulation is a repeatable trait affected by successive handling in zebra finches. J. Comp. Physiol. B Biochem. Syst. Environ. Physiol. 190, 455–464. https://doi.org/10.1007/s00360-020-01283-4

Moon, J., Ikeda-Araki, A., Mun, Y., 2024. Night shift work and female breast cancer: a two-stage dose-response meta-analysis for the correct risk definition. BMC Public Health 24, 1–16. https://doi.org/10.1186/s12889-024-19518-2

Niu, S.F., Chung, M.H., Chu, H., Tsai, J.C., Lin, C.C., Liao, Y.M., Ou, K.L., O'Brien, A.P., Chou, K.R., 2015. Differences in cortisol profiles and circadian adjustment time between nurses working night shifts and regular day shifts: A prospective longitudinal study. Int. J. Nurs. Stud. 52, 1193–1201. https://doi.org/10.1016/j.ijnurstu.2015.04.001

Opperhuizen, A.L., van Kerkhof, L.W.M., Proper, K.I., Rodenburg, W., Kalsbeek, A., 2015. Rodent models to study the metabolic effects of shiftwork in humans. Front. Pharmacol. 6, 1–20. https://doi.org/10.3389/fphar.2015.00050

Oster, H., Challet, E., Ott, V., Arvat, E., de Kloet, E.R., Dijk, D.J., Lightman, S., Vgontzas, A., Van Cauter, E., 2017. The functional and clinical significance of the 24-hour rhythm of circulating glucocorticoids. Endocr. Rev. 38, 3–45. https://doi.org/10.1210/er.2015-1080

Otalora, B.B., Vivanco, P., Madariaga, A.M., Madrid, J.A., Rol, M.Á., 2010. Internal temporal order in the circadian system of a dual-phasing rodent, the octodon degus. Chronobiol. Int. 27, 1564–1579. https://doi.org/10.3109/07420528.2010.503294

Ouyang, J.Q., Davies, S., Dominoni, D., 2018. Hormonally mediated effects of artificial light at night on behavior and fitness: Linking endocrine mechanisms with function. J. Exp. Biol. 221. https://doi.org/10.1242/jeb.156893

Paul, M.J., Galang, J., Schwartz, W.J., Prendergast, B.J., 2009. Intermediate-duration day lengths unmask reproductive responses to nonphotic environmental cues. Am. J. Physiol. - Regul. Integr. Comp. Physiol. 296, 1613–1619. https://doi.org/10.1152/ajpregu.91047.2008

Perfito, N., 2010. The reproductive and stress physiology of Zebra Finches in context: Integrating field and laboratory studies. Emu 110, 199–208. https://doi.org/10.1071/MU09091

Perfito, N., Kwong, J.M.Y., Bentley, G.E., Hau, M., 2008. Cue hierarchies and testicular development: Is food a more potent stimulus than day length in an opportunistic breeder (Taeniopygia g. guttata)? Horm. Behav. 53, 567–572. https://doi.org/10.1016/j.yhbeh.2008.01.002

Pilcher, J.J., Lambert, B.J., Huffcutt, A.I., 2000. Differential effects of permanent and rotating shifts on self-report sleep length: A meta-analytic review. Sleep 23, 155–163. https://doi.org/10.1093/sleep/23.2.1b

Preiser, J.C., Thooft, A., Tironi, R.M., 2016. Stress hyperglycemia. Stress Response Crit. Illn. Metab. Horm. Asp. 89–94. https://doi.org/10.1007/978-3-319-27687-8_8

Rao, R., Androulakis, I.P., 2019. The physiological significance of the circadian dynamics of the HPA axis: Interplay between circadian rhythms, allostasis and stress resilience. Horm. Behav. 110, 77–89. https://doi.org/10.1016/j.yhbeh.2019.02.018

Remage-Healey, L., Romero, L.M., 2000. Daily and Seasonal Variation in Response to Stress in Captive Starlings (Sturnus Vulgaris): Glucose. Gen. Comp. Endocrinol. 119, 60–68. https://doi.org/10.1006/gcen.2000.7492

Rojas-Morales, P., Pedraza-Chaverri, J., Tapia, E., 2020. Ketone bodies, stress response, and redox homeostasis. Redox Biol. 29, 101395. https://doi.org/10.1016/j.redox.2019.101395

Spierings, M.J., Cate, C. Ten, 2016. Zebra finches as a model species to understand the roots of rhythm. Front. Neurosci. 10, 1–3. https://doi.org/10.3389/fnins.2016.00345
Sweazea, K.L., 2022a. Revisiting glucose regulation in birds – A negative model of diabetes complications. Comp. Biochem. Physiol. Part - B Biochem. Mol. Biol. 262, 110778. https://doi.org/10.1016/j.cbpb.2022.110778
Sweazea, K.L., 2022b. Revisiting glucose regulation in birds – A negative model of diabetes complications. Comp. Biochem. Physiol. Part - B Biochem. Mol. Biol. 262, 23332973. https://doi.org/10.1016/j.cbpb.2022.110778
Tabatabaei Dakhili, S.A., Yang, K., Stenlund, M.J., Ussher, J.R., 2025. The multifaceted roles of ketones in physiology. Exp. Physiol. 1–13. https://doi.org/10.1113/EP092243
Tolla, E., Stevenson, T.J., 2020. Sex differences and the neuroendocrine regulation of seasonal reproduction by supplementary environmental cues. Integr. Comp. Biol. 60, 1506–1516. https://doi.org/10.1093/icb/icaa096
van Dalfsen, J.H., Markus, C.R., 2018. The influence of sleep on human hypothalamic–pituitary–adrenal (HPA) axis reactivity: A systematic review. Sleep Med. Rev. 39, 187–194. https://doi.org/10.1016/j.smrv.2017.10.002
Van, N.T.H., Hoang, T., Myung, S.K., 2021. Night shift work and breast cancer risk: A meta-analysis of observational epidemiological studies. Carcinogenesis 42, 1260–1269. https://doi.org/10.1093/carcin/bgab074
Walker, W.H., Walton, J.C., DeVries, A.C., Nelson, R.J., 2020. Circadian rhythm disruption and mental health. Transl. Psychiatry 10. https://doi.org/10.1038/s41398-020-0694-0
Watts, H.E., Macdougall-Shackleton, S.A., Hahn, T.P., 2015. Variation among individuals in photoperiod responses: Effects of breeding schedule, photoperiod, and age-related photoperiodic experience in birds. J. Exp. Zool. Part A Ecol. Genet. Physiol. 323, 368–374. https://doi.org/10.1002/jez.1929
Zisapel, N., 2018. New perspectives on the role of melatonin in human sleep, circadian rhythms and their regulation. Br. J. Pharmacol. 175, 3190–3199. https://doi.org/10.1111/bph.14116

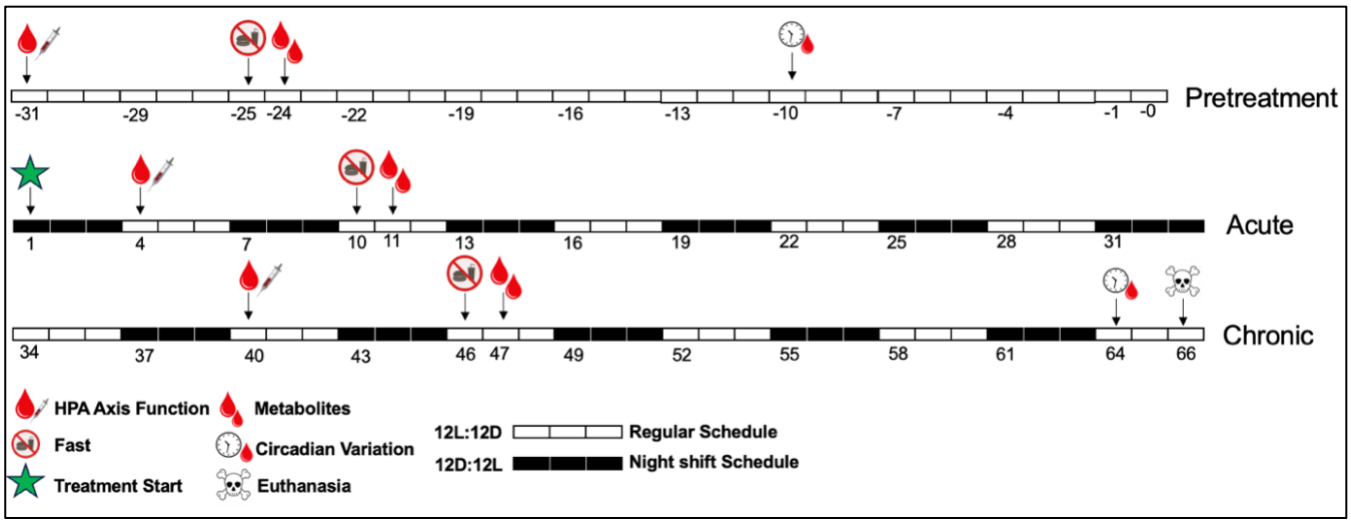

Figure 18. Experimental schematic of pretreatment sample collection. Each singular white bar represents one day on a regular light/dark schedule (lights on at 6am with lights off at 6pm). Numbers with a negative sign indicate days prior to treatment start (pretreatment). Blood icon with syringe on day -31 indicates when pretreatment HPA axis dynamics was tested (baseline, post-restraint, and post-dexamethasone corticosterone levels). On Day -25, birds were fasted 1 hour prior to lights off at 6pm, which is indicated by a crossed out burger and shake icon and bled the following morning on day -24 (one week later) indicated by double blood icons. Circadian variation in circulating hormones were measured on day -10 (two weeks later), indicated by the clock and blood icon. The green star indicates treatment start, in which birds experienced their first night shift condition by experiencing darkness from 6am-6pm (ZT0-ZT12pm). Then, light hours began from 6pm-6am (ZT12-ZT24). Here, three solid white bars indicate three days on a regular light/dark schedule (12L:12D) and three solid dark bars indicating three days on a night shift schedule (12D:12L). This schedule persisted for a total of 66 days and light schedules switched every three days. Euthanasia and tissue collection is indicated by the skull and crossbones.

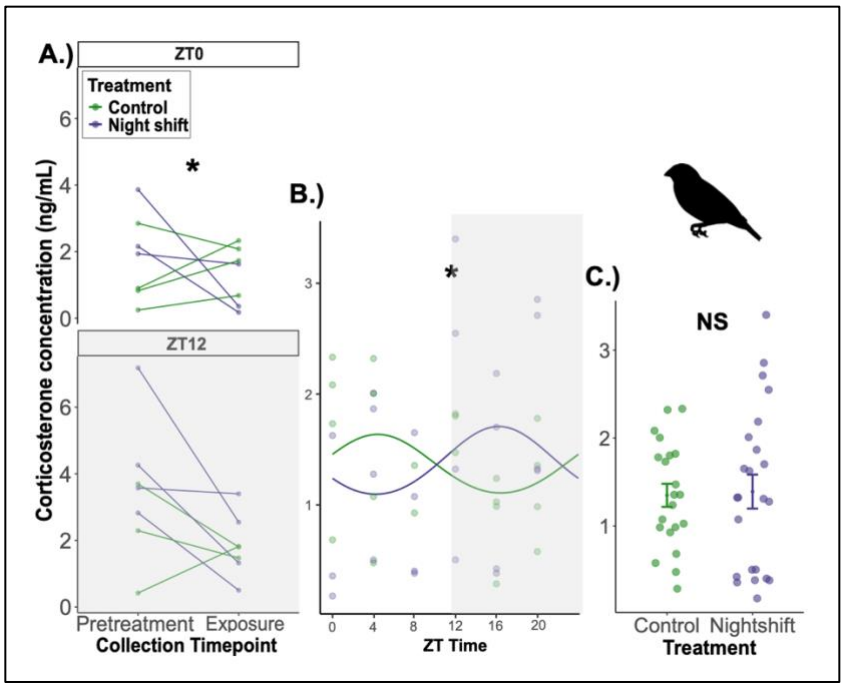

Figure 19. Corticosterone levels regarding circadian variation. A.) Corticosterone levels within birds before and after exposure simulated night shift work at specific ZT collection timepoints; B.) across 24-h period at exposure only, and C.) between treatment groups at exposure only. In all graphs, controls are depicted in green, while birds exposed to simulated night shift work are depicted in blue. A.) The X-axis indicates collection timepoint, while the Y-axis indicates corticosterone levels tracked between each unique individual before and after exposure to treatment. B.) The X-axis depicts the six ZT collection timepoints in which corticosterone levels were quantified. A sine wave is fit using GLMMcosine. C.) The X-axis indicates treatment groups, with average levels of corticosterone on the Y-axis using raw data on exposure data only. Error bars indicate the standard error of the mean (SEM). Gray boxes indicate the dark phase. Asterisks denote statistical differences; $*P < 0.05$.

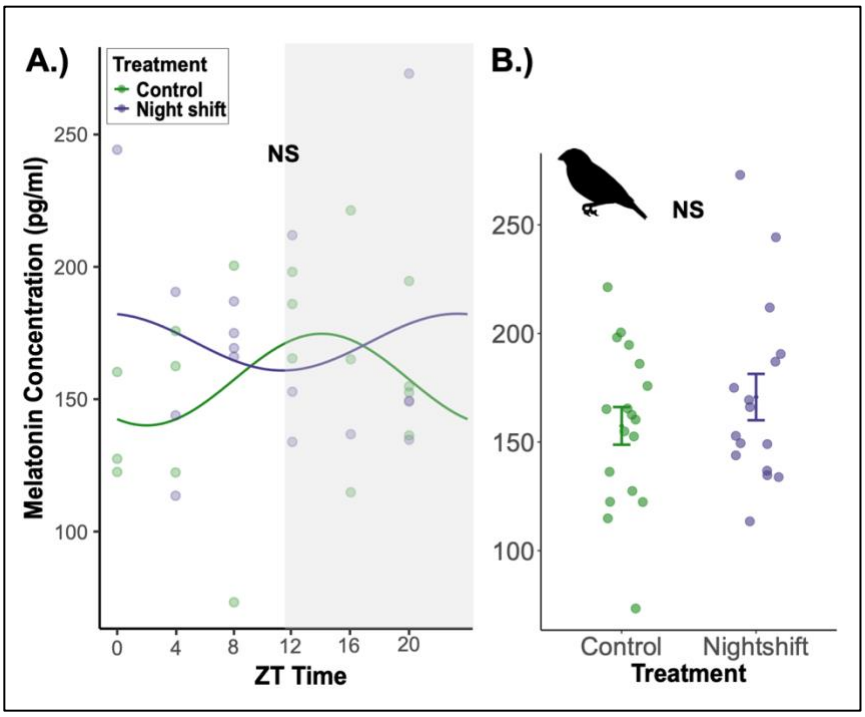

Figure 20. Melatonin rhythms and average hormone levels after exposure to night shift work. In all graphs, controls are depicted in green, while birds exposed to simulated night shift work are shown in blue. A.) The X-axis indicates six ZT collection times in which melatonin levels were quantified, while the Y-axis indicates melatonin levels (pg/mL). A best fit sine wave is fitted using GLMMcosine. B.) The X-axis depicts treatment group with the y-axis indicating melatonin levels. Average levels are plotted using raw data with error bars representing the standard error of the mean (SEM). Melatonin rhythms were significant, however, there was no difference in the acrophase or average difference in hormone levels between treatment groups.

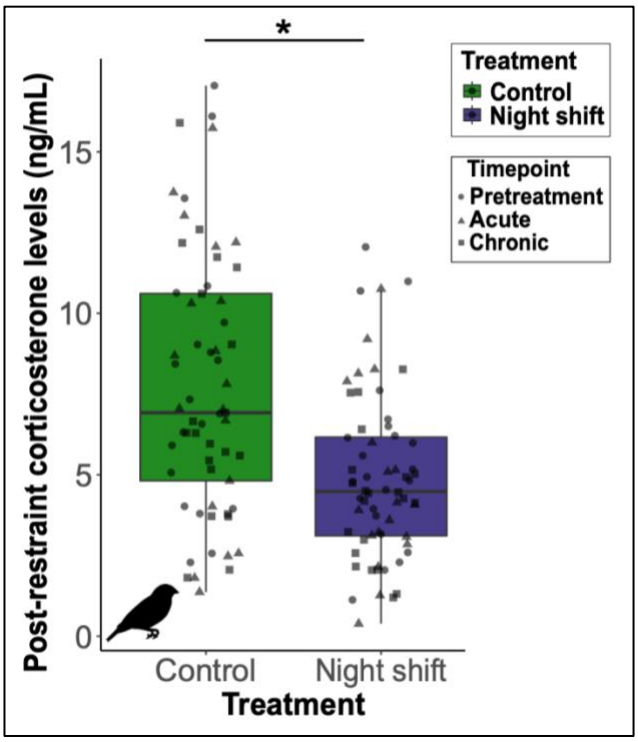

Figure 21. 30 min post-restraint corticosterone levels between treatment groups represented as a box-and-whisker plot. The solid black line indicates the median value, with the upper 75% quartile and lower 25% quartile depicted, and the interquartile representing 50% of the observed data. The X-axis depicts experimental groups, with control birds represented by the green bar and night shift birds represented by the blue bar. The Y-axis depicts corticosterone levels measured in ng/mL. Timepoints across the experiment are represented in shapes. Circle = Pretreatment, triangle = 3 night shifts, and square = 21 night shifts. Statistical significance is denoted with a solid black line with a single asterisk, with an associated *P-v*alue < 0.05).

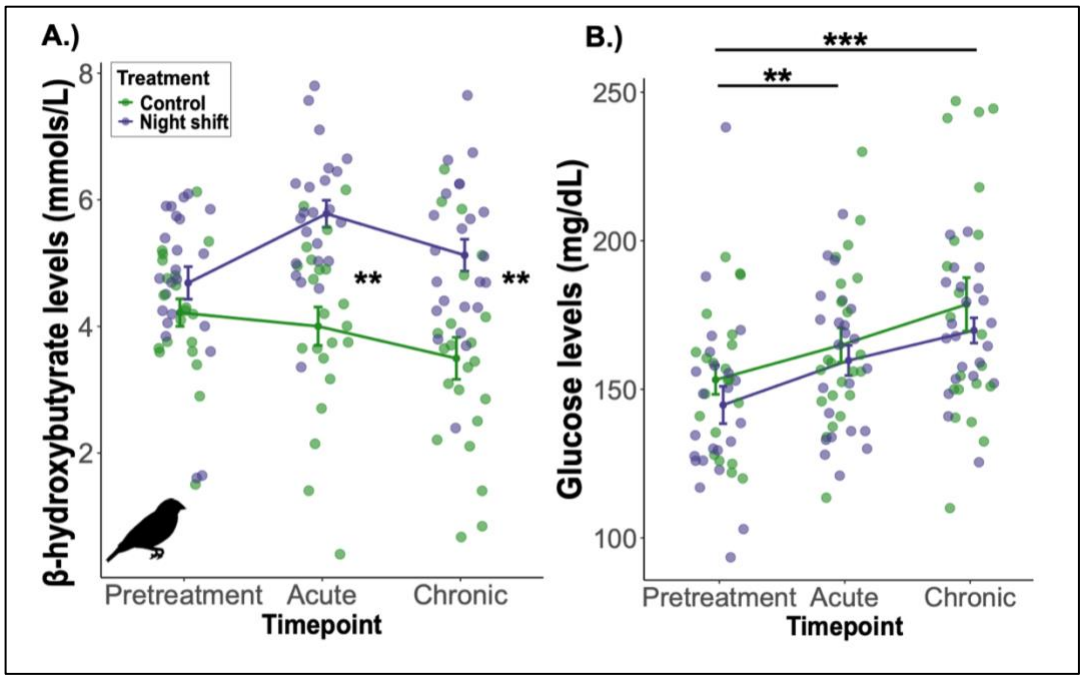

Figure 22. β-hydroxybutyrate and glucose levels between experimental groups over the duration of the experiment. For both graphs, the green line indicates controls, while the blue line indicates treatment birds. Averages are plotted using raw data, with error bars indicating the standard error of the mean (SEM). A.) The X-axis indicates Timepoint, while the Y-axis indicates circulating β-hydroxybutyrate levels (mmols/L). B.) The X-axis indicates timepoint, while the Y-axis indicates circulating glucose levels (mg/dL). Asterisks denote statistical differences; $^{**}P < 0.01$, $^{***}P < 0.001$.

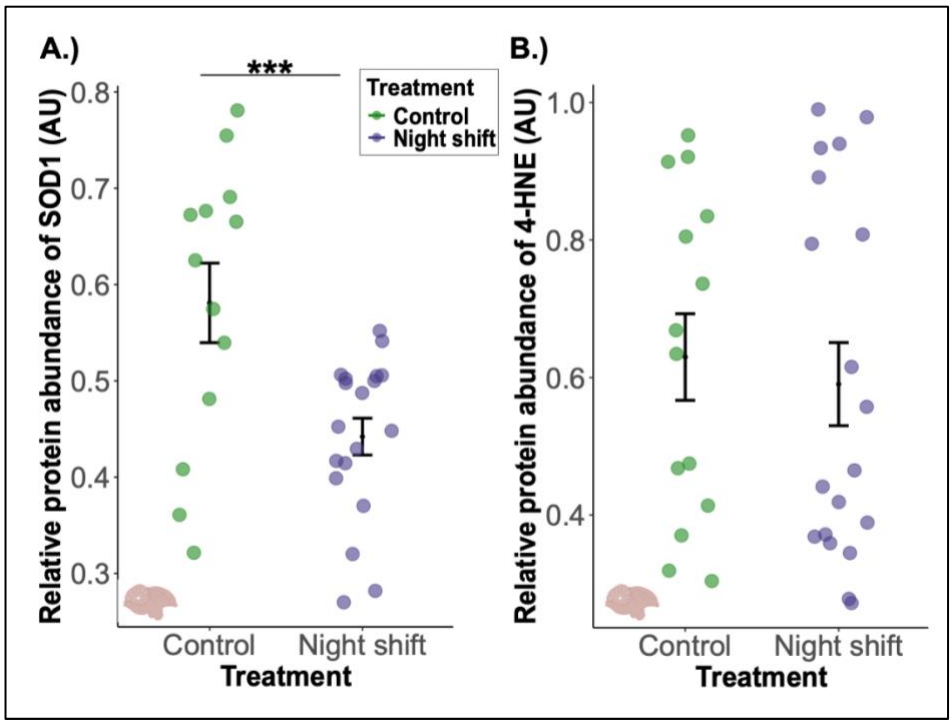

Figure 23. Relative abundance of SOD1 and 4-HNE protein levels in the brain. In both graphs, controls are depicted by the blue line, while birds exposed to night shift work are shown by the green line. The X-axis depicts treatment groups, while the Y-axis indicates relative protein abundance. A.) Sample size for this analysis was n = 13 for controls, and n = 19 for treatment birds. B.) Sample size for this analysis was n = 14 for controls, and n = 19 for treatment birds. Averages are plotted using raw data, with error bars indicating the standard error of the mean (SEM). Note that we show untransformed data, while in the statistical analysis, we log transform both response variables. Asterisks with lines denote statistical differences; ***$P < 0.001$.

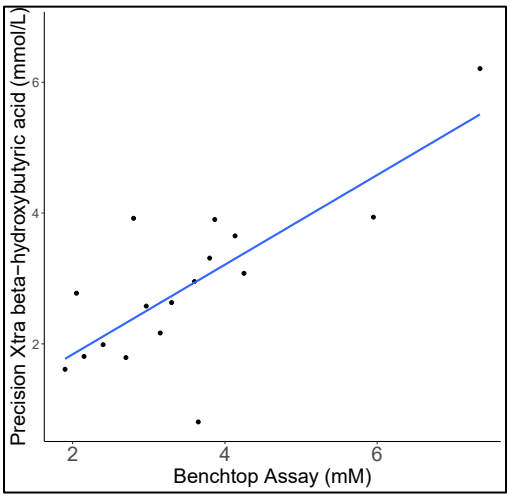

Figure S9. Linear regression between benchtop assay and point-of-care measurement of β-hydroxybutyrate. The X-axis indicates values obtained via the commercial EIA kit, while the Y-axis indicates values obtained via the PrecisionXtra point-of-care device. The best fit line is indicated by a blue line, with 95% confidence intervals shown in gray shading.

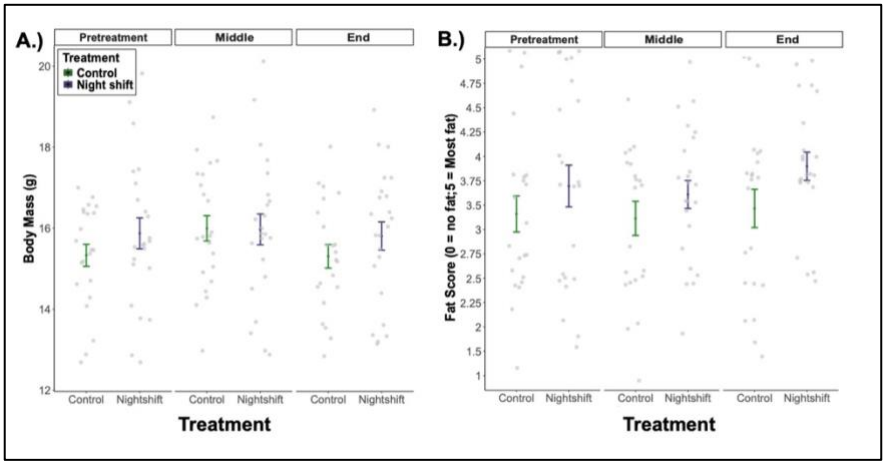

Figure S10. Morphometric measures taken throughout the experiment. The X-axis depicts different experimental groups, with control birds represented by a slate blue line and night shift birds represented by a forest green line. A.) The Y-axis depicts average body mass (g) between groups at each timepoint. B.) The Y-axis depicts average fat score between groups at each timepoint. Error bars represent standard error of the mean (SEM).

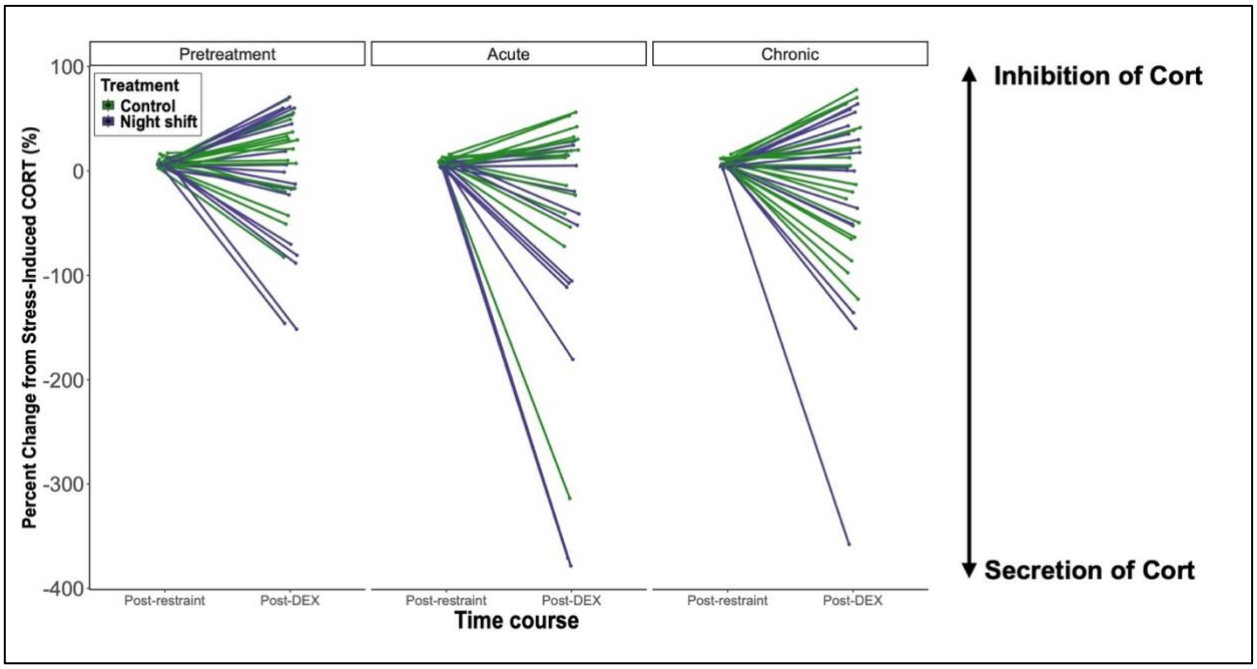

Figure S11. Relative reduction in corticosterone levels 30 min between post-restraint to after the dexamethasone challenge. The X-axis depicts the time course in corticosterone secretion, with control birds represented by a slate blue bar and night shift birds represented by a forest green bar. The Y-axis depicts the percent change (%) in corticosterone levels between post-restraint to post-DEX. Each individual point represents an individual's corticosterone level between the two corticosterone quantification timepoints. Also represented is each timepoint in which we measured corticosterone throughout the experiment. Positive slopes represent % inhibition of corticosterone, while negative slopes indicate % increase in corticosterone secretion.

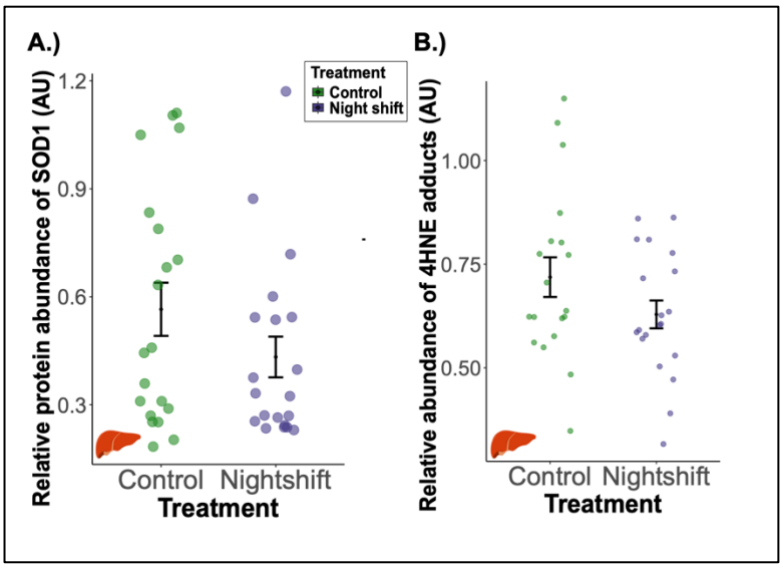

Figure S12. Relative abundance of SOD1 and 4-HNE protein levels in the liver. In both graphs, controls are depicted in dark slate blue, while birds exposed to night shift work are shown in forest green. The X-axis depicts treatment groups, while the Y-axis indicates relative protein abundance. A.) Sample size for this analysis was n = 19 for controls, and n = 20 for treatment birds. B.) Sample size for this analysis was n = 19 for controls, and n = 20 for treatment birds. Averages are plotted using raw data, with error bars indicating the standard error of the mean (SEM). Note that we show untransformed data, while in the statistical analysis, we log transform both response variables.

Chapter 6: General Conclusions and future directions

Light at unnatural times, at varying intensities, spectra, patterns, or durations poses a novel challenge in both wild and human populations, and the physiological consequences underlying this challenge can lead to long-term health and fitness outcomes. Yet, through my work, I have revealed that female diurnal zebra finches were not only able to recover from a constant light environment but were also able to escape persistent DNA and oxidative damage across tissues, emphasizing the value and importance of identifying an organism's capacity to recover from stressors. Additionally, I found a stimulatory effect, in which wild-derived female house mice exposed to constant light for six weeks had enhanced maximum mitochondrial respiratory function, specifically in the liver, with no cost in lipid peroxidation. Lastly, female zebra finches exposed to alternating patterns of light at night, similar to what night shift workers may experience, were able to maintain significant hormone rhythms, albeit inverted of their natural rhythm, and escape lipid peroxidation in the brain and liver.

Overall, my dissertation emphasizes the importance of resilience, and highlights key knowledge gaps in the literature that encompass physiological ecology studies in birds, to rodents and human epidemiological studies regarding shift work in humans. Perhaps one the main assumptions is that stressors have lingering, persistent effects that may translate into damage, fitness, or health-related costs. However, it is critical to evaluate the capacity at which organisms recover from stressors. By focusing on the role of recovery and resilience, we may be able to identify the mechanisms underlying an organism's response to mitigate detrimental outcomes, especially in the face of human-induced environmental change.

My dissertation also underscores the important of relevant animal models to investigate the effects of light at night by leveraging the unique physiology and circadian plasticity of birds,

and the utility of wild-derived rodent models that capture natural variation in physiological responses under controlled laboratory environments. Most work that has informed public health decisions regarding the deleterious effects of sleep loss and circadian rhythm disruption are done in nocturnal rodents. If we do not acknowledge opposing patterns or do not extend beyond artificially selected models, we will delay and prevent our ability to capture the unique mechanisms and responses that animals employ in order to combat environmental perturbations.

These interpretations and messages are echoed across my four data chapters. Zebra finches are resilient to light at night. Firstly, body mass and glucose levels collected within three min of capture were able to rebound and return to levels prior to exposure to light at night, indicating stress resilience; however, the glucose stress response did not show a similar recovery trend, indicating a persistent physiological effect of light at night that blunted the response. Secondly, while there were no average differences in DNA, lipid, or protein damage after the recovery period, but path analysis revealed physiological network rewiring between the control and treatment group with regards to lipid and protein damage. This rewiring between physiological traits revealed condition-dependency of HPA axis reactivity, and strong coupling between physiological traits in control birds that disappeared, reduced in magnitude, or were different in their direction of change in birds recovering from light. Physiological network rewiring may have been a response to prevent damage from accruing in birds recovering from constant light, or a long-lasting effect from light exposure; however, I am unable to determine if changes in physiological network connectivity is adaptative, as I did not have measures of performance or fitness. Nevertheless, my first two chapters identifies that zebra finches are able to recover from light exposure at unnatural times, potentially through shifts in physiological

relationships underlying damage outcomes and perhaps the mechanism enabling recovery and underlying stress resilience.

In chapter 4, I revealed that female wild-derived mice are able to effectively respond to constant light exposure by increasing mitochondrial respiratory function in the liver at no physiological cost. The lack of treatment effects on body mass, and fat pads is in direct opposition compared to many other studies investigating nighttime light in rodent models. Perhaps the most important difference between my study and others is that we leveraged a model that retained their sensitivity to stressors. As a consequence of inbreeding, specific traits such as aggression have been bred out, such that mice are easy models to handle. Yet, it is likely that traits underlying their flexibility in response to stressors have unintentionally been affected, possibly narrowing the range of their responses. Thus, my study leverages this plasticity, and I found a pattern yet to be discovered; maximum mitochondrial function (state 3) was enhanced in response to constant light. Yet, the physiological or molecular mechanism underpinning this enhanced respiratory rate in the liver cannot be identified within my study. This opens up the path to use a valuable and ecologically relevant model to investigate the deleterious effects of light at night and reinform our understanding of circadian rhythm biology relating to mammalian physiology. Moreover, the investigation of the subcellular capacity of mitochondria and how it relates to the metabolic costs under light at night will prove beneficial.

In my last chapter, I bridged together avian, mammalian, and human biomedical literature and asked how simulated night shift work affects the physiology of zebra finches, given their resilience found in my previous chapter. I found that zebra finches display the ability to resynchronize to imposed changes in the nighttime environment. This circadian plasticity closely mimics some studies in humans, suggesting that zebra finches have a similar ability to quickly

realign rhythms. The ability to quickly realign and display circadian plasticity opens the door to many questions regarding tolerance to nighttime exposure to mitigate detrimental costs.

While I detected interesting effects throughout my dissertation, perhaps one of the main limitations is such a targeted focus on physiology and could have been improved with the incorporation of behavioral measurements, an extremely important marker describing circadian rhythm disruption, as well as gene expression profiles. To remedy this, future work should investigate the role of simulated night shift work on behavior and cognitive flexibility, given that zebra finches seem to show resilience to physiological damage and quickly realign circadian oscillators. Zebra finches are social songbirds and extremely useful in evaluating the neural mechanisms underlying song learning. Thus, they are an insightful model to evaluate behavioral and cognitive flexibility in response to circadian rhythm disruption and sleep loss, which is associated with learning disabilities, mood disorders, and mental health illness in humans.

Measurement of behavioral and cognitive flexibility, coupled with a functional genomics approach targeting the eye and brain would be a critical first step to evaluate which genes are associated with behavioral responses to circadian rhythm disruption and which genes facilitate a recovery to sleep loss which may underlie learning outcomes.

In conclusion, the evidence gathered in this dissertation underscores the next path of research that I would partake on - investigating the role of circadian plasticity and resilience underlying cognition and behavior. Dr. Barbara Helm has called for this integration between chronobiologists and ecologists, with a focus on phenotypic plasticity. Given a bird's unique tolerance to disruption in nighttime lighting patterns, evaluating within-individual responses to behavioral assays in combination with aspects of repeatability may be an interesting avenue to evaluate if circadian rhythm disruption does indeed lead to short-term or long-term memory

deficits. Yet, the underlying mechanism is even more exciting – perhaps a downregulation of synaptic plasticity related genes? Or a reduction in the number of neurons able to be formed due to sleep loss? There could also be interesting physiological perspective given that neurons are vulnerable to reactive oxygen species, and energetically demanding.